PREDICTION OF DYNAMIC BENDING STRESSES OF SHIPS AT SEA

FREDERICK ROGERS

PREDICTION OF DYNAMIC BENDING STRESSES OF SHIPS AT SEA

BY

© FREDERICK ROGERS, B.Eng.

A thesis submitted to the School of Graduate

Studies in partial fulfillment of the

Requirements for the degree of

Master of Engineering

Faculty of Engineering and Applied Science

Memorial University of Newfoundland

May 1999

St. John's Newfoundland Canada

For my wife Roxanne, and son Andrew

ABSTRACT

A new method for the prediction of a ship's dynamic bending stresses at sea is presented and examined in this paper. The method uses a ship's heave and pitch motion to determine the dynamic bending moment at a point along the ship's length. This can be combined with the known still water bending moment, and known ship sectional properties to determine deck and keel stresses. A combination of mathematical modeling, the random decrement, and neural network techniques have been used to determine the relationship between ship motion and bending moment, without any prior knowledge of the wave excitation level.

To test this method, two sets of model experiments have been used. One set from a Great Lakes bulk carrier, the other from a Canadian patrol frigate. In each experiment, the mean and variance of the bending moment have been successfully predicted, demonstrating this method as a valid approach.

ACKNOWLEDGEMENTS

I would like to thank my supervisor, Dr. M. R. Haddara for his guidance and patience over the last two years. Without his help, this work would have never gotten off the ground.

I would also like to thank both David Molyneux at the Institute for Marine Dynamics and Lt. Commander Steve Gibson of the Department of National Defense for their kind donation of model experiment data. The level of the experiments performed went well beyond the means of a Masters program.

I appreciate the financial support from the Faculty of Engineering and the School of Graduate Studies for teaching assistantships, graduate funding and scholarship recommendations. Also, the National Research Council of Canada and the Department of Education were extremely generous.

Most importantly, I have to thank my wife Roxanne and son Andrew to whom this thesis is dedicated. They make all the work worthwhile.

Table of Contents

List of Figures

List of Tables

1.0 INTRODUCTION

Ship safety is becoming increasingly important as larger ships are built and required to operate in harsher environments. Extreme wave loading conditions have been known to produce dynamic stresses, which could result in structural damage. Without an accurate means of measuring and predicting stresses at critical locations in the ship, the ship's captain has no information that can help him make an enlightened decision to change a ship's course and speed to reduce these stresses.

Methods to predict the ship stresses are available, but normally require knowledge of the wave excitation level. This is extremely difficult to obtain in the open sea. Monitoring systems also exist, but they are expensive and can only measure stress where instrumentation is placed.

A new method has been developed to predict ship stresses using the measured ship motions of heave and pitch. A combination of mathematical modeling, the random decrement, and neural network techniques has been used to determine the relationship between ship motion and bending moment, without any prior knowledge of the wave excitation level.

To test this method, two sets of model experiments have been used. One set from a Great Lakes bulk carrier, the other from a Canadian patrol frigate.

2.0 LITERATURE SURVEY

The relationship between ship motion and ship bending moment is clearly defined by Lewis [1] in Principles of Naval Architecture. There, the motion is used to determine the forces acting on a section of the ship that are caused by the displacement, velocity and acceleration of the ship at this section. However, the wave properties at that section need to be known. Then the force is double integrated (over the length of the ship) to obtain the bending moment at a particular instant in time. This has been the focus for predictive methods of bending moment.

Strip theory has traditionally been used to predict bending moment in a known sea. This is a linear theory and the usual calculation takes the form of a wave spectrum multiplied by a bending moment response amplitude operator to produce the bending moment spectrum. This calculation cannot account for non-linear contributions to the loads. Buckley [2] discusses his recommended engineering approach to the determination of ship loads and motions. He states "The assessment of nonlinear behavior is regarded as a basic requirement in all aspects of the seaway environment and ship responses to it."

These non-liner contributions can come from various sources. Vulovich *et al* [3] analyzed full-scale deck stress measurements taken on a large containership in rough seas. They concluded that foredeck stresses vary directly with the slamming forces on the bow flare while the stresses in the midship portion are highly influenced by the

whipping vibration caused by the same bow flare slamming. Guedes Soares and Schellin [4] applied a method of long-term formulation for the non-linear wave induced vertical load effects on ships. This method is based on an empirical correction factor and was applied to three tanker hulls of different sizes. For the larger tankers, they concluded the correction factor had an insignificant effect, however for the smaller tanker, significant non-linear values were obtained. The main difference between the tankers was the non-vertical sides present in the smaller ones. In conclusion, they state that the non-linearity of ship response is caused mainly by ship's non-vertical sides.

Such non-linearities have been added to improve load estimating methods. Chiu and Fujino [5] used traditional strip theory with a non-linear component to predict the bending moment of a high-speed craft in waves. Strip theory was used to determine the ship's properties of added mass, damping and restoring coefficients as well as the hydrodynamic forces of a ship running in calm water. The non-linear portion of the forces was determined using time step calculations by computing the wave properties along the ship's length and determining the forces due to it. Chan [6] used a 3-D oscillating source and a 3-D translating pulsating source method to predict the wave loads on catamarans. Again, this was a time-step calculation that computed the wave properties along the length of the ship.

The method discussed by the author accounts for any non-linearity in the system. The ship's heave and pitch motions are influenced by whatever wave the ship experiences and by the ship's shape. Thus non-linearity effects would be included in the

heave and pitch measurements. Also, by requiring only the heave and pitch motions to be measured, the wave system can be totally arbitrary and doesn't need to be known. This is the main difference between this method and other predictive methods.

The removal of the requirement to know the wave system is accomplished using a mean value operator known as the random decrement. The Random Decrement Technique is mainly used to determine a one-degree of freedom system's free vibration characteristics from its response to a random excitation. Haddara *et al* [7] extended the technique and successfully applied it to the non-linear roll motion of a ship, predicting the ship's natural frequency in roll. In this paper, the random decrement curve closely matched the free roll decay curve. Ibrahim [8] demonstrated that the random decrement could be used in multi-degree of freedom systems, assuming the measured values were dynamically coupled and measured simultaneously. Heave, pitch and bending moment satisfy these criteria. Haddara [9] also demonstrated that a hybrid approach combining random decrement, classical parametric identification and neural network techniques could be used to identify the stability parameters of a ship at sea. Haddara modeled the essential physics of the system and lumped the other unknown parameters into one non-linear function. He used a feed-forward neural net, with one hidden layer to evaluate the function.

3.0 THEORY

The relationship between a ship's bending moment/bending moment squared and between heave and pitch motions, can be determined by considering static beam theory.

First, we consider bending moment. We assume there is no appreciable flexure in the structure. This would remove the need to determine any bending moment component due to hull whipping. Now we recognize that the bending moment at any location (x) is given by the following equation.

$$M(x) = \iint q(x_i)\, dx\, dx \tag{3.1}$$

where:
x_i *goes from* 0 *to location* x
$M(x)$ = *Bending Moment*
$q(x_i)$ = *Force at* x_i

The force at each location x_i, is made up of various components as follows.

$$q(x) = g(x) + b(x) - w(x) \tag{3.2}$$

where:
$g(x)$ = *force due to motion and waves*
$b(x)$ = *buoyancy force at* x
$w(x)$ = *weight at* x

Both the buoyancy force and weight are static variables and are determined from the loading condition and ship particulars. In the prediction, it is assumed that these forces are zero, and that bending moment due to static loading can be superimposed on the prediction. In other words, only the dynamic bending moment of the ship is being predicted.

The force due to motion and waves can be further broken down into the following: see Lewis [1].

$$g(x) = z(x)\left(c_{33}(x) + \frac{\omega_o}{\omega_e}\left[\omega_e^2\, a_{33}(x) - i\omega_e\, b_{33}(x)\right]\right) \tag{3.3}$$
$$+(\zeta_3 - l\zeta_5)c_{33}(x) + (\dot{\zeta}_3 - l\dot{\zeta}_5)b_{33}(x) + (\ddot{\zeta}_3 - l\ddot{\zeta}_5)(m(x) + a_{33}(x))$$

where:

l = *distance from center of buoyancy*

$z(x)$ = *wave height at* x

$a_{33}(x), b_{33}(x), c_{33}(x)$ = *added mass, damping and stiffness coefficients*

$m(x)$ = *mass at* x

ω_o, ω_e = *wave frequency and encounter frequency*

ζ_3, ζ_5 = *heave and pitch displacement*

$\dot{\zeta}_3, \dot{\zeta}_5$ = *heave and pitch velocity*

$\ddot{\zeta}_3, \ddot{\zeta}_5$ = *heave and pitch acceleration*

Now the relationship between bending moment and ship motion becomes obvious. Unfortunately, there is a calculation based on wave height along the length of the ship and wave frequency. Even in controlled testing conditions, neither of these is

accurately known. So the next step is to eliminate these quantities using a mean value operator.

To summarize the above,

$$M(x) = f(wave) + f(displacement) + f(velocity) + f(acceleration) \tag{3.4}$$

The wave function is assumed to be a stationary zero mean Gaussian white noise random process. When a mean value operator is applied to the wave function, it becomes zero. As a result, we get

$$\overline{M}(x) = f(\overline{H}_m, \overline{H}_v, \overline{H}_a, \overline{P}_m, \overline{P}_v, \overline{P}_a) \tag{3.5}$$

where:

$\overline{H}_m, \overline{H}_v, \overline{H}_a$ = *Mean Value of Heave displacement, velocity and acceleration*

$\overline{P}_m, \overline{P}_v, \overline{P}_a$ = *Mean Value of Pitch displacement, velocity and acceleration*

Similarly, the bending moment squared is a function of the heave and pitch motions and the wave. Since the function will contain terms of the wave squared, the wave effect cannot be removed using a mean value operator. However, one may assume that the bending moment squared is implicitly dependent on the wave condition through

the heave and pitch motion, and that the squared portion of the wave may be neglected. Thus, when applying the mean value operator, the bending moment squared becomes

$$\overline{M}^2(x) = f'\left(\overline{H}_m, \overline{H}_v, \overline{H}_a, \overline{P}_m, \overline{P}_v, \overline{P}_a\right) \tag{3.6}$$

If the above functions are known, both the mean values of the bending moment and the bending moment squared can be predicted based purely on the ship's heave and pitch motion. These values can then be used to determine the probable bending moment being experienced by the ship.

The Random Decrement Method is used as the mean value operator. It essentially filters out the randomness of a response and leaves the response's free decay curve. This is discussed further in section 5.2. The form of the function relating heave and pitch random decrement to the bending moment and bending moment squared random decrement can be determined by neural network methods. This is discussed further in section 5.3.

4.0 EXPERIMENTAL DATA

To validate the above theory, two sets of experimental data were used. The experiments were performed at the Institute for Marine Dynamics (IMD), St. John's, Newfoundland, a division of the National Research Council of Canada (NRC). Both experiments involved the use of a segmented model to measure the bending moment at multiple locations. The first model was a Great Lakes Bulk Carrier [10] tested in October 1992 and the second was a Canadian Patrol Frigate [11] tested in May 1993. It should be stressed that neither of these experiments were performed for this thesis work, but were part of a much larger test program. The author had no involvement with the Laker experiments, but was involved in both testing and analysis of the CPF experiments while employed at IMD. Details of the models and experiments are given in the following sections.

4.1 Great Lakes Bulk Carrier

4.1.1 Model Description

The model used for this experiment is representative of a self-unloading 217 metre bulk carrier. A summary of the principal particulars is given in Table 4.1, while a body plan of the ship is given in Figure 4.1. From here onward, this model is referred to as the Laker.

	Full Scale	Model Scale
Length, L_{BP} (m)	216.83	6.43
Beam (m)	23.12	0.69
Draught at FP (m)	10.41	0.31
Draught at midships (m)	10.41	0.31
Draught at AP (m)	10.41	0.31
Trim by bow (m)	0	0
Displacement (tonnes)	48820	1.27
Model Scale		33.7312
LCB (fwd midships) (m)	2.64	0.078
C_B	0.912	0.912
C_P	0.913	0.913
C_W	0.956	0.956
C_M	0.999	0.999

Table 4.1: Principal Particulars of a Great Lakes Bulk Carrier

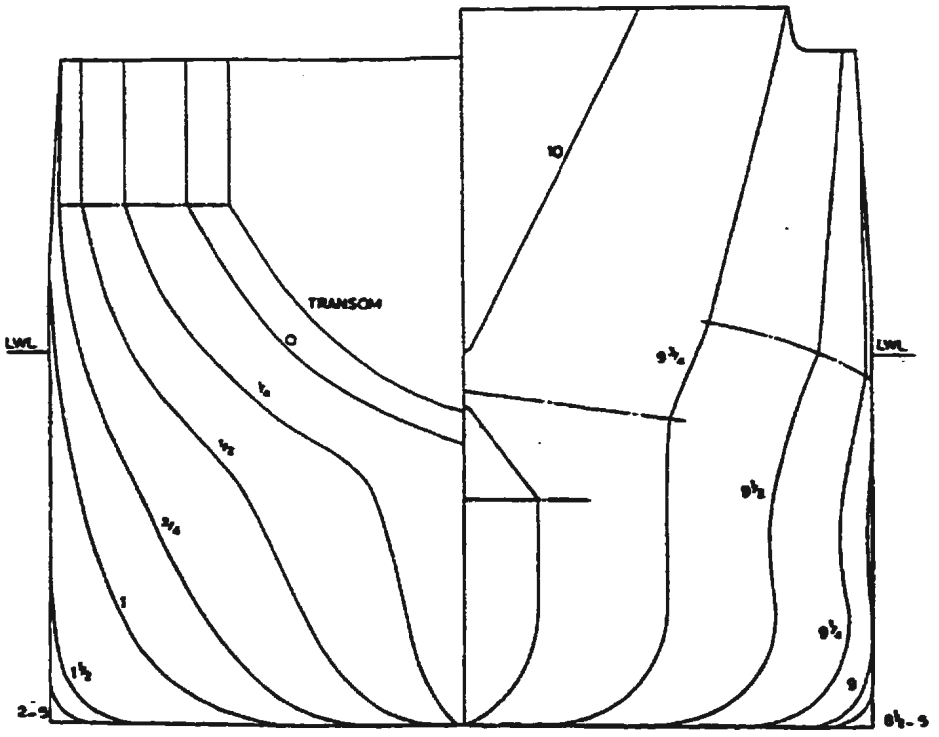

Figure 4.1: Body Plan of a Great Lakes Bulk Carrier

The model was constructed of glass reinforced plastic and segmented at stations 2, 3.5, 5 (midships), 6.5 and 8 with the forward perpendicular being at station 0 of 10. Each model segment was connected to its neighbor by two aluminum bars (one port and one starboard) outfitted with strain gauges for bending moment measurement. Each bar was outfitted with two strain gauges for a total of four strain gauges at each location. These four gauges were connected together to form a full Wheatstone bridge, and the aluminum bars horizontal axis corresponded to the neutral axis of the ship. A gap of 4 mm was maintained between the segments and covered with thin latex strips to maintain water tightness without compromising the elastic properties of the model. A diagram of the setup is shown in Figure 4.2.

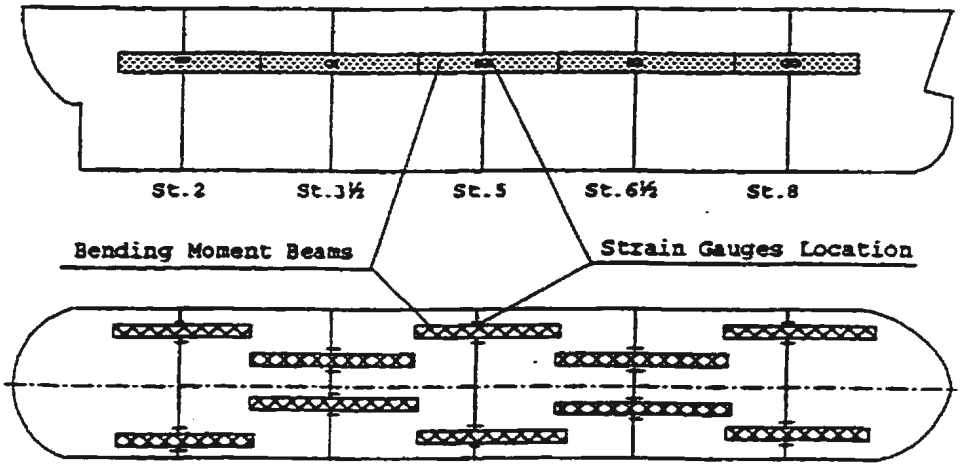

Figure 4.2: Bending Moment Measurement of a Great Lakes Bulk Carrier

For the experiments, the model was ballasted to the 0.3 m waterline, its L_{CG} from the AP was 3.292 m, its V_{CG} was 0.118 m and the longitudinal radius of gyration was 0.265 L_{BP} (target of 0.25 L_{BP}). The model's longitudinal weight distribution is shown in Figure 4.3. During the experiment, the model was self-propelled and free to heave, pitch and surge. Vertical guide poles restrained roll, sway and yaw motion.

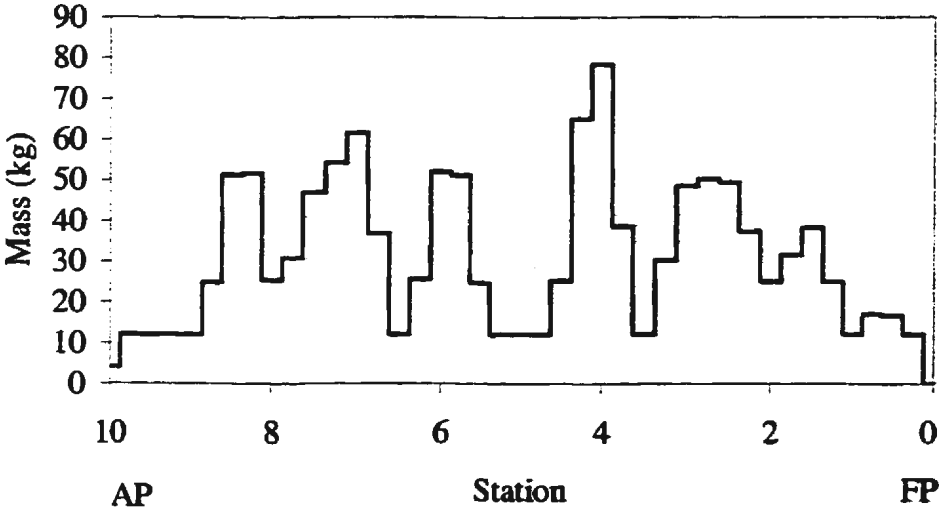

Figure 4.3: Longitudinal Weight Distribution of a Great Lakes Bulk Carrier

4.1.2 Model Calibration

Before use, the aluminum bars and strain gauges were calibrated using an in-situ calibration. For this calibration, the model was fully outfitted, but ballasted only to maintain positive transverse stability and level trim. The calibration was done for each station separately in the sag and hog directions by the application and movements of known weights to and from predefined initial locations. This would apply a known bending moment change to the station that could be compared to the change in the strain gauge output.

4.1.3 Data Collection

Table 4.2 lists the parameters measured during the Laker experiments. Not all of these measurements are required for the purpose of the current work, and those that are used are indicated by an *. While model speed and wave height are indicated as being used, their only purpose was to ensure that in the selected region of a test run, the model speed was constant and the wave had reached the model. All measured data were recorded at 40 Hz.

It should be noted here that the output from strain gauges located at station 3.5 were no stable during the model experiments. A calibration check of this station after the experiments were over indicated a significant change in the calibration constants. The station is analyzed and presented, but is ignored in the discussion of the results.

*Model Speed	m/sec
*Wave Elevation	cm
Shaft Rotation	1/sec
Relative Motion at Station 9.75	cm
Duct Thrust	N
Propeller Thrust	N
Propeller Torque	Nm
Heave Acceleration at FP	g
Surge Acceleration at LCB	g
*Heave Acceleration at LCB	g
Heave Acceleration at AP	g
*Pitch Angle	deg
Surge Displacement	cm
*Bending Moment at Station 2	Nm
*Bending Moment at Station 3.5	Nm
*Bending Moment at Station 5	Nm
*Bending Moment at Station 6.5	Nm
*Bending Moment at Station 8	Nm

Table 4.2: Measured Parameters in the Great Lakes Bulk Carrier Experiments

4.1.4 Experiments

The model was tested in two Bretschneider irregular wave spectra with significant wave heights of 3.05 and 6.10 metres full scale, and at speeds of 12.15 and 14.76 knots. This provides two conditions at each speed, allowing the use of one wave height for network training with the other for prediction and validation. For training purposes, the significant wave height of 6.10 metres is used.

4.2 Canadian Patrol Frigate

4.2.1 Model Description

The model for this experiment was based on the current patrol frigates used by the Canadian Navy. The principal particulars for this ship are given in Table 4.3 and a body plan is shown in Figure 4.4. From here onward, this model is referred to as the CPF.

	Full Scale	Model Scale
Length, L_{BP} (m)	124.5	6.225
Beam (m)	14.8	0.740
Draught at FP (m)	4.988	0.249
Draught at midships (m)	4.970	0.248
Draught at AP (m)	4.951	0.248
Trim by bow (m)	0.037	0.002
Displacement (tonnes)	4735.4	0.578
Model Scale		20
LCB (aft midships) (m)	2.775	0.139
C_B	0.490	0.490
C_P	0.610	0.610
C_W	0.772	0.772
C_M	0.801	0.801

Table 4.3: Principal Particulars of a Canadian Patrol Frigate

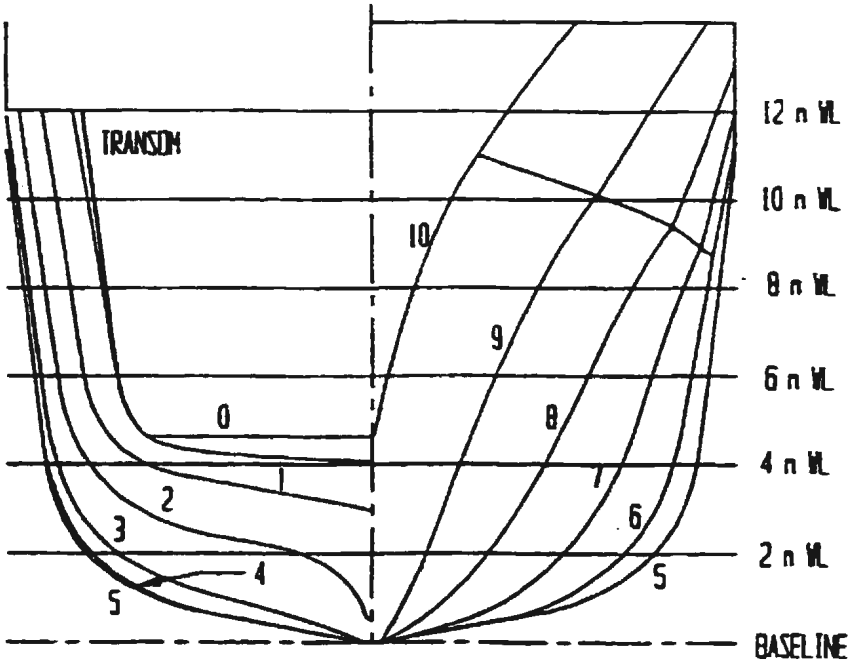

Figure 4.4: Body Plan of a Canadian Patrol Frigate

The model was constructed from fiberglass and was segmented at stations 2.5, 5, 7.5, 10 (midships) and 13.7 with the forward perpendicular at station 0 of 20. The six model segments were connected together by using a single longitudinal backbone seated on mounts made of aluminum plating and hardwood. Great care was taken to ensure the mounts were at the same horizontal level above the keel, making a near perfect seating of the backbone inside the model. As well, the neutral axis of the backbone was situated at the vertical neutral axis of the model (0.28 m above the keel). A gap of 10 mm was maintained between the segments and covered with thin latex strips to maintain water tightness. The setup for the CPF is shown in Figure 4.5.

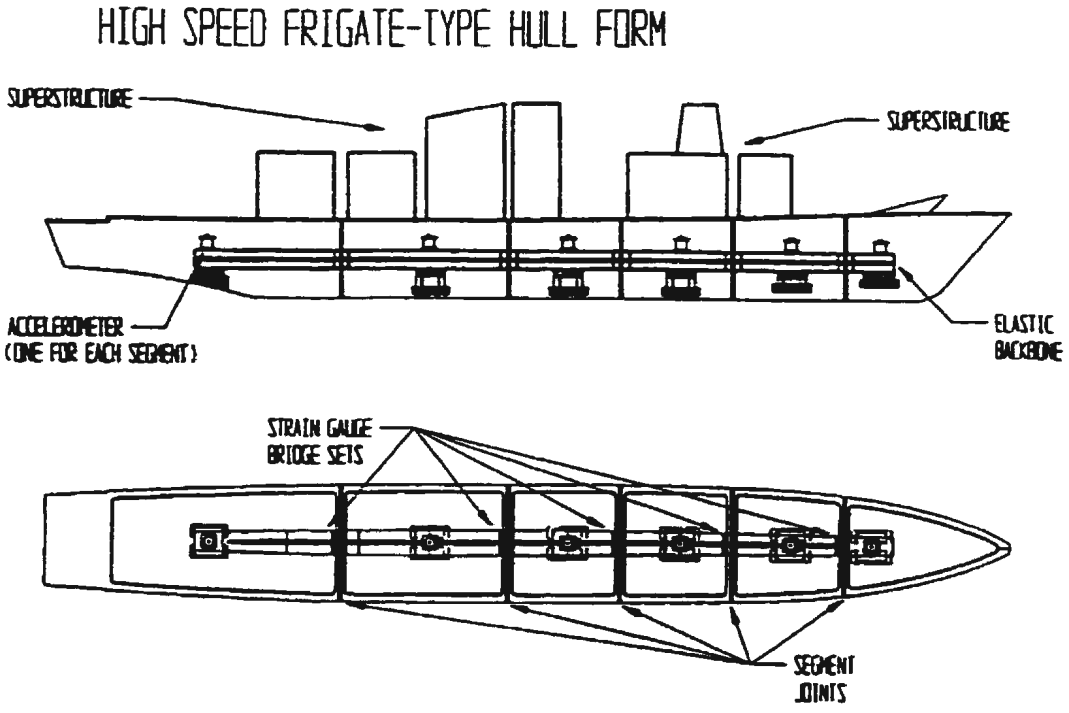

Figure 4.5: Bending Moment Measurement of a Canadian Patrol Frigate

The backbone was primarily comprised of four continuous stiffeners of carbon fiber composite material. These stiffeners were housed in a box made of Lexan webs, which were attached to the stiffeners. At the six mounting points, solid hardwood bulkheads were added. These bulkheads were approximately located at the longitudinal centers of gravity of each hull segment. It should be noted that the bulkheads and the Lexan webs were not longitudinally continuous, the carbon fiber stiffeners are the only longitudinal structural members of the model. At each segment joint, the backbone was outfitted with a series of strain gauges in full Wheatstone bridge formation to measure vertical bending, vertical shear, horizontal bending, horizontal shear, and torsion. During

backbone construction, primary attention was given to modeling the vertical bending stiffness, with the vertical shear, lateral bending and lateral shear stiffness given secondary importance. No effort was made to model the torsional properties correctly.

For the experiment, the model was ballasted to the 0.232 m waterline, its L_{CG} aft of midships was 0.139 m, its V_{CG} was 0.316 m, and the longitudinal pitch radius of gyration was 0.238 L_{BP} (target of 0.25 L_{BP}). The model was also ballasted so that the calm water bending moment distribution was reasonably accurate. The model's longitudinal weight distribution is shown in Figure 4.6. During the experiment, the model was completely self-propelled and free to move in all six degrees of freedom. The only connection was a set of slack lines to ensure model safety.

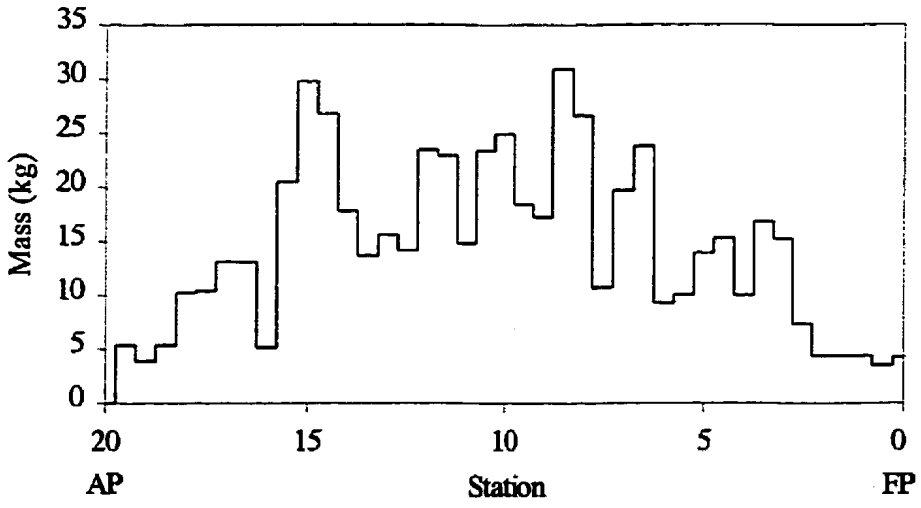

Figure 4.6: Longitudinal Weight Distribution of a Canadian Patrol Frigate.

4.2.2 Model Calibration

Before use, the backbone needed to be calibrated. This was done with the backbone outside of the model, and simply supported on rollers. Known weights were applied to various locations along the backbone length, creating known bending moment and shear forces. These forces would be compared to the output from the strain gauge sets. However, due to the complexity of the backbone and the fact that creating a perfectly symmetrical backbone is nearly impossible, "cross-talk" occurred. This means that even when the backbone was loaded in the purely vertical direction, some small lateral moment or torsion would occur. This cross-talk was accounted for during the calibration and analysis. During calibration, when subjected to pure loading in one direction, the outputs from all directions were measured. This then allowed the subtraction of the cross-talk component during analysis.

4.2.3 Data Collection

Table 4.4 lists the parameters measured during the CPF experiments. Not all of these measurements are required for the purpose of the current work, and those that are used are indicated by an *. As with the Laker, the model speed and wave height were only used to ensure that in the selected region of a test run, the model speed was constant and the wave had reached the model. The horizontal bending/shear, vertical shear and

*Model Speed	m/sec
*Wave Elevation	cm
Surge Displacement	cm
*Pitch Angle	deg
Roll Angle	deg
Yaw Angle	deg
*Heave Acceleration	g
Sway Acceleration	g
Surge Acceleration	g
Pitch Rate	deg/s
Roll Rate	deg/s
Yaw Rate	deg/s
Rudder Angle	deg
Port Propeller	rps
Stbd. Propeller	rps
Relative Motion at FP	m
Segment 1 Acceleration	g
Segment 2 Acceleration	g
Segment 3 Acceleration	g
Segment 4 Acceleration	g
Segment 5 Acceleration	g
Segment 6 Acceleration	g
Segment joints at Stations 2.5, 5, 7.5, 10 & 13.7	
*Vertical Bending	Nm
*Horizontal Bending	Nm
*Vertical Shear	N
*Horizontal Shear	N
*Torsion	Nm

Table 4.4: Measured Parameters in the Canadian Patrol Frigate Experiments

4.2.4 Experiments

The model was tested in three Bretschneider irregular wave spectra with significant wave heights of 4.0, 5.0 and 6.0 metres, and at speeds of 4.1, 8.2, 13.6 and

17.0 knots. This provides three conditions at each speed, allowing the use of one wave height for network training with the other two for prediction and validation. For training purposes, the significant wave height of 6.0 metres is used.

5.0 METHODOLOGY

The following sections outline the way in which the experimental data was analyzed and how the random decrement method was applied. Also, the neural network method is discussed along with the neural network program NeuroShell2®.

5.1 Data Analysis

Both the Laker and CPF data analysis were done in the same way. This was possible since both sets of experiments included the same required measurements as was indicated in Tables 4.2 and 4.4. The steps are listed in point form for convenience, and any minor differences in analysis are indicated. At various stages, the time series were visually checked to ensure the programs were working properly.

1. The data was sampled using IMDs DAS (Data Acquisition System) format. This had to be converted into a form that the main analysis package at IMD could use. This package is known as the GEDAP software suite. GEDAP is developed between various sections of NRC, and its components are thoroughly tested to ensure they work properly.

2. Visual examinations of each run were performed, and portions where the model speed was constant and the model experienced waves were selected.

3. Runs with a common speed and wave system were spliced together. This is done to obtain long records of the model in a particular wave. Run lengths of 250-300 seconds (model scale) were obtained for the Laker and lengths of 500-600 seconds (model scale) were obtained for the CPF.

4. CPF only. A program developed at IMD was used to remove the cross talk components from the backbone measurements.

5. The pitch displacement was converted from degrees to radians using a scale factor of 0.0174533.

6. The mean value was removed from the bending moment channels. This removed components due to still water bending.

7. After doing a spectral analysis on the pitch and bending moment channels, each was filtered to remove high frequency noise. This noise was most likely due to motor vibration.

8. The heave acceleration was converted from g's to m/s^2 and integrated twice to obtain the heave displacement. During integration, the heave was also filtered to remove high frequency noise.

9. Heave and pitch displacement data were differentiated to obtain heave and pitch velocity and then differentiated again to obtain heave and pitch acceleration. This then resulted in six heave and pitch measurements and five bending moment measurements on which the random decrement needed to be applied. The heave accelerations were then compared with those measured as a check of the integration and differentiation steps.

10. The random decrement of each measurement was determined, and these were fed into the neural network program; first for training, and then for prediction. As mentioned in section 4, in the case of training, the wave height of 6.1 m was used for the Laker, and the wave height of 6.0 m was used for the CPF. Prediction was performed on measurements obtained from the Laker wave height of 3.05 m, and CPF wave heights of 4.0 and 5.0 m.

Both the random decrement method and the neural network deserve some extended discussion. This can be found in the following sections.

5.2 Random Decrement

As mentioned previously, the random decrement was used as a mean value operator. It is based on the fact that the random response of a system due to random input is made up of two parts; the deterministic part and the random part. The random part is assumed to have a zero average. By averaging enough samples of the response,

the random component will average out to zero, leaving the deterministic component. This component is the free decay curve of a particular ship response. Here, we determined the decay curve of heave displacement/velocity/acceleration, pitch displacement/velocity/acceleration, bending moment and bending moment squared. The input into this particular system was the irregular wave, and it is assumed to be a Gaussian excitation with zero mean.

The calculation of the random decrement for a one-degree of freedom system is very simple. First, the length of the time window is chosen that would cover several zero crossings in the system response. This length is usually chosen by inspection and will be the total time length of the resulting random decrement curve. Second, a threshold value is chosen, also by inspection. The idea is to make sure there are enough samples to add together to create a meaningful average. Third, the time series is scanned till threshold values are found where the curve has a positive slope. At each threshold, a section of data the size of the window is triggered out and saved for later use. Fourth, the entire time series is rescanned at the same threshold but this time at points where the curve has a negative slope. These sections are saved for later use. The double scan along the time series is to remove any potential cause of bias. Finally, all of the triggered out sections of data from steps three and four and added together by superposition and averaged by the number of sections. This produces the final random decrement curve. Since portions of the response are random, the superposition and averaging remove the random component. These sections are averaged with the others, producing the final random decrement curve.

When determining the random decrements of a multi-degree of freedom system that are dynamically coupled, care must be taken to ensure the time phase between random decrements is maintained. This was particularly important in this case since the heave and pitch responses were to be compared with the bending moment and bending moment squared response. In order to maintain the time phase, the random decrements needed to be determined a little differently. Instead of using a threshold value for each individual response, one response needed to be used as the master time series. The threshold value is applied to this response, and the time the value occurs is used for all other responses. This is most clearly demonstrated in Figure 5.1.

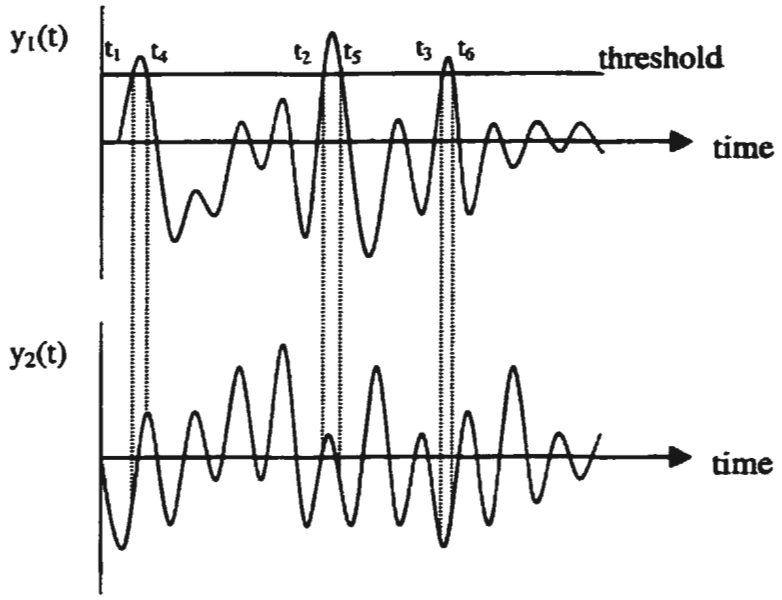

Figure 5.1: Random Decrement Determination for a Multi-degree of Freedom System

For this work, heave displacement was chosen as the master response. The time window was set at 5 seconds and the threshold was nominally chosen as 25% of the peak heave response. These threshold values are shown in Table 5.1, along with the number of sections used to determine the random decrements at each condition.

Model	Speed (knots)	Wave Ht. (m)	Threshold (m)	Num. Sections
LAKER	12.15	3.05	0.005	81
		6.1	0.02	83
	14.76	3.05	0.01	49
		6.1	0.025	59
CPF	4.1	4	0.03	108
		5	0.03	208
		6	0.04	199
	8.2	4	0.02	48
		5	0.03	162
		6	0.03	198
	13.6	4	0.03	185
		5	0.03	169
		6	0.03	186
	17	4	0.03	98
		5	0.03	155
		6	0.03	152

Table 5.1: Random Decrement Thresholds and Number of Sections Used

Although a 5 second window was used, the first 1.75 seconds of the Random Decrements provide the information needed to see peak response and frequency. Therefore, for the sake of efficiency in analyses, the latter 3.25 seconds of the random decrements are not used. An example of the first 1.75 seconds of the displacement, velocity and acceleration random decrements for the Laker and CPF are presented in Figures 5.2 and 5.3. The complete set of random decrements can be found in Appendix A. These are both the input random decrements used for training, and those used for prediction. Note the phase lag between the various inputs can be clearly seen. The bending moment and bending moment squared random decrements are presented later during the network training and network prediction discussion.

LAKER

Figure 5.2: Motion Random Decrements

Ship Speed: 12.15 knots Sig. Wave Height: 3.05 m Bretschneider Spectra

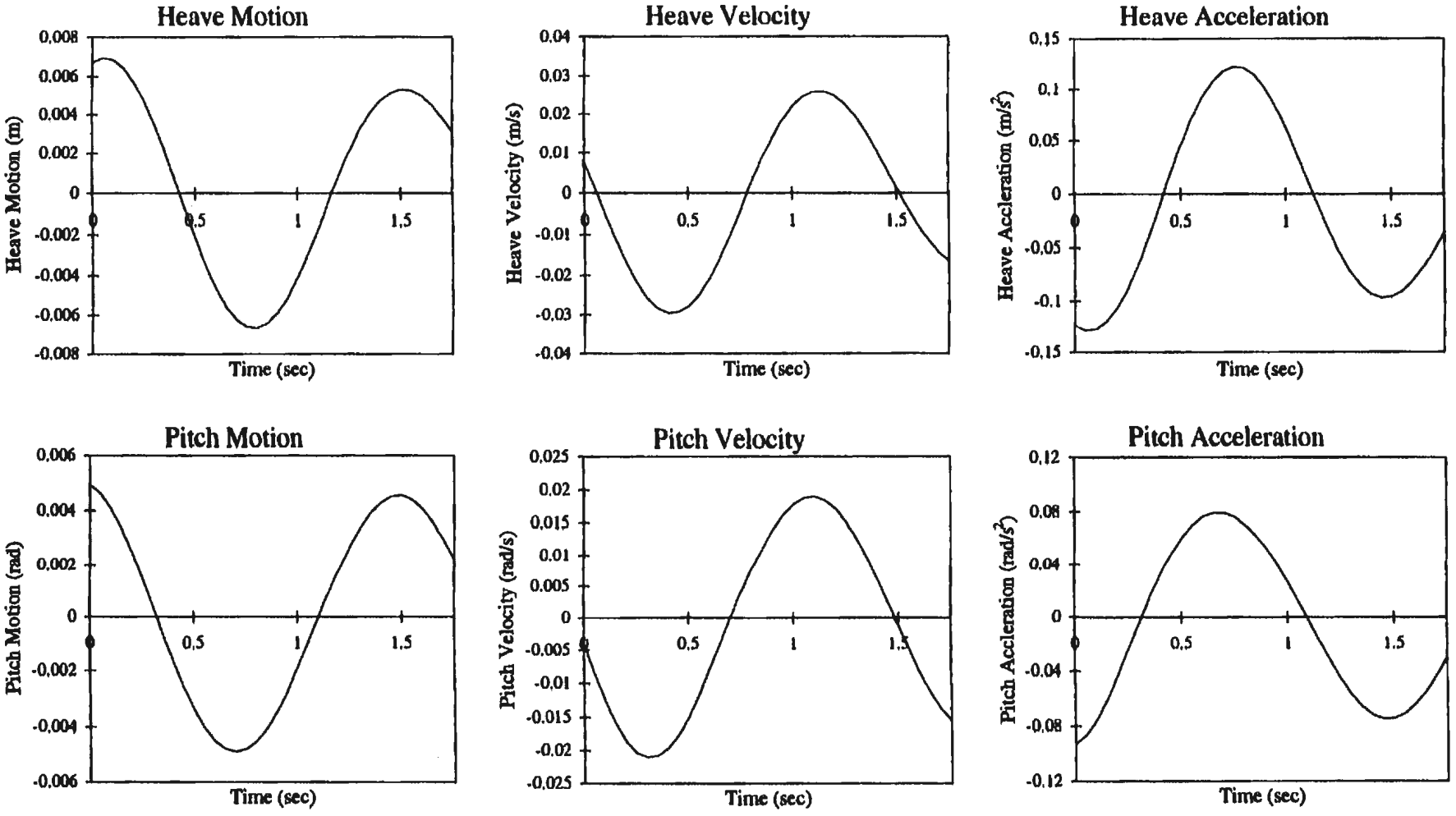

CPF

Figure 5.3: Motion Random Decrements

Ship Speed: 4.1 knots Sig. Wave Height: 4 m Bretschneider Spectra

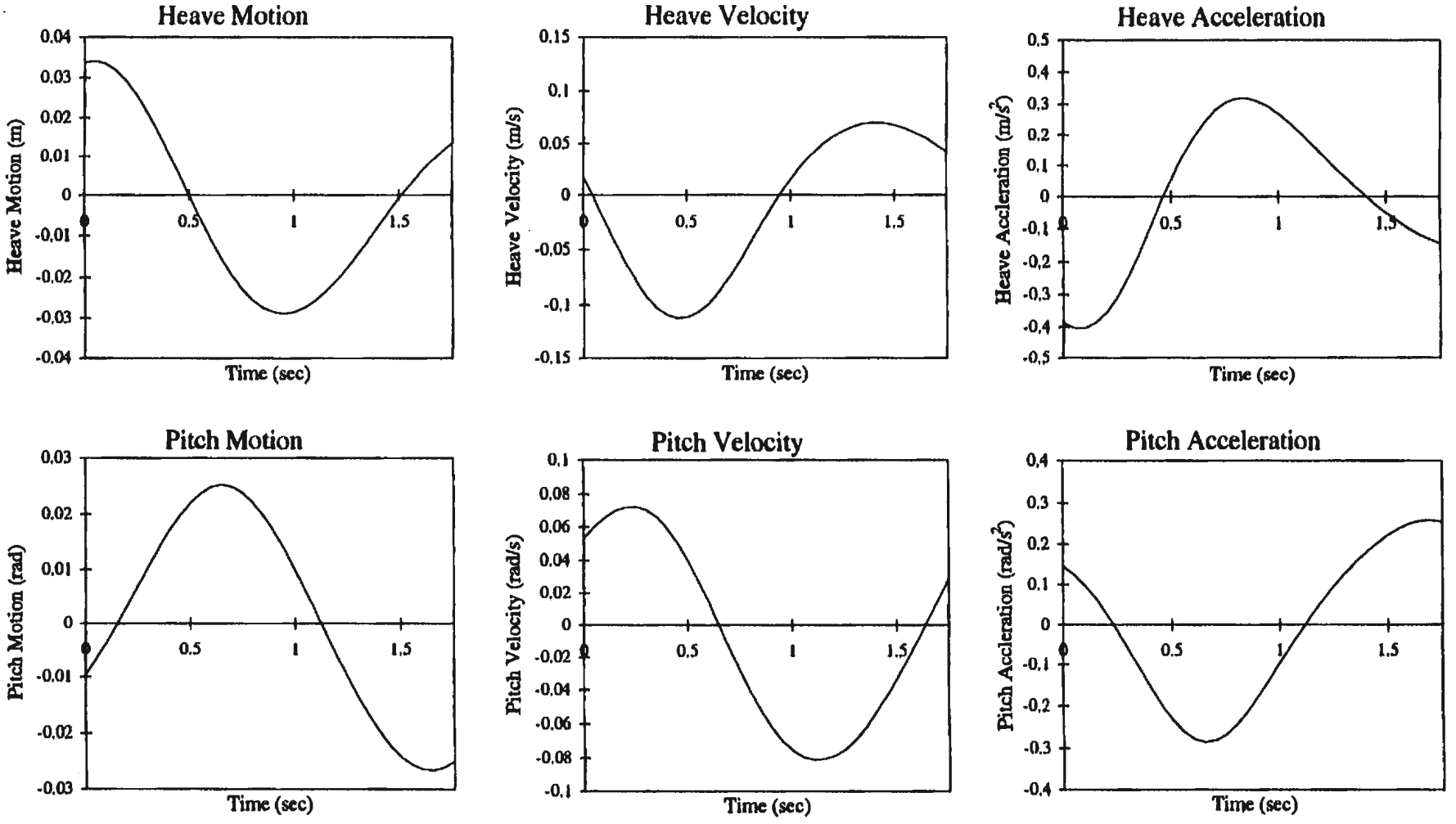

5.3 Neural Network

As mentioned above, we want to determine the relationship between the Random Decrement of the bending moment and the Random Decrements of the ship heave and pitch responses. This relationship can be determined using neural network techniques. The technique is similar to regression, but infinitely more flexible as one does not assume any final form of the relationship equation.

A neural network in nature, as shown in Figure 5.4, consists of dendrites, neurons and axons. The dendrites feed information into each neuron through a synapse that controls the strength of the signal fed in. The neuron then sums up all its inputs from the synapses and sends a signal along the axon if it exceeds a certain threshold.

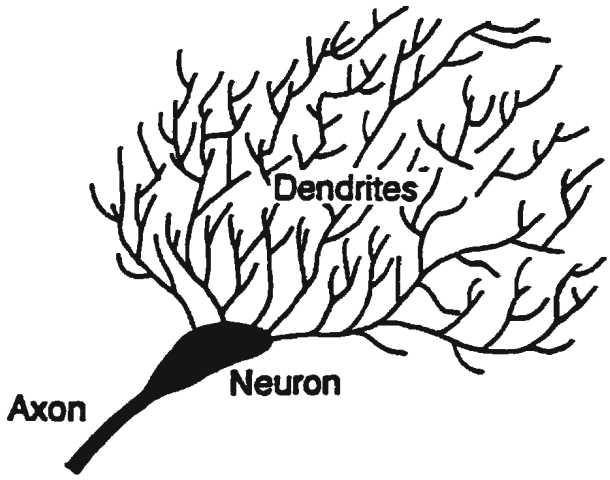

Figure 5.4: Biological Neural Network

An artificial network attempts to mimic this process. Consider the diagram in Figure 5.5.

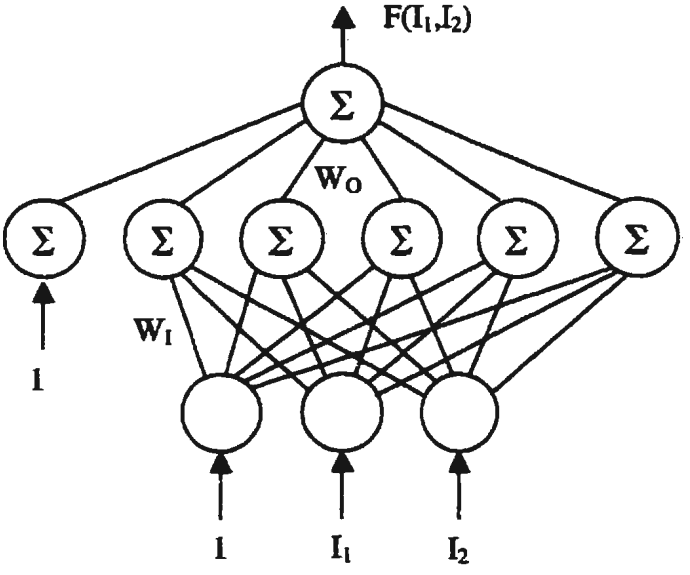

Figure 5.5: Artificial Neural Network Example

The input layer with inputs of 1, I_1 and I_2 feeds into a hidden layer the way the dendrites feed into the neurons. The synapse strength between the input and hidden layer is defined as a weighting value (W_I) applied at each connection. Then, all of the summations from the hidden layer are then weighted by another value (W_O) and summed together to form the output. The diagram shown is a simplified version of the network used to determine the relationship between bending moment/bending moment squared and the ship response. The network used has six inputs, plus a bias input of unity in the first layer, there are thirteen inputs plus bias in the hidden layer, and a single output.

The summed inputs in the hidden layer are processed with a squashing function as they pass through the neuron. The squashing function used is known as the logistic function and is given by

$$f(x)=\frac{1}{1+e^{-x}} \tag{5.1}$$

This function simulates the firing action of neurons where information flows forward through the net from input to output. To update the synaptic weights and improve the training, a method of back-propagation is used, and numerous iterations are performed until an acceptable error level is reached. Thus, the neural network model is known as a feed-forward, back-propagation network. In mathematical form, the neural network model for bending moment can be given as

$$BM = \sum_{k=1}^{13} W_{Ok} f(H_k) \tag{5.2}$$

$$H_k = \sum_{j=1}^{7} W_{ij} y_j$$

Here, BM is the bending moment, W_{Ok} is the k^{th} output weight from the hidden layer, H_k is the input to the k^{th} node of the hidden layer, W_{ij} is the weight between the input layer and hidden layer for input j and node k, and y_j is the input to the j^{th} node.

The training of the network was done using a commercial program called NeuroShell2®. It is discussed in the next section.

5.4 NeuroShell2®

NeuroShell2® is a commercial program purchased by Memorial University of Newfoundland for general student use. It is written by Ward Systems Group, and the version used here is 3.0. This program enables the user to build complex neural networks. Basically, one tells the program what one is trying to predict, and the program learns the patterns from the training data and makes its own predictions when presented with new data. The available options in the program are varied, and the ones used for this work are discussed.

The neural network used was the basic feed forward, back propagation net. It is the simplest form of a neural network and the easiest to train. The inputs consisted of the heave and pitch random decrement responses, the single hidden layer had 13 neurons, and the training output was bending moment and bending moment squared random decrements. It should be noted that the bending moment and bending moment squared were trained separately. Each layer is known as a slab, with the connections between the slabs known as links.

Each slab has its own scaling or activation function. That is how the data within the slab is scaled for the neural network to use. The input slab was scaled using a linear function with no clipping. Basically, all inputs were scaled between 0 and 1, and later during the prediction, values below 0 and above 1 were allowed. The hidden slab used

the logistic activation function mentioned earlier. The output slab, like the input, had a linear scaling function.

The links between the slabs require two important values. These are the learning rate and the momentum. During training, the error between the calculated output and the actual output is determined. A percentage of this error is used to modify the weights to improve the prediction. This percentage is a combination of the learning rate and the momentum. The change in weight is given by the following equation.

$$\Delta weight = (learning\ rate + momentum * \Delta weight_{old}) * error \qquad (5.3)$$

The momentum is used to prevent the oscillation of weight changes that can prevent the network from being properly trained. The learning rate used here was 0.05 with a momentum of 0.5. These values were for both links.

Another useful part of NeuroShell2® is its ability to prevent overtraining and network memorization by the use of calibration. To put it simply, the program takes a small portion of the input and output data and doesn't use it in the regular training cycles. Instead, this portion is used every so many cycles to check on the training. Since it is outside of the training set, it is representative of other possible inputs and thus keeps the network training generalized. It is also a better indication of when the network has been trained enough for practical use. For this work, the calibration was performed every 200 cycles and training was stopped when the average error was less than $2x10^{-6}$ kNm or $(kNm)^2$.

6.0 RESULTS AND DISCUSSION

6.1 Training

As mentioned previously, the data used for network training were the conditions in the Laker test where the wave height was 6.1 metres and the condition in the CPF test where the wave height was 6.0 metres. In each case, the six inputs to the neural network were the random decrements of heave displacement, heave velocity, heave acceleration, pitch displacement, pitch velocity and pitch acceleration. The outputs were the bending moment and the bending moment squared random decrements. It should be noted that these two outputs were trained independently.

Examples of the training plots for the Laker and CPF are presented in Figures 6.1 and 6.2. The full set of training plots can be found in Appendix B. For each, the training stopped when the average error reached $2\text{-}10^{-6}$ kNm for the bending moment and $2\text{-}10^{-6}$ $(\text{kNm})^2$ for the bending moment squared. From each plot, it can be seen the training has been done very accurately.

LAKER

Figure 6.1: Training of Bending Moment Random Decrements

Ship Speed: 12.15 knots Sig. Wave Height: 6.1 m Bretschneider Spectra

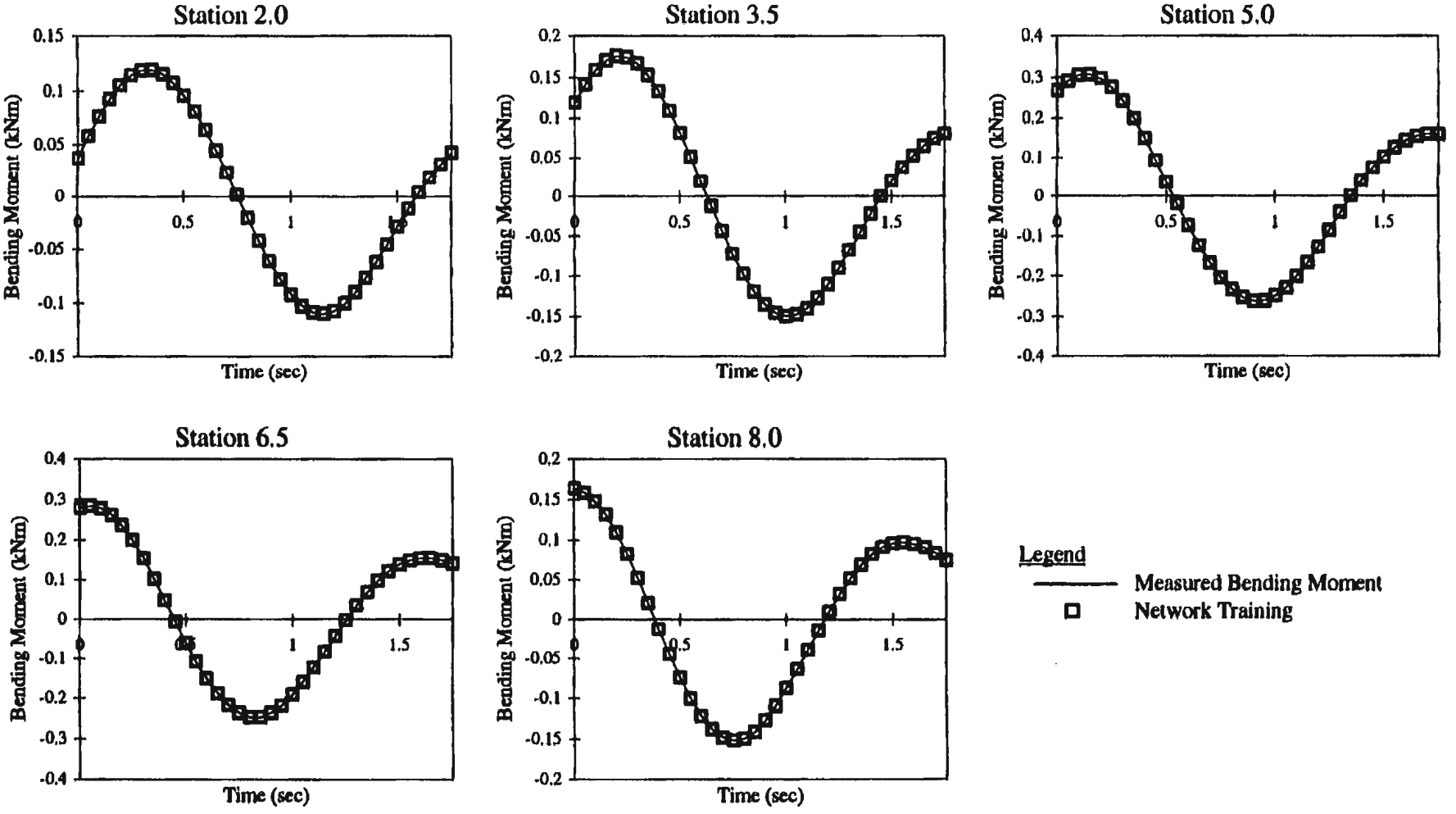

CPF

Figure 6.2: Training of Bending Moment Random Decrements

Ship Speed: 4.1 knots Sig. Wave Height: 6 m Bretschneider Spectra

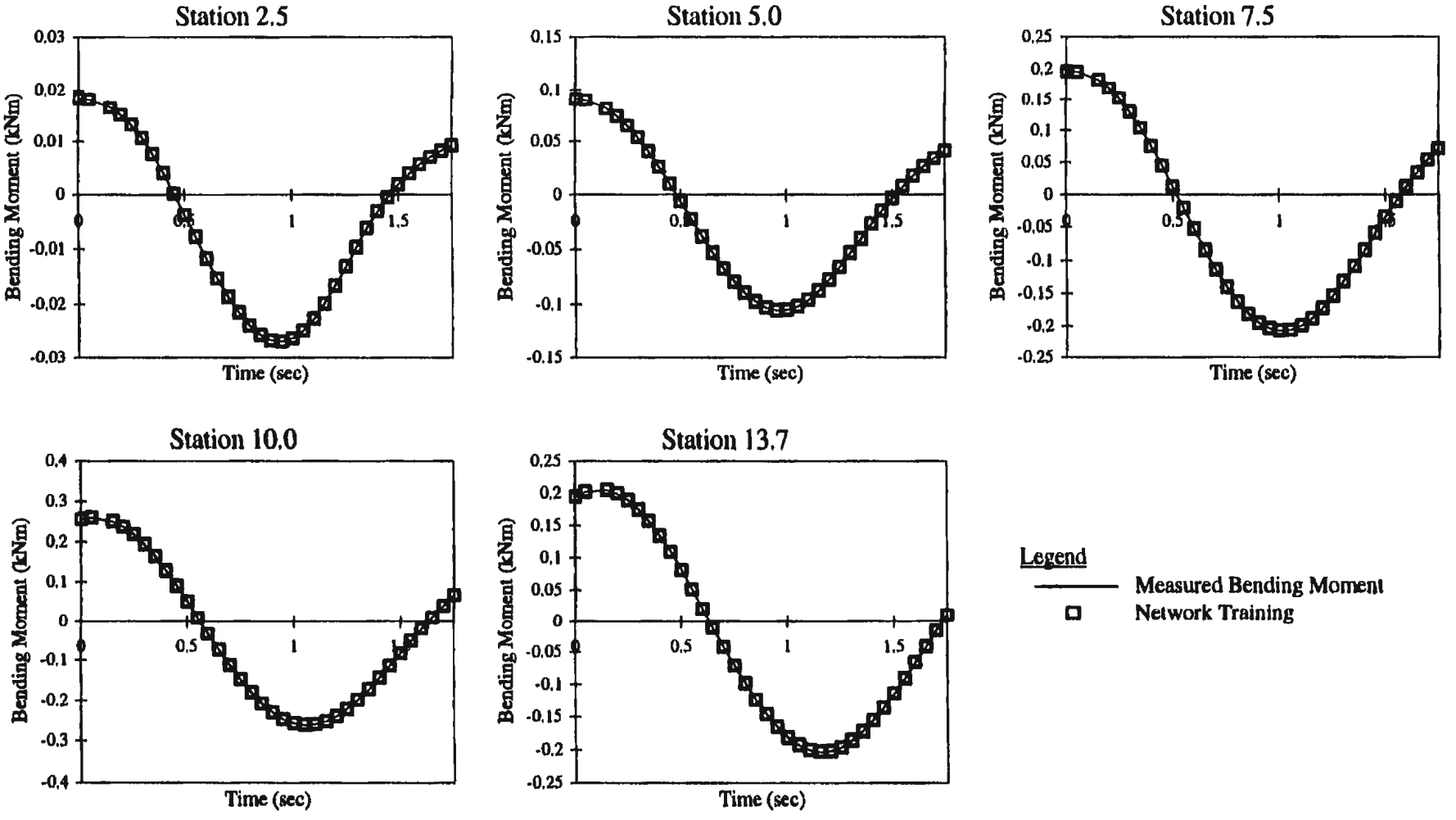

For the most part, the bending moment random decrement curves are very smooth and have no sharp changes in curvature. The only exception is the CPF at 17 knots, station 2.5 (Figure B11). Here, the random decrement has a sharp bend at its lower bound. However, the more important part of the curve, the upper bound, looks fine.

It should be noted that the bending moment random decrement curves are slightly different in shape between the Laker and CPF in the forward stations. Specifically, looking at the Laker, (Figure B3 - Station 2.0) and at the CPF, (Figure B9 - Station 5.0), we see that the Laker curve starts lower and then increases to its peak, while the CPF curve starts at its maximum and decreases. This demonstrates the phase difference between the heave displacement and the bending moment. Generally, for the CPF, the maximum bending moment occurred at the point of maximum heave, while in the forward section of the Laker, the maximum bending moment occurred slightly after the maximum heave.

The bending moment squared random decrement curves are also fairly smooth with no sharp changes in curvature. However, in a few cases, there is a clear double peak. This is especially evident in the forward sections of each ship. While no definitive reason has been found for this phenomenon, slamming may be a factor. The general shape of the random decrement curves is also highly similar between the two ships over the range of speeds.

6.2 Contribution

Contribution factors are a part of NeuroShell2® calculations. These factors give a rough measure of the importance of a particular variable in predicting the network's output. Contribution factors can only be compared within training sets, or different training of the same type of data in different conditions. Here, contribution factors are shown along the length of the ship to try and get an indication of which factor affects the response most.

Examples of contribution factors for the Laker and CPF are shown in Figures 6.3 and 6.4. The complete set of contribution factors can be found in Appendix C.

LAKER

Figure 6.3: Contibution Factor Vs. Station for Bending Moment

Ship Speed: 12.15 knots Sig. Wave Height: 6.1 m Bretschneider Spectra

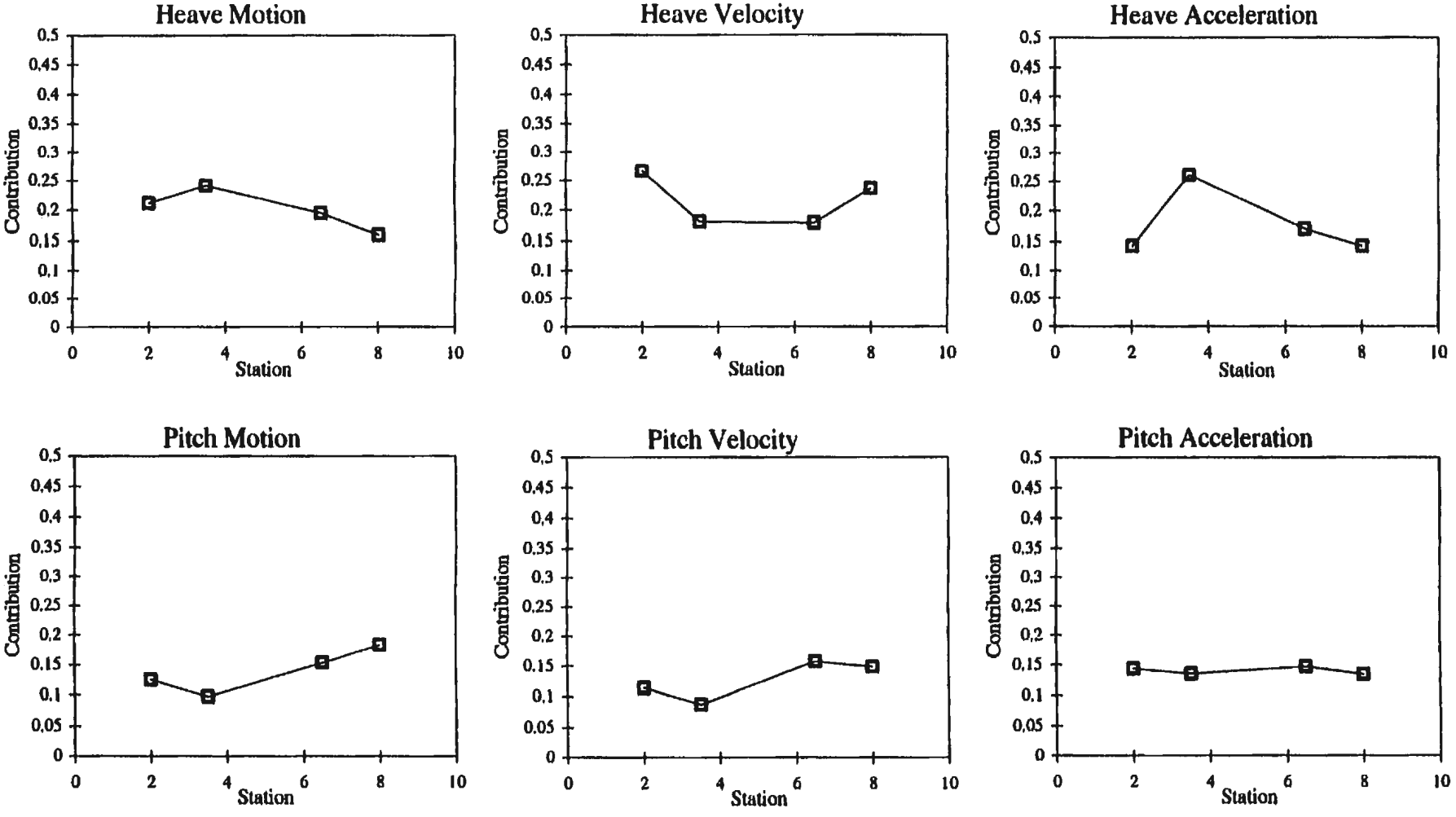

CPF

Figure 6.4: Contibution Factor Vs. Station for Bending Moment

Ship Speed: 4.1 knots Sig. Wave Height: 6 m Bretschneider Spectra

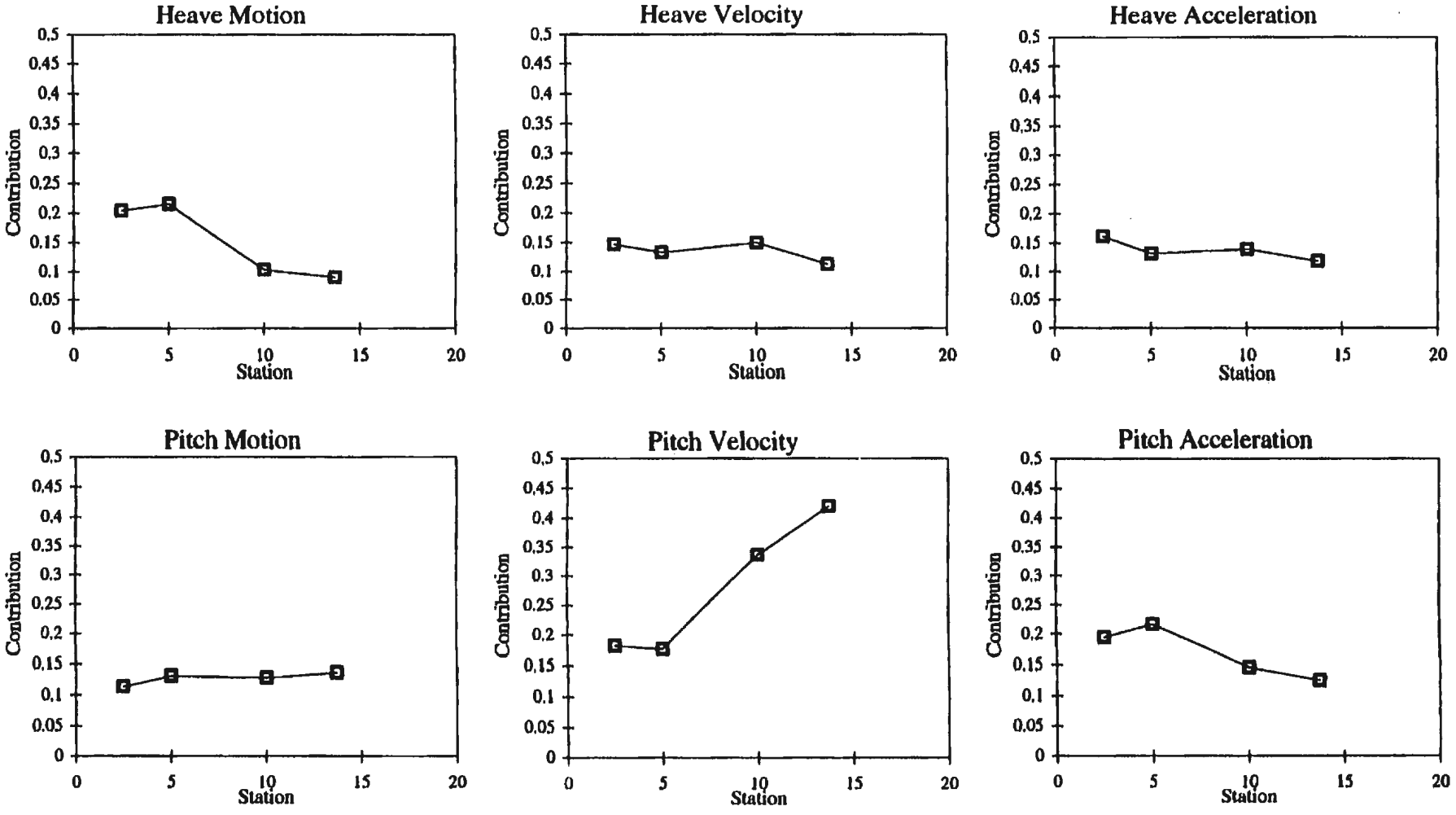

It is difficult to explain the contribution trends of the input responses to the bending moment and bending moment squared responses. However, broad generalizations based on the majority of the information are made.

For the most part, all six of the input responses appear to have a fairly equal contribution to the bending moment training. This contribution seems to fluctuate between 0.1 and 0.2 with a couple of exceptions. Most notably, the pitch velocity for the CPF at 4.1, 8.2 and 13.6 knots reaches just over a contribution of 0.3 at station 13.7 (Figures C5, C7 & C9). These higher contributions are reflected by a lower contribution in pitch acceleration that would appear to indicate that overall pitch response has a constant effect.

Over the length of the CPF, the heave displacement, heave velocity, heave acceleration and pitch displacement are fairly constant. The pitch velocity on the other hand appears to have a more important effect toward the middle and aft sections, while the pitch acceleration has a lesser effect to the aft. This pitch velocity trend is seen in the Laker, but to a much lesser degree. Also, the Laker's heave velocity has a lower contribution at midships, but a higher heave acceleration contribution. Again this would indicate that, like pitch, the overall heave response contribution is constant.

The same basic trends hold for the bending moment squared contribution factors. Overall response in pitch and heave appears to be fairly constant within a range of 0.1 to

0.2. The pitch displacement at 13.6 and 17 knots for the CPF is an exception (Figures C10 & C12). In both, the pitch contribution increases to 0.3 at station 13.7.

6.3 Prediction

To predict the bending moment and bending moment squared at a certain ship speed and wave height, the trained weights from the same ship speed and the trained wave heights are used. These trained weights are applied to the random decrements of the heave and pitch responses to produce the bending moment and bending moment squared responses. From these two predictions, the average bending moment and the variance of the bending moment are known. For example, to predict the bending moment and bending moment squared random decrements for the CPF at 4.1 knots, wave height 4.0 m and 5.0 m, the training from 4.1 knots, 6.0 m was used.

6.3.1 Laker

Example predictions for the Laker are shown in Figures 6.5. The experimental random decrements are also shown to demonstrate the accuracy of the prediction. The complete set of prediction plots is given in Appendix D.

LAKER

Figure 6.5: Prediction of Bending Moment Random Decrements

Ship Speed: 12.15 knots Sig. Wave Height: 3.05 m Bretschneider Spectra

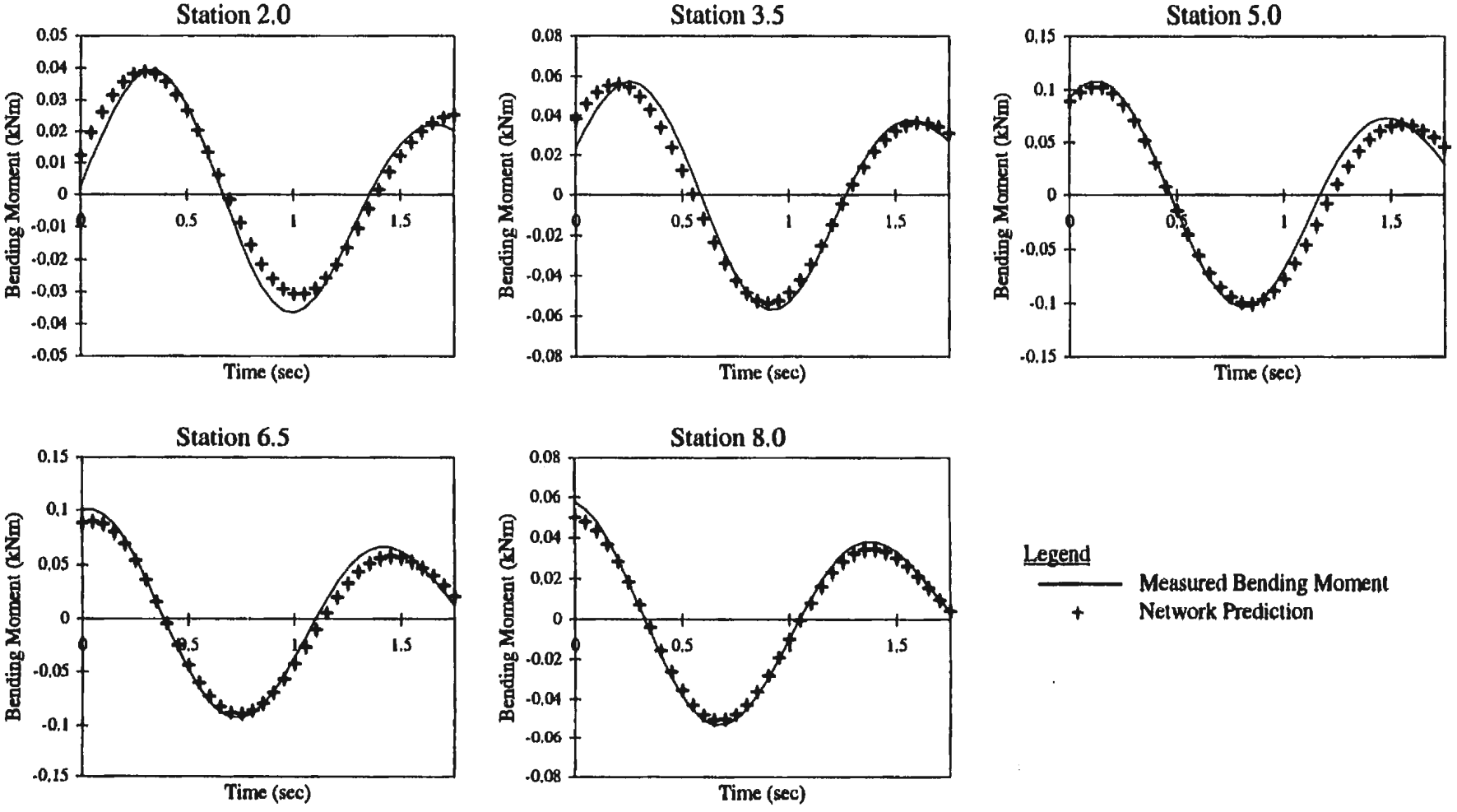

The predictions show a high degree of accuracy in the prediction of bending moment, particularly at the important maximum value. The random decrement trend and frequency are maintained, and the prediction is particularly good at stations 5 to 8. This also demonstrates the neural network has not been overtrained and can generalize.

The maximum bending moment values occurred at midships as expected, however there was appreciable moment in both station 2.0 and 8.0. In both cases, the bending moment was on the order of 25% to 50% that of the midships bending moment. It should also be noted the maximum and minimum values are fairly symmetrical about the zero value. This indicates near equal dynamic bending moment in both directions.

The bending moment squared prediction isn't as accurate as the bending moment. However, the general shape of the random decrement curve is maintained, and the maximum value and frequency is reasonably well predicted. It is also noted, that the maximum value is never under-predicted with the better predictions near the midships area. This poorer prediction indicates the assumption of neglecting the wave squared term and allowing it to be implicitly present in the motion measurements may not be entirely accurate.

6.3.2 CPF

Example predictions for the CPF are presented in Figure 6.6. As with the Laker, the entire set of predictions can be found in Appendix D.

CPF

Figure 6.6: Prediction of Bending Moment Random Decrements

Ship Speed: 4.1 knots Sig. Wave Height: 4 m Bretschneider Spectra

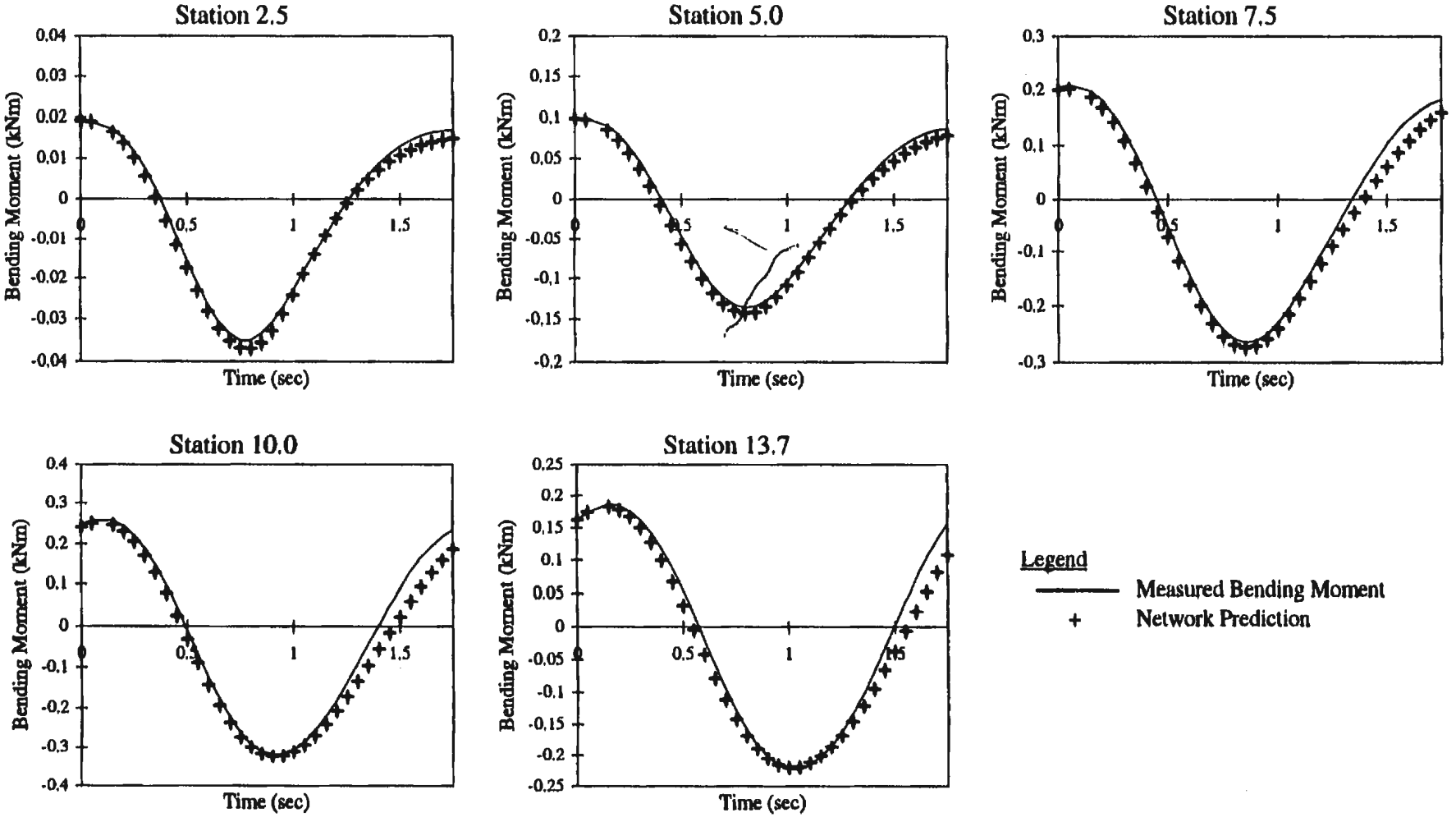

As with the Laker, these predictions show a fairly high degree of accuracy in the prediction of bending moment, particularly at the lower speeds. As the speed of the ship increases, the predictions at the forward stations begins to get a little worse in the latter half of the random decrement curve. However, the important maximum value at the beginning of each curve is well predicted. It is suspected that ship slamming is the underlying cause.

Again, similar to the Laker, the bending moment squared predictions are not as accurate as the bending moment. At the lower speed of 4.1 knots (Figures D6 & D8), the prediction is very good with both the curve trends and maximum values maintained. At 8.2 knots, (Figures D10 & D12) the prediction is fairly good. However, the double peak that was trained into the forward sections is reproduced in the prediction, but doesn't exist in the measured random decrement. Also, the predicted maximum values at the 4-metre wave height are about 20% off at stations 5 and 13.7.

For the speeds of 13.6 and 17 knots, the bending moment squared prediction is still generally reasonable. The curve trends are maintained, but again the double peak that was trained into the network at the forward sections is reproduced in the prediction. Interestingly enough, the maximum values are well predicted at 17 knots, but poorly predicted in the forward sections at 13 knots, especially at the lower wave height. This gives further evidence that ship slamming is the cause of the larger predicted maximum value.

It is possible that, at the trained wave height of 6 m, slamming occurred, and the bending moment reflected the presence of slamming. At 17 knots in the lower wave heights, slamming still occurred, so the prediction was accurate. However, at 8.2 and 13.6 knots, slamming in the lower wave heights may not have been as much of a factor, resulting in the poorer prediction. Regardless, this would tend to conservatively predict the bending moment, assuming the training was always done at the higher wave height.

7.0 Conclusions

The bending moment has been successfully predicted from the heave and pitch response in a full form bulk carrier and a slender form frigate. In the prediction, no knowledge of the wave excitation level was required. Thus the random decrement method can be confidently used to monitor and predict ship stress, assuming the weights of the neural network are pre-known. This system could also be used to evaluate the historical bending moment experienced by a ship where past heave and pitch measurements have been made.

From a design standpoint, the random decrement predictions could be used to develop bending moment distributions, along a ship's length, from predicted heave and pitch motion distributions. These distributions could then be used in probability failure analysis.

This can be done in one of two ways. Firstly, there is what is known as the auto-correlation function. This function is exactly the same as the random decrement multiplied by a constant. By using a calibration, this constant could be determined. Once the auto-correlation function is known, its maximum value is the variance of the bending moment. Considering that the bending moment is a narrow band process, the variance is basically the square of the amplitude of a sinusoidal expression. The random decrement of the bending moment squared can then be used to determine the range of error in the

expressions amplitude. The main frequency of the sinusoidal expression can be measured by the time difference between zero crossings in the random decrement.

Secondly, the random decrement predictions of bending moment and bending moment squared could be used to determine the mean and variance of the bending moment by assuming a suitable distribution for the bending moment. This distribution would be best assumed to be similar to the heave or pitch motion distribution, since all are a function of the wave spectrum the vessel is experiencing.

The advantage of this method over others is that the wave doesn't need to be known for accurate results. Thus, predictions can be made on full-scale vessels in real time with little instrumentation. While the bending moment squared predictions were not as accurate as hoped, they were still within 10% of the measured values.

It is noted that the training and predictions were done within a constant speed. Further work could attempt to determine the forward speed effect, which would allow successful cross speed predictions.

8.0 References

1. Lewis, Edward V. , Editor, "Principles of Naval Architecture" Volume I. The Society of Naval Architects and Marine Engineers, 1988.

2. Buckley, William H., "The Determination of Ship Loads and Motions: A Recommended Engineering Approach", Naval Engineers Journal, Vol. 102, No. 3, May 1990, pp. 209-227.

3. Vulovich, Rod. Hirayama, Toshitsugu. Toki, Naoji. And Mizuno, Hiroyuki. "Characteristics of Hull Stresses Measured on a Large Containership in Rough Seas". SNAME Transactions, Vol. 97, 1989, pp. 397-428.

4. Guedes Soares, C. and Schellin, T. E. "Nonlinear Effects on Long Term Distributions of Wave Induced Loads for Tankers" Proceedings of the Fifteenth International Conference on Offshore Mechanics and Arctic Engineering, Vol. II, 1996, pp. 79-85.

5. Chiu, Forng-chen and Fujino, Masataka "Nonlinear Prediction of Vertical Motions and Wave Loads of High-speed Crafts in Head Seas" Int. Shipbuilding Progress, Vol. 36, no. 406, 1989, pp. 193-232.

6. Chan, H. S. "On the Calculation of Ship Motions and Wave Loads of High-speed Catamarans" Int. Shipbuilding Progress, Vol. 42, no. 431, 1995, pp.181-195.

7. Haddara, M. R., Wishahy, M., Wu, X. "Assesment of Ship's Tranverse Stability at Sea" Ocean Engineering, Vol. 21, no. 8, 1994, pp. 781-800.

8. Ibrahim, S. R., "Random Decrement Techniques for Modal Identification of Structures", The AIAA Journal of Space-Craft, Col. 14, no. 11, 1977, pp. 696-700.

9. Haddara, M. R., "On the Use of Neural Network Techniques for the Identification of Ship Stability Parameters at Sea", Proceedings of the Fourteenth International Conference on Offshore Mechanics and Arctic Engineering, Vol. II, Copenhagen, Denmark, pp. 127-135.

10. Hermanski, G., "Model Experiments to Determine Wave Induced Bending Moment on a Great Lakes Bulk Carrier" IMD report TR-1993-02, October 1992.

11. Datta, I., Hermanski, G., Molyneux, D., and Rogers, F. "CPF Hydro-Elastic Model Tests in Severe Seas: Phase I – Head Seas Tests in the Towing Tank" IMD Reoprt Tr-1993-17, September 1993.

Appendix A: Motion Random Decrements

LAKER

Figure A1: Motion Random Decrements

Ship Speed: 12.15 knots Sig. Wave Height: 3.05 m Bretschneider Spectra

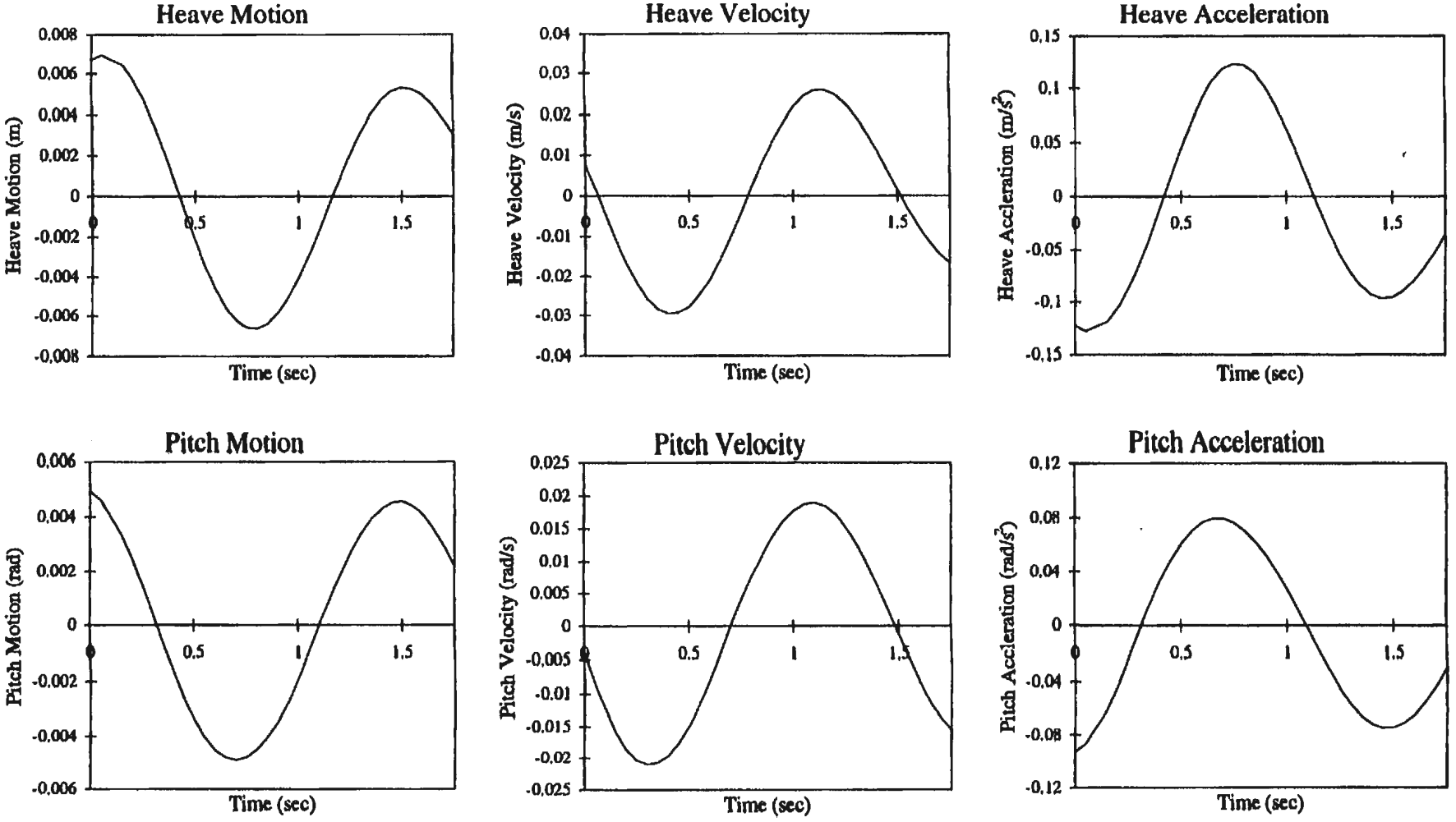

LAKER

Figure A2: Motion Random Decrements

Ship Speed: 12.15 knots Sig. Wave Height: 6.1 m Bretschneider Spectra

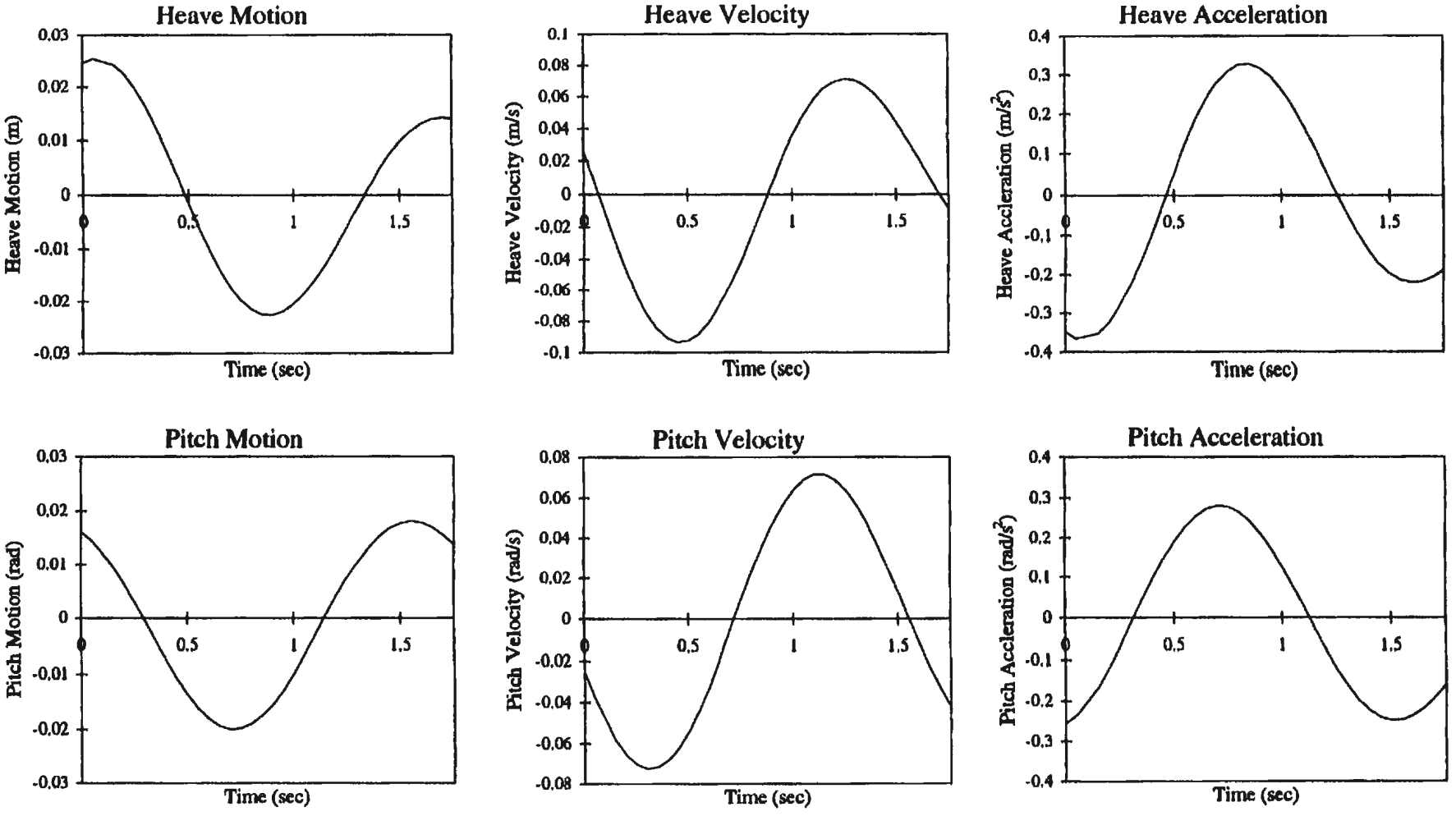

LAKER

Figure A3: Motion Random Decrements

Ship Speed: 14.76 knots Sig. Wave Height: 3.05 m Bretschneider Spectra

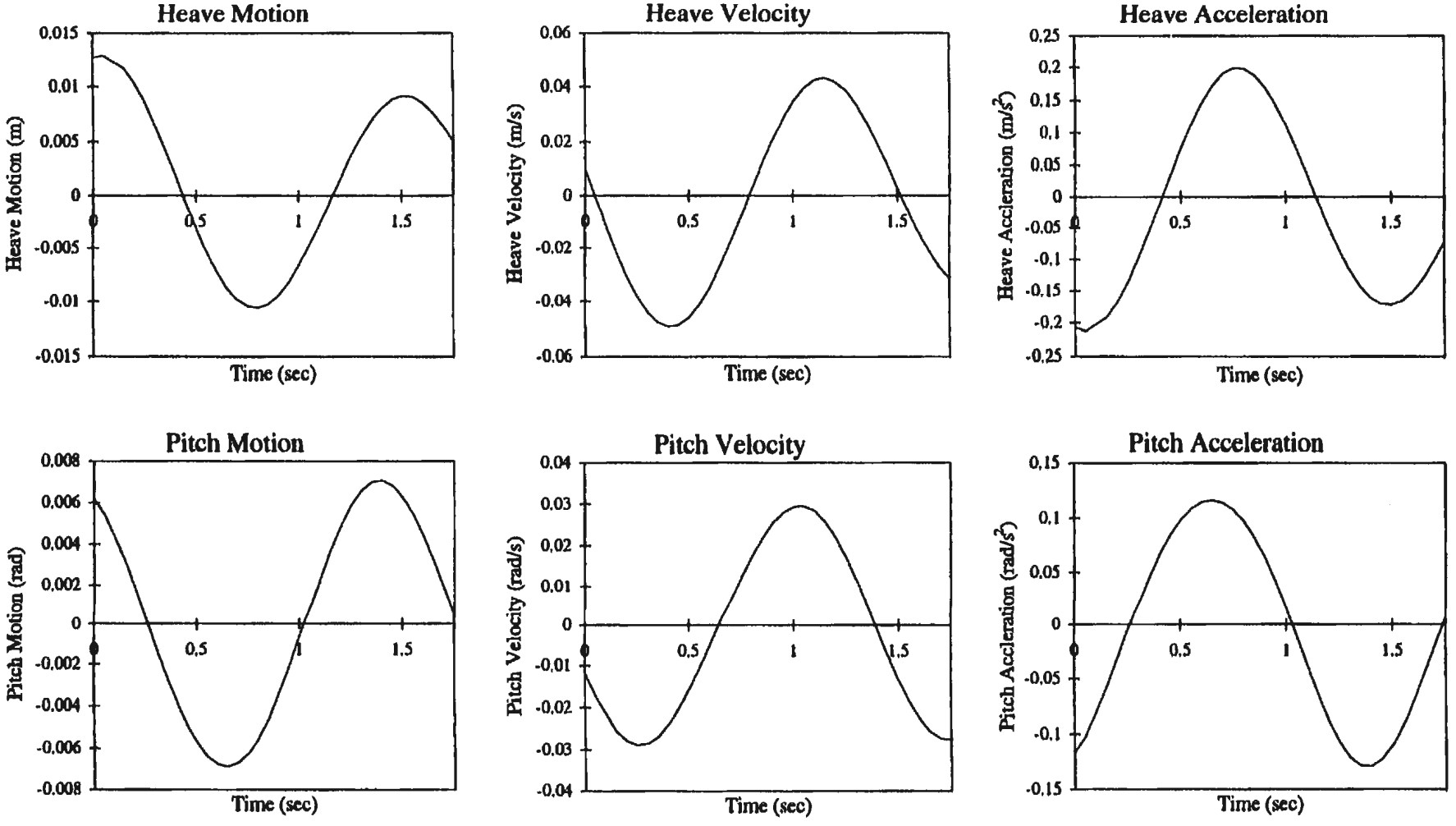

LAKER

Figure A4: Motion Random Decrements

Ship Speed: 14.76 knots Sig. Wave Height: 6.1 m Bretschneider Spectra

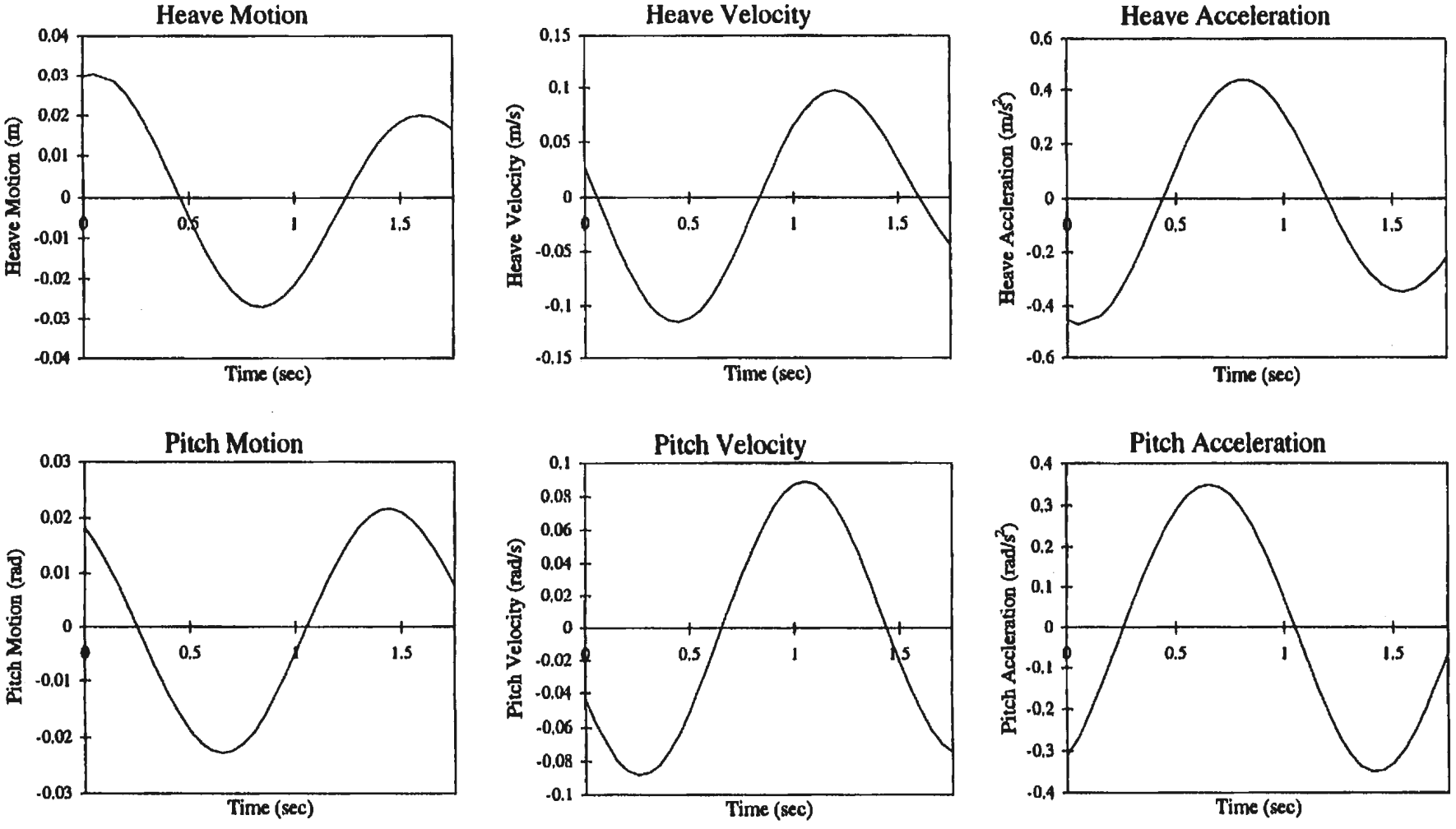

CPF

Figure A5: Motion Random Decrements

Ship Speed: 4.1 knots Sig. Wave Height: 4 m Bretschneider Spectra

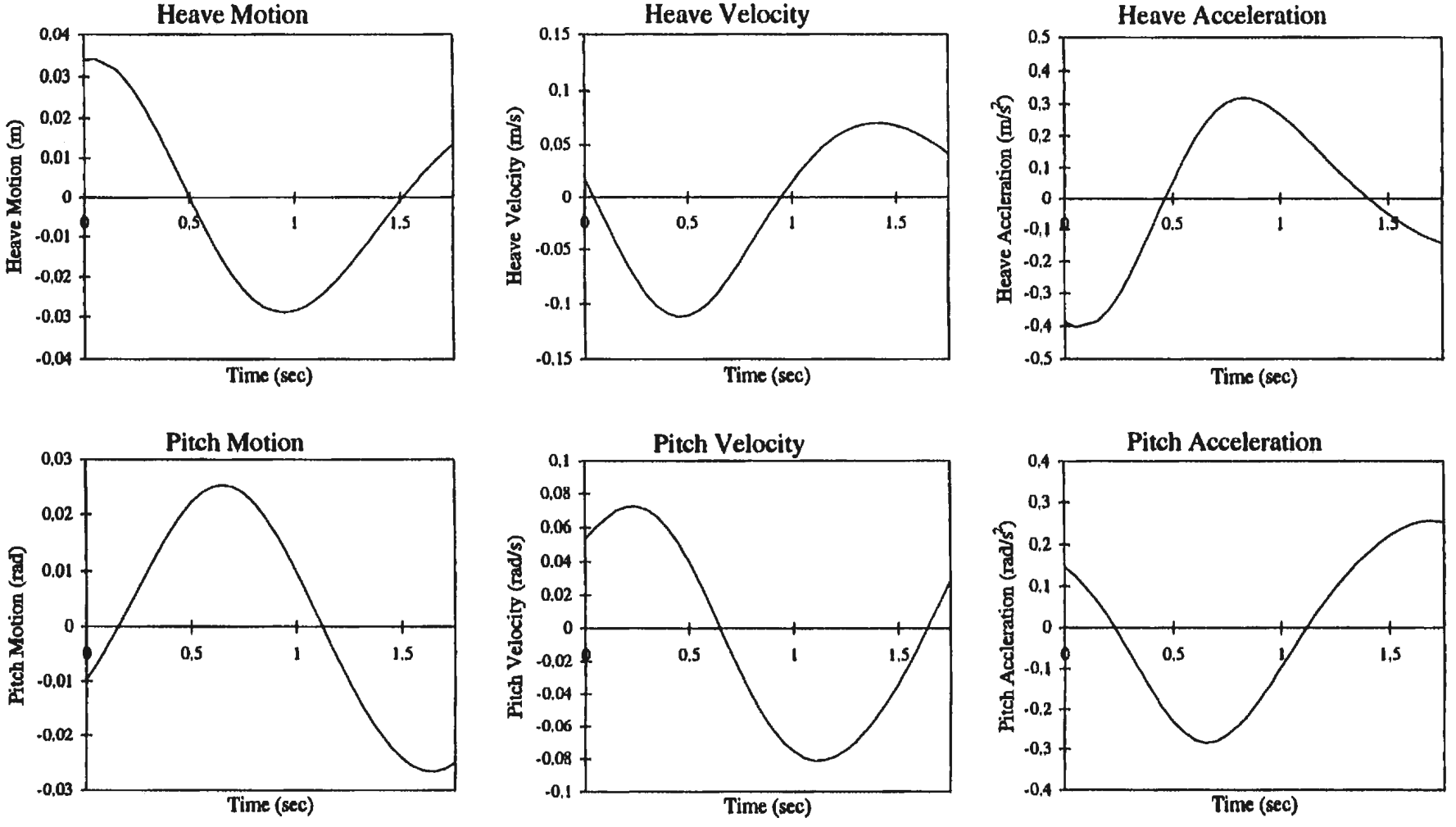

CPF

Figure A6: Motion Random Decrements

Ship Speed: 4.1 knots Sig. Wave Height: 5 m Bretschneider Spectra

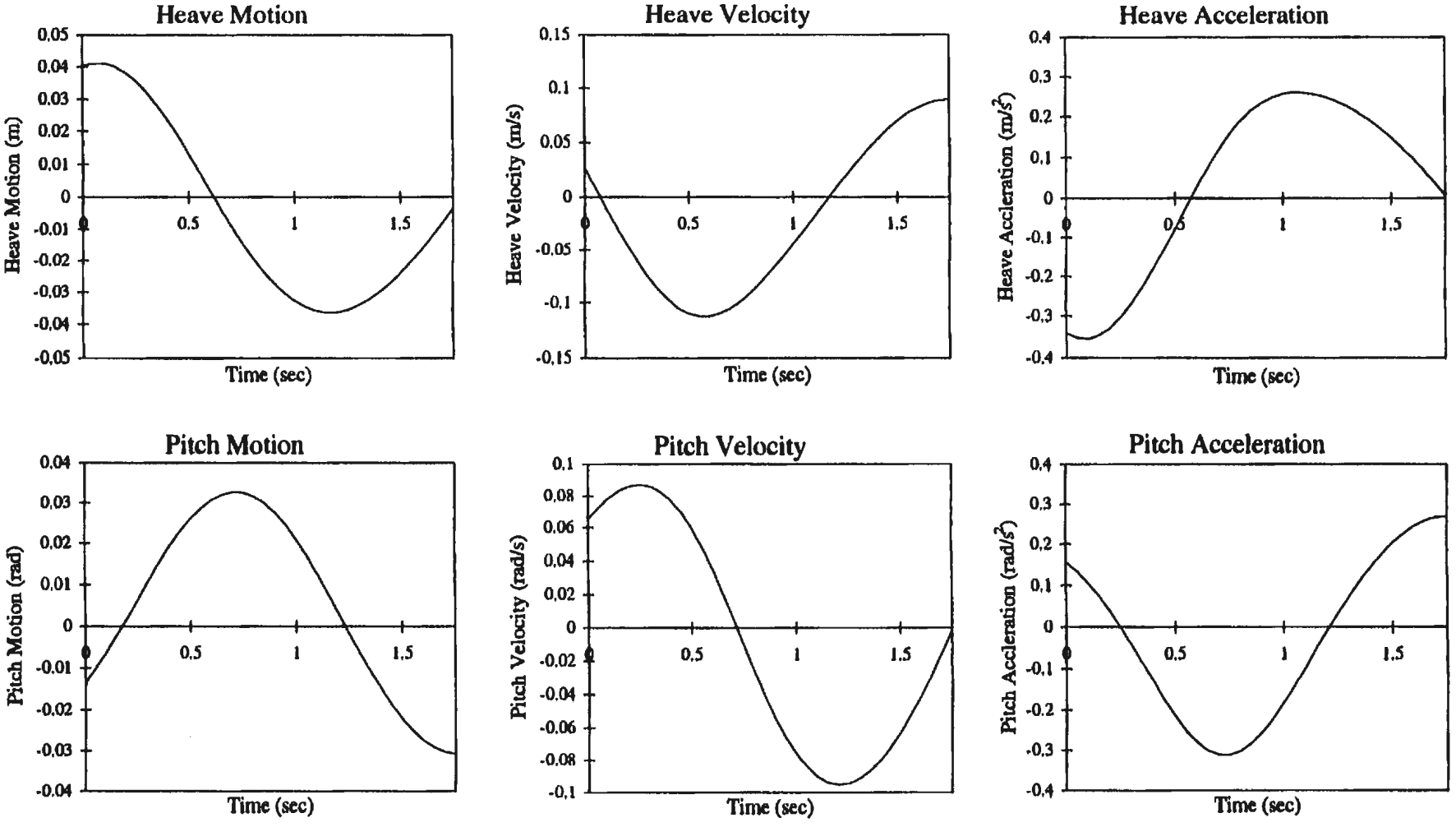

CPF

Figure A7: Motion Random Decrements

Ship Speed: 4.1 knots Sig. Wave Height: 6 m Bretschneider Spectra

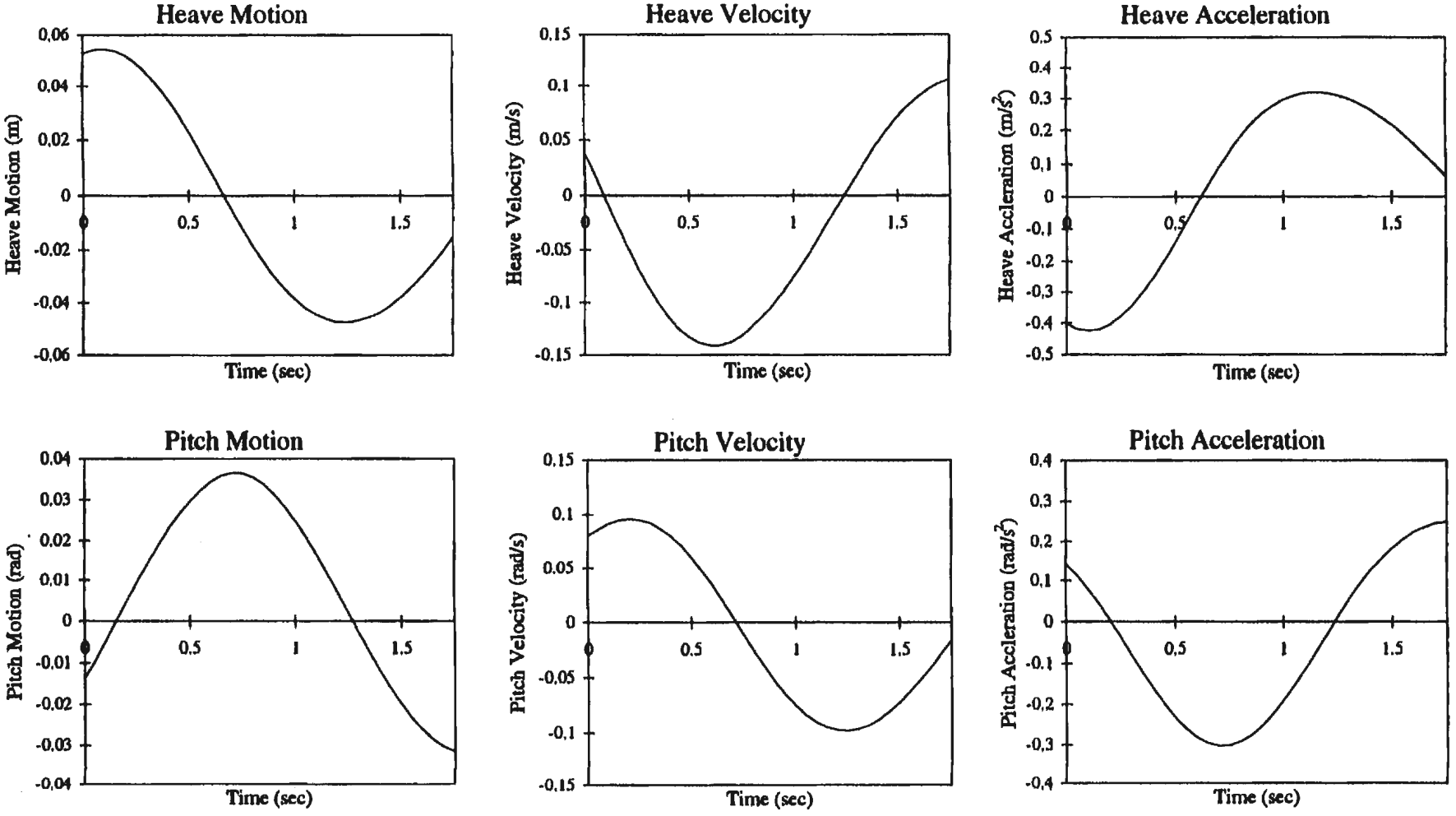

CPF

Figure A8: Motion Random Decrements

Ship Speed: 8.2 knots Sig. Wave Height: 4 m Bretschneider Spectra

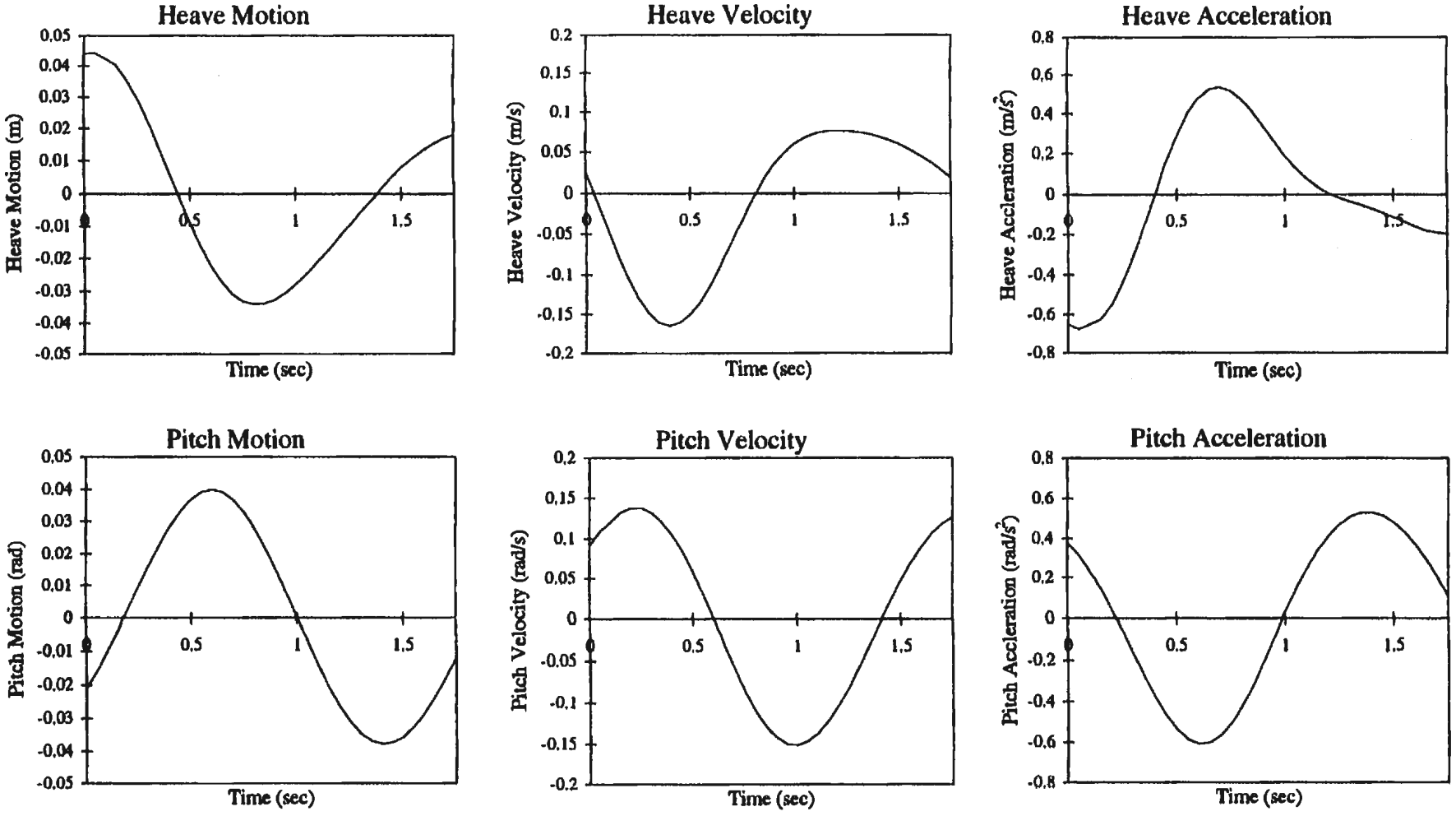

CPF

Figure A9: Motion Random Decrements

Ship Speed: 8.2 knots Sig. Wave Height: 5 m Bretschneider Spectra

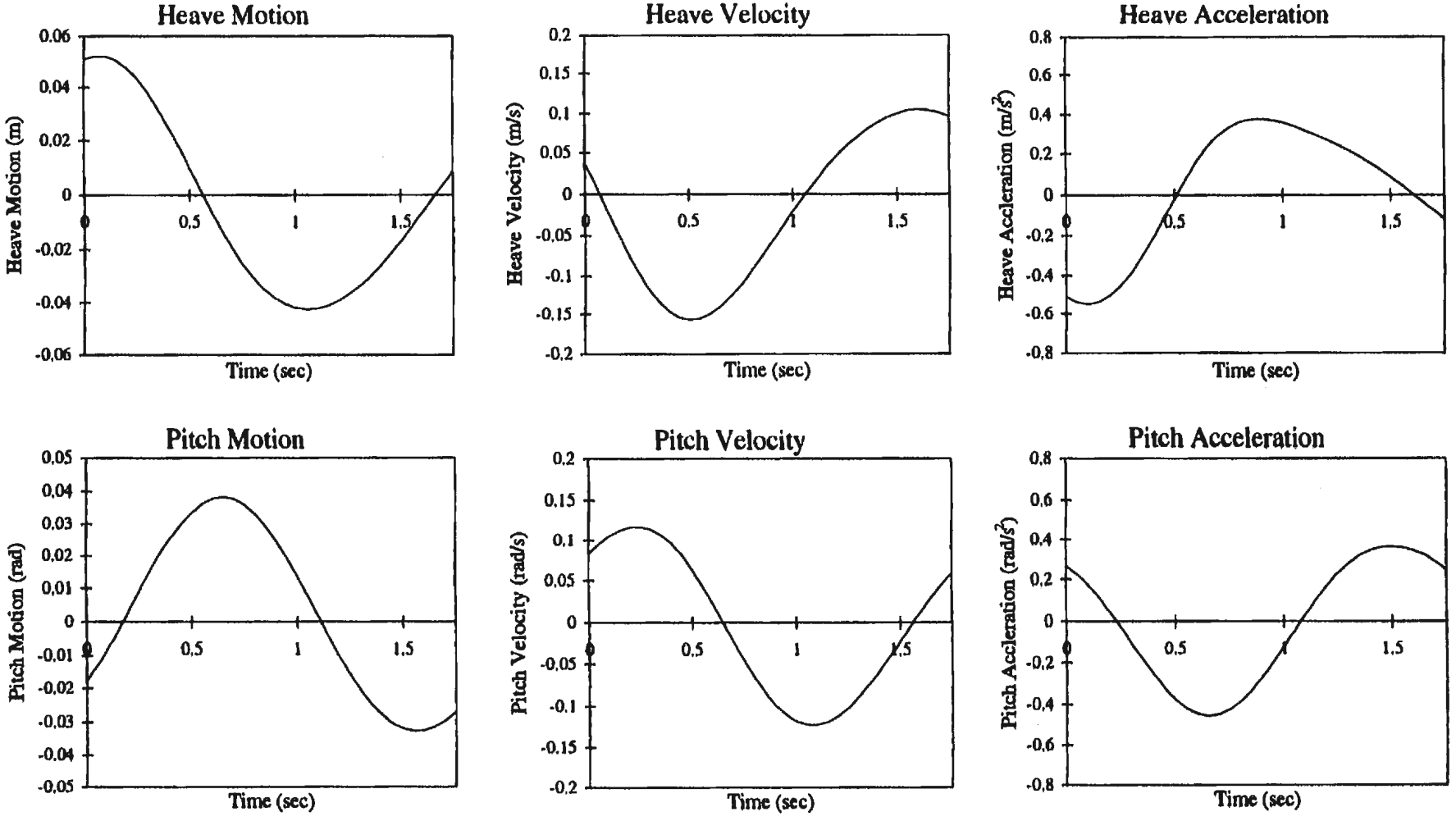

CPF

Figure A10: Motion Random Decrements

Ship Speed: 8.2 knots Sig. Wave Height: 6 m Bretschneider Spectra

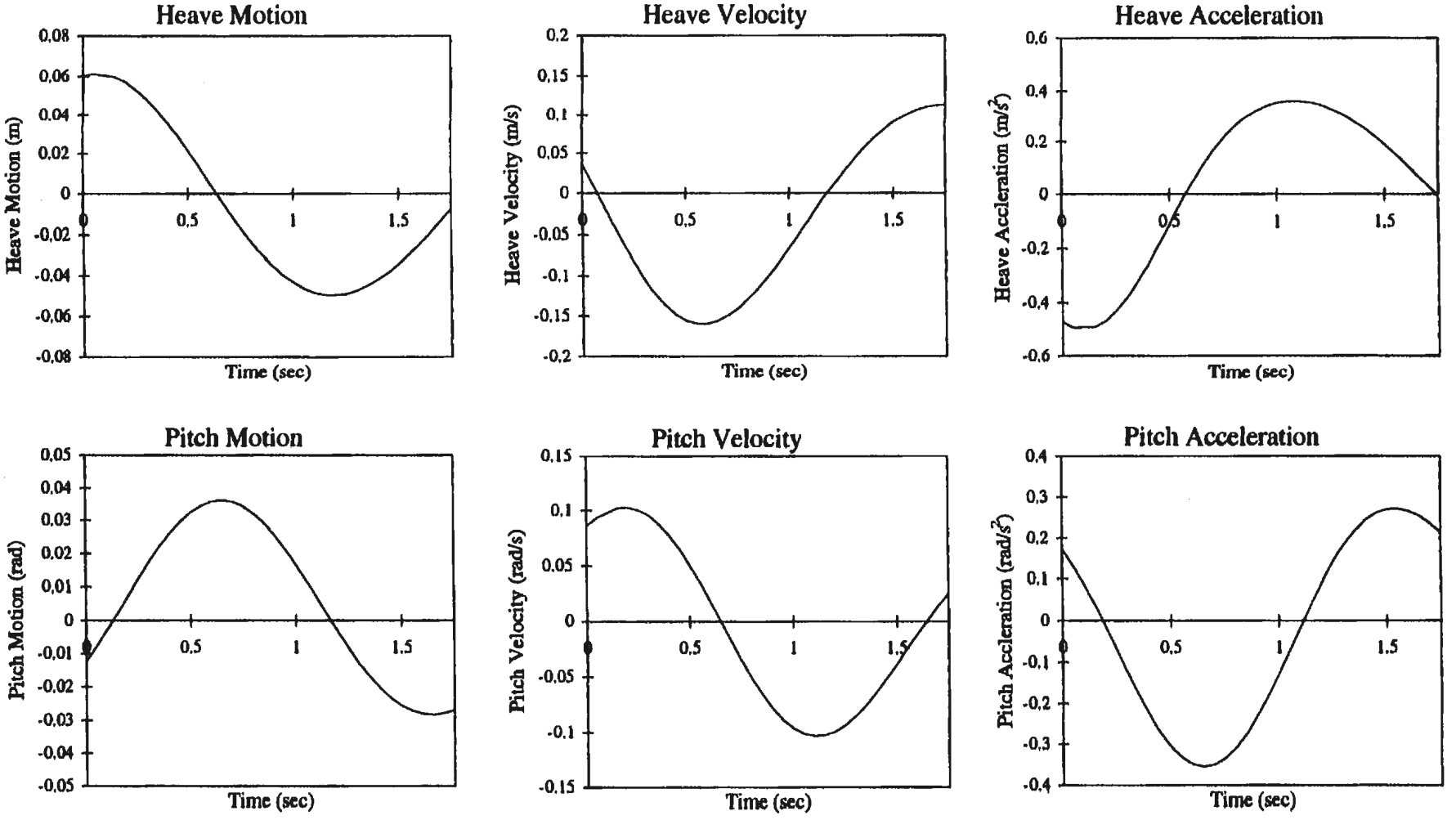

CPF

Figure A11: Motion Random Decrements

Ship Speed: 13.6 knots Sig. Wave Height: 4 m Bretschneider Spectra

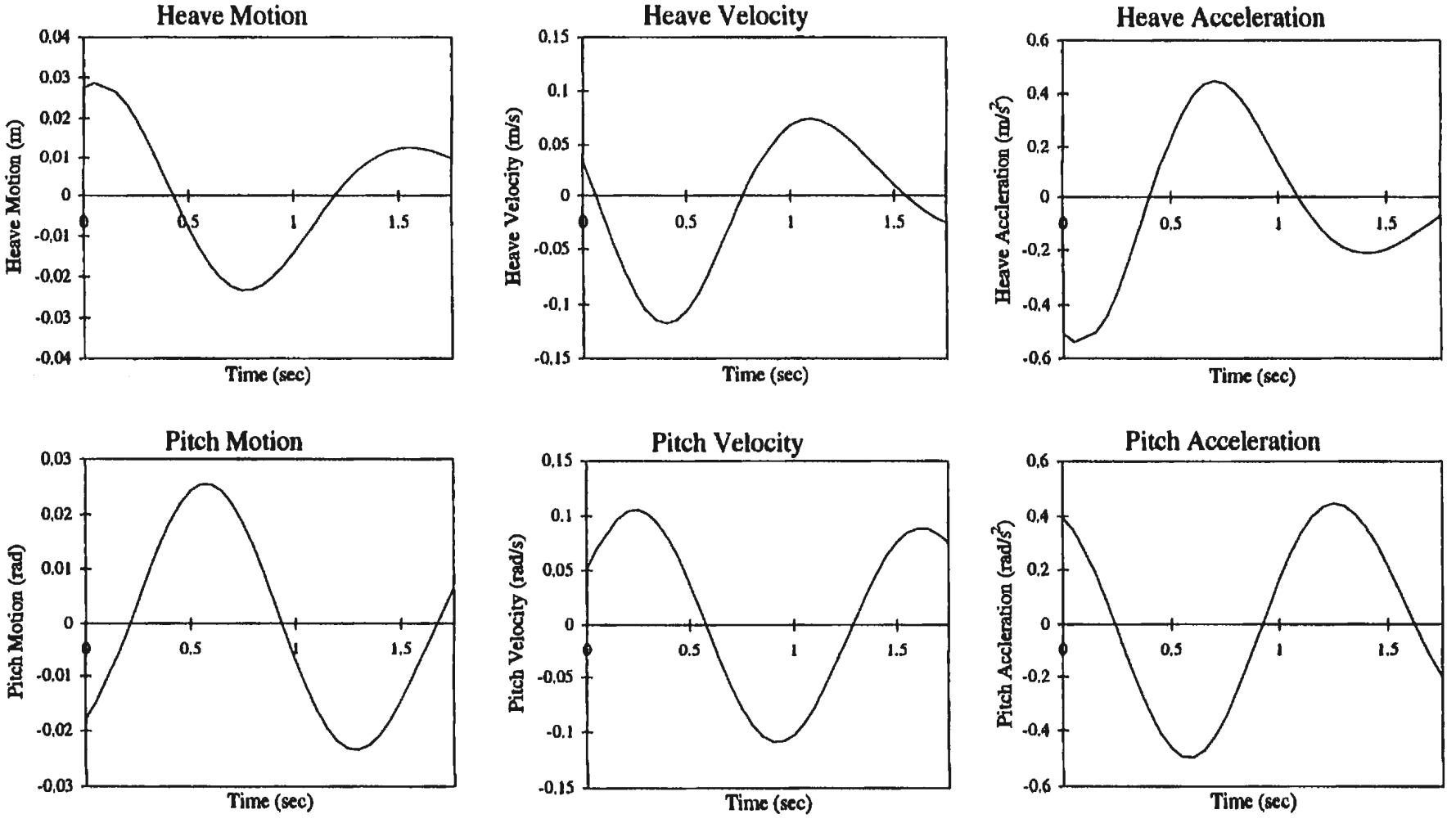

CPF

Figure A12: Motion Random Decrements

Ship Speed: 13.6 knots Sig. Wave Height: 5 m Bretschneider Spectra

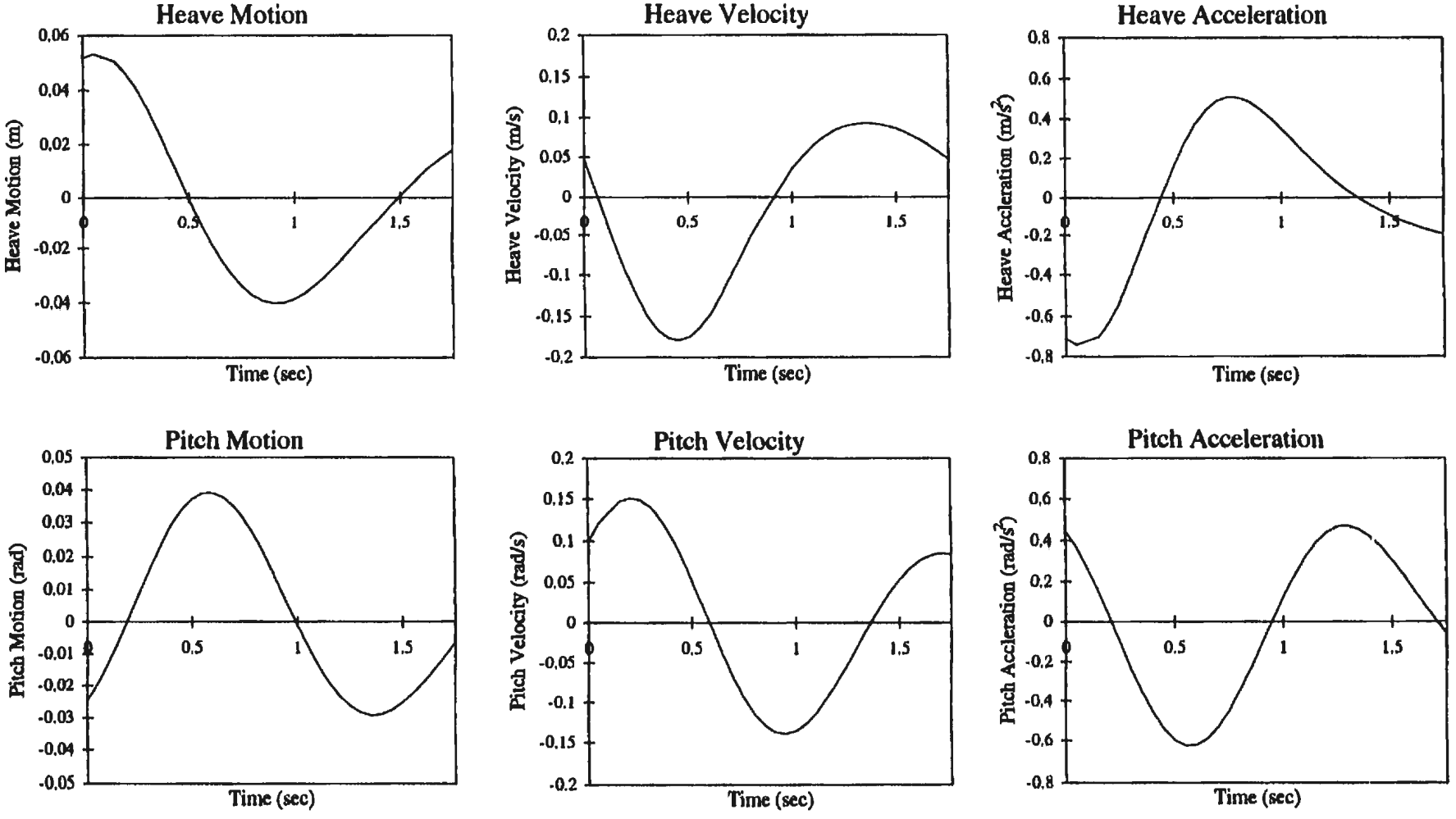

CPF

Figure A13: Motion Random Decrements

Ship Speed: 13.6 knots Sig. Wave Height: 6 m Bretschneider Spectra

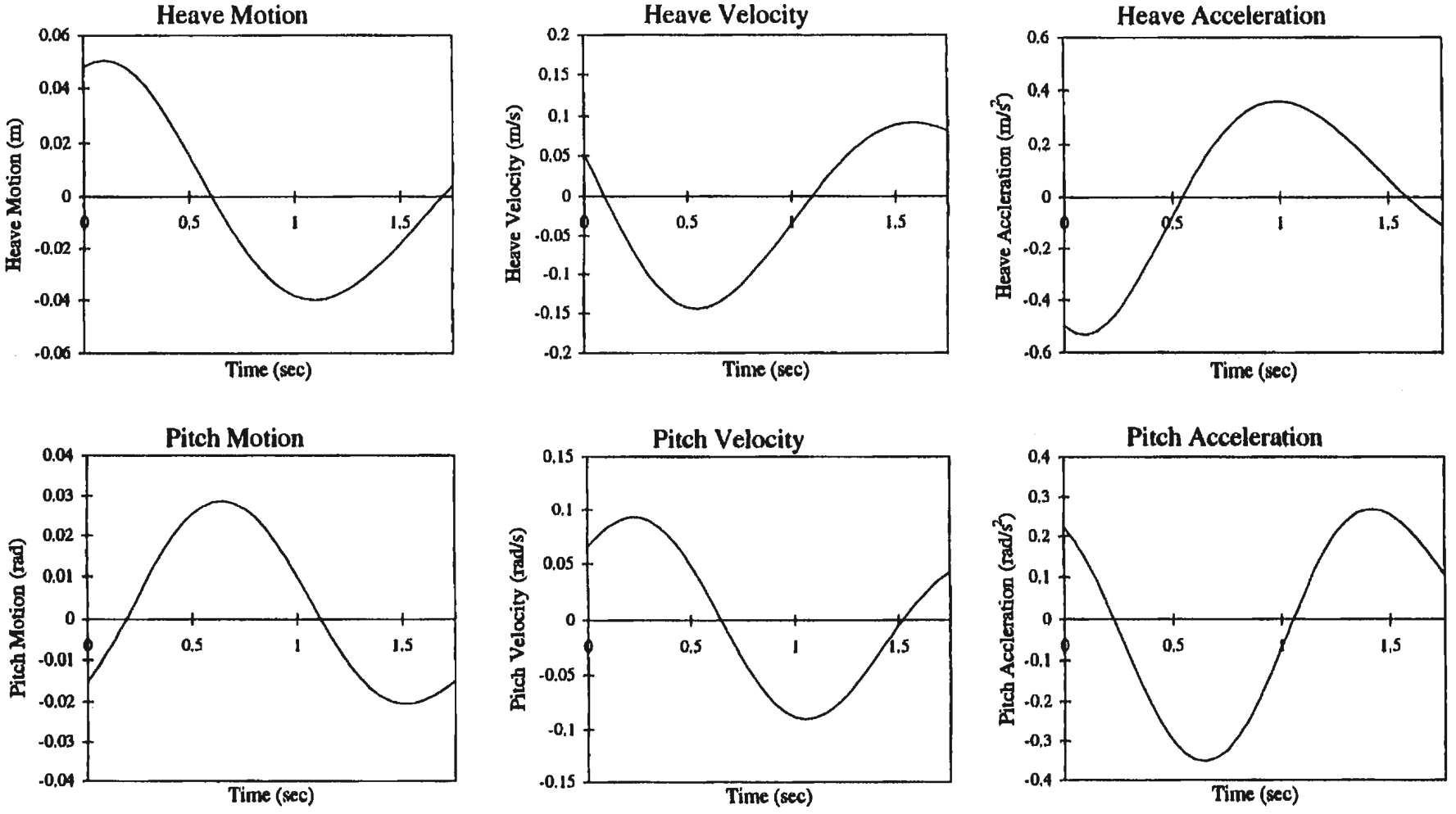

CPF

Figure A14: Motion Random Decrements

Ship Speed: 17 knots Sig. Wave Height: 4 m Bretschneider Spectra

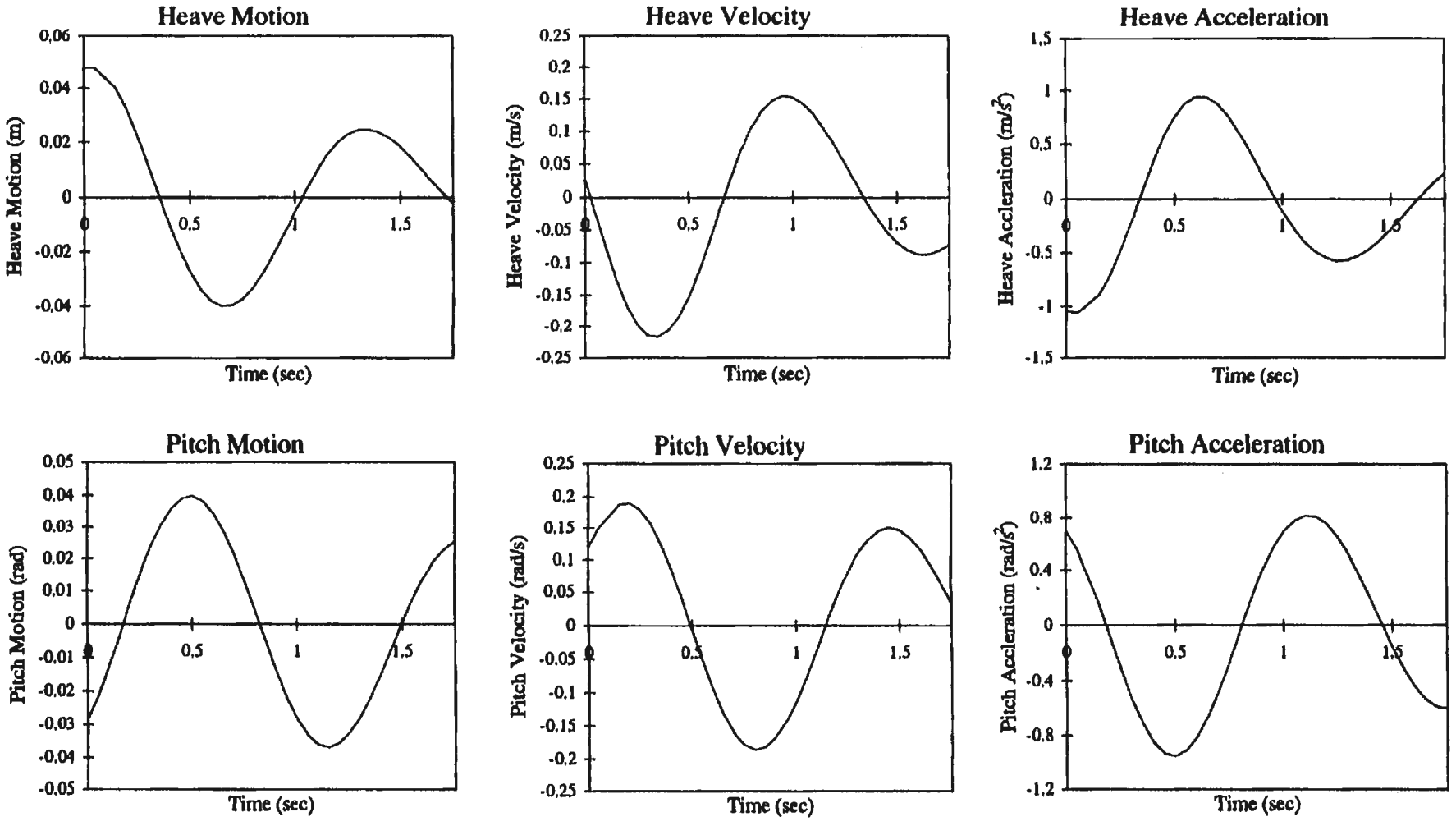

CPF

Figure A15: Motion Random Decrements

Ship Speed: 17 knots Sig. Wave Height: 5 m Bretschneider Spectra

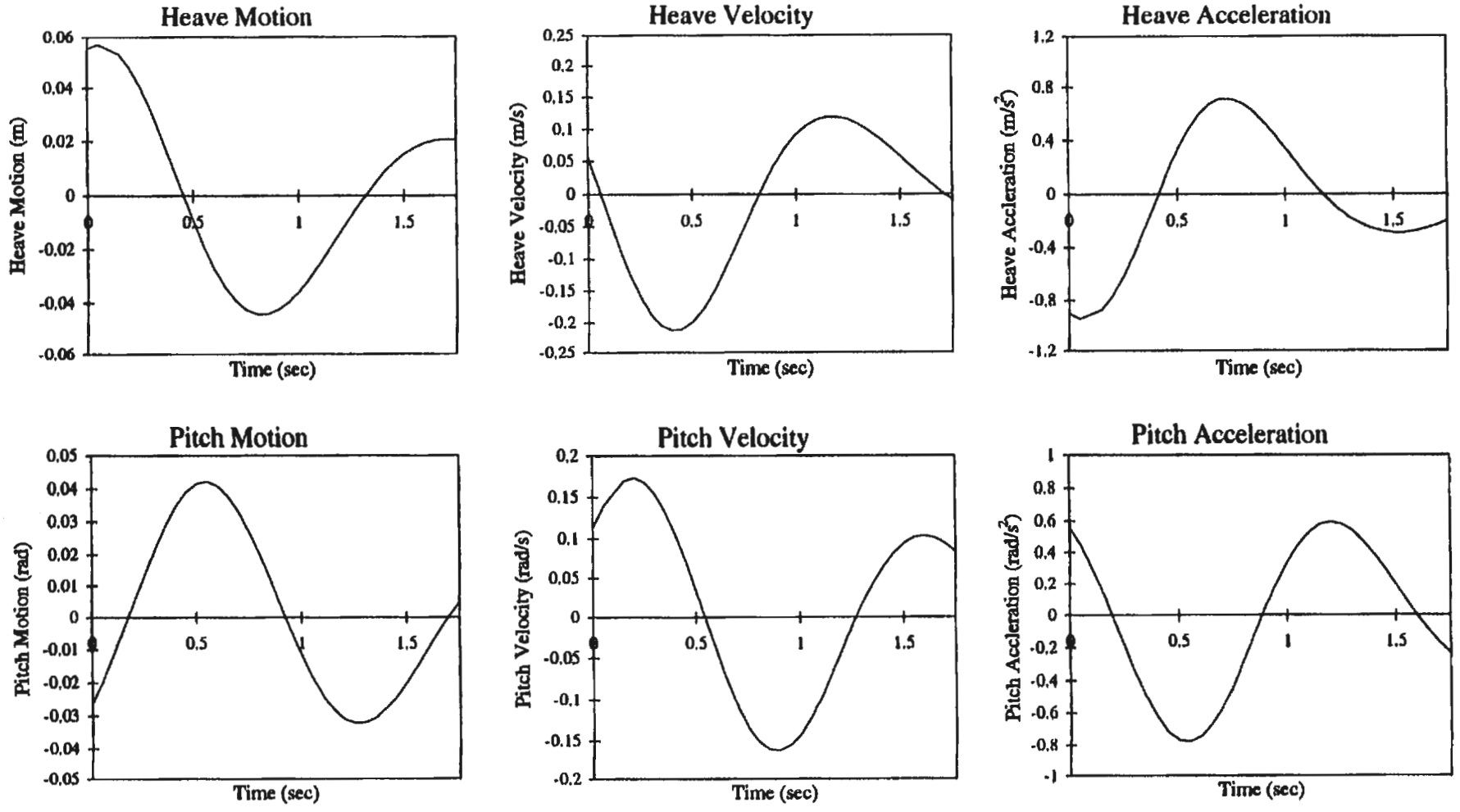

CPF

Figure A16: Motion Random Decrements

Ship Speed: 17 knots Sig. Wave Height: 6 m Bretschneider Spectra

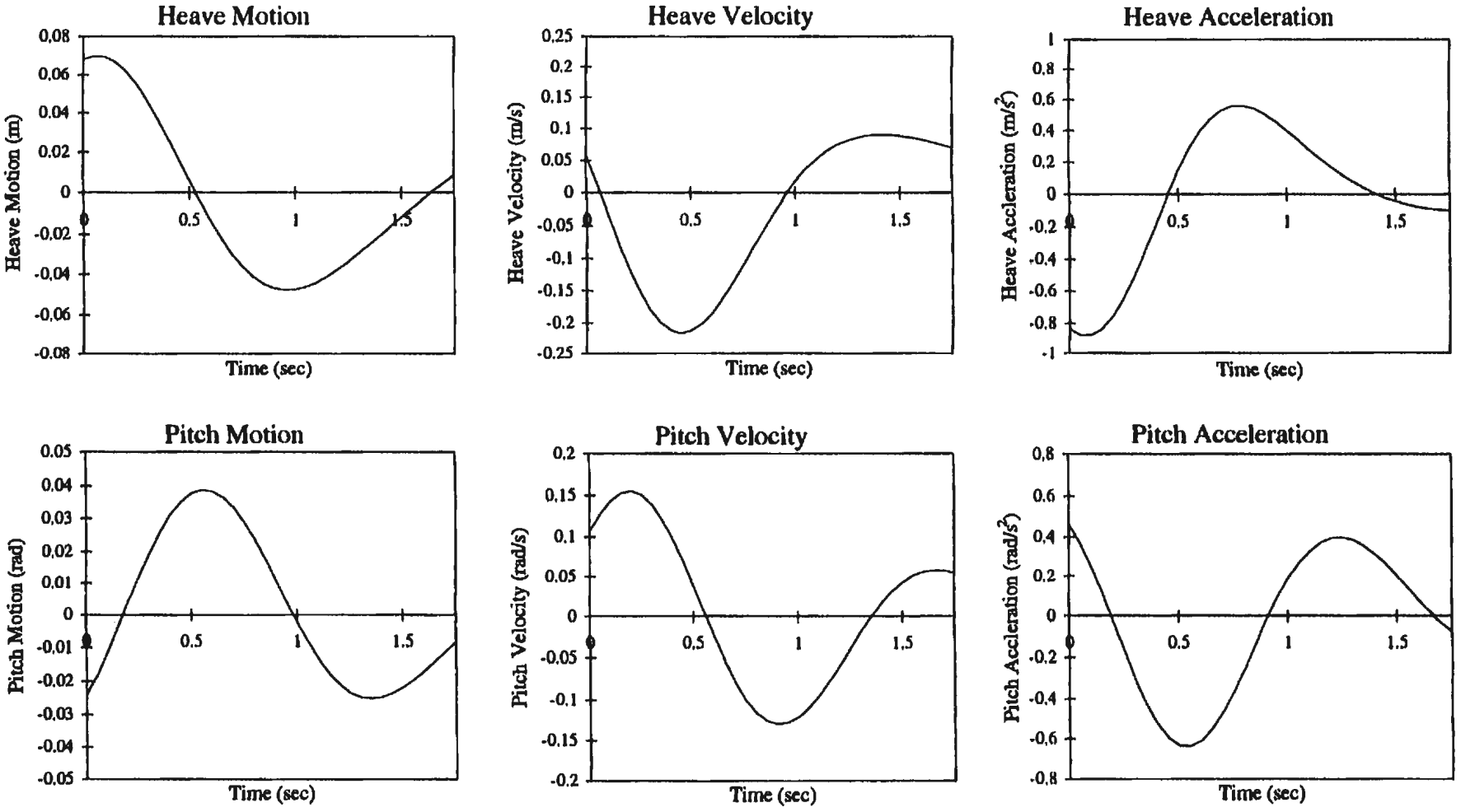

Appendix B: Motion Random Training

LAKER

Figure B1: Training of Bending Moment Random Decrements

Ship Speed: 12.15 knots Sig. Wave Height: 6.1 m Bretschneider Spectra

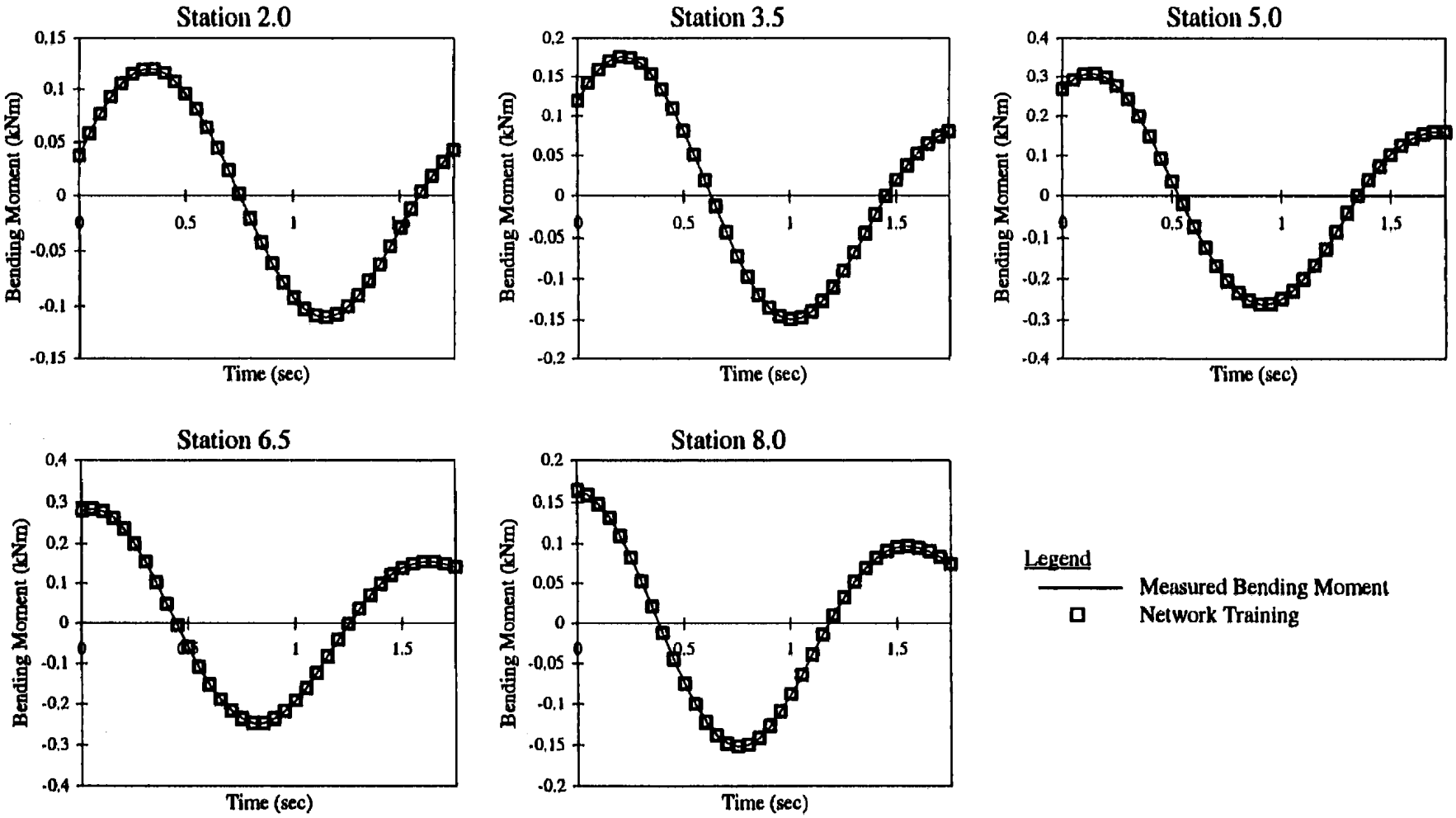

LAKER

Figure B2: Training of Bending Moment^2 Random Decrements

Ship Speed: 12.15 knots Sig. Wave Height: 6.1 m Bretschneider Spectra

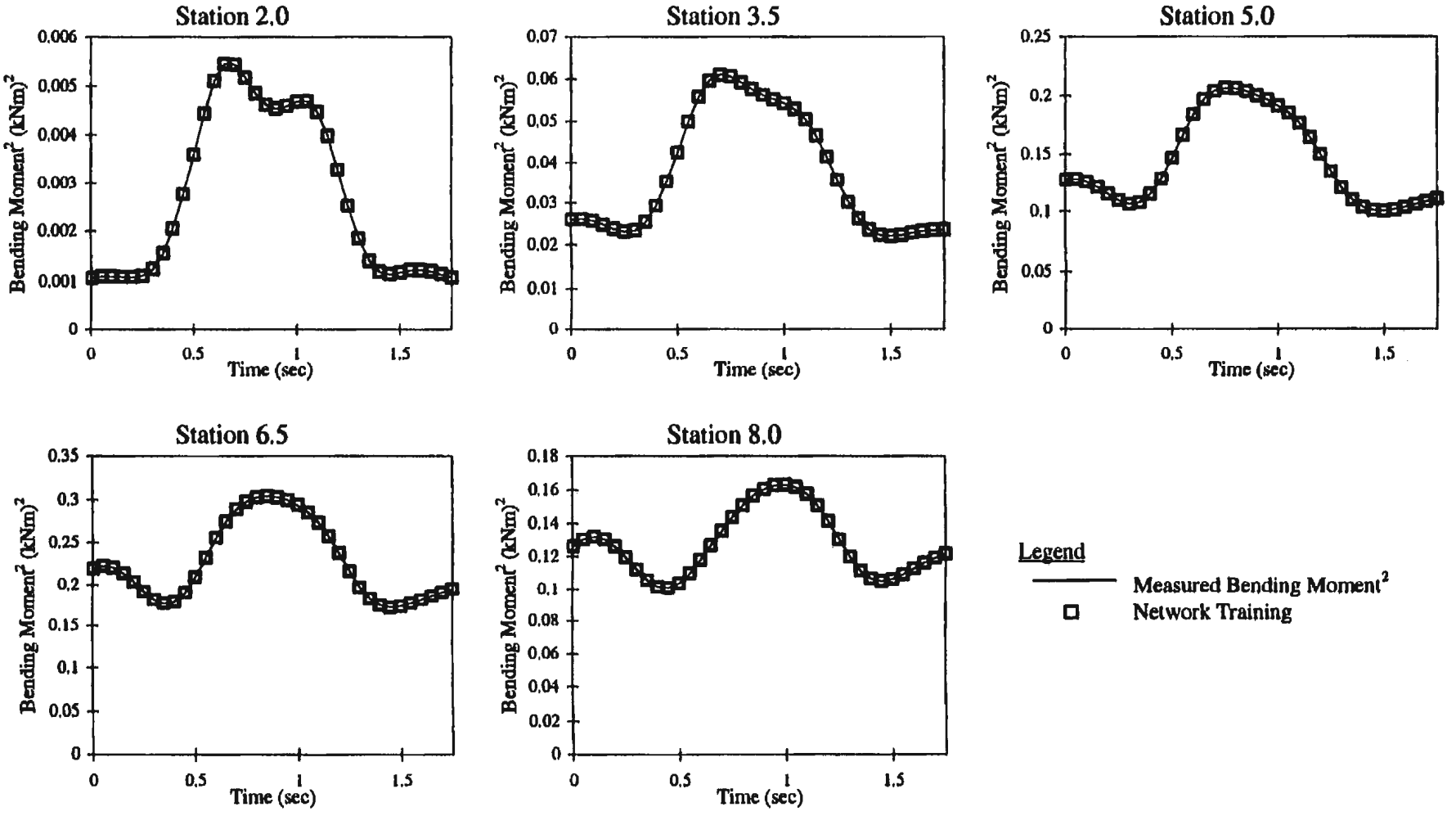

LAKER

Figure B3: Training of Bending Moment Random Decrements

Ship Speed: 14.76 knots Sig. Wave Height: 6.1 m Bretschneider Spectra

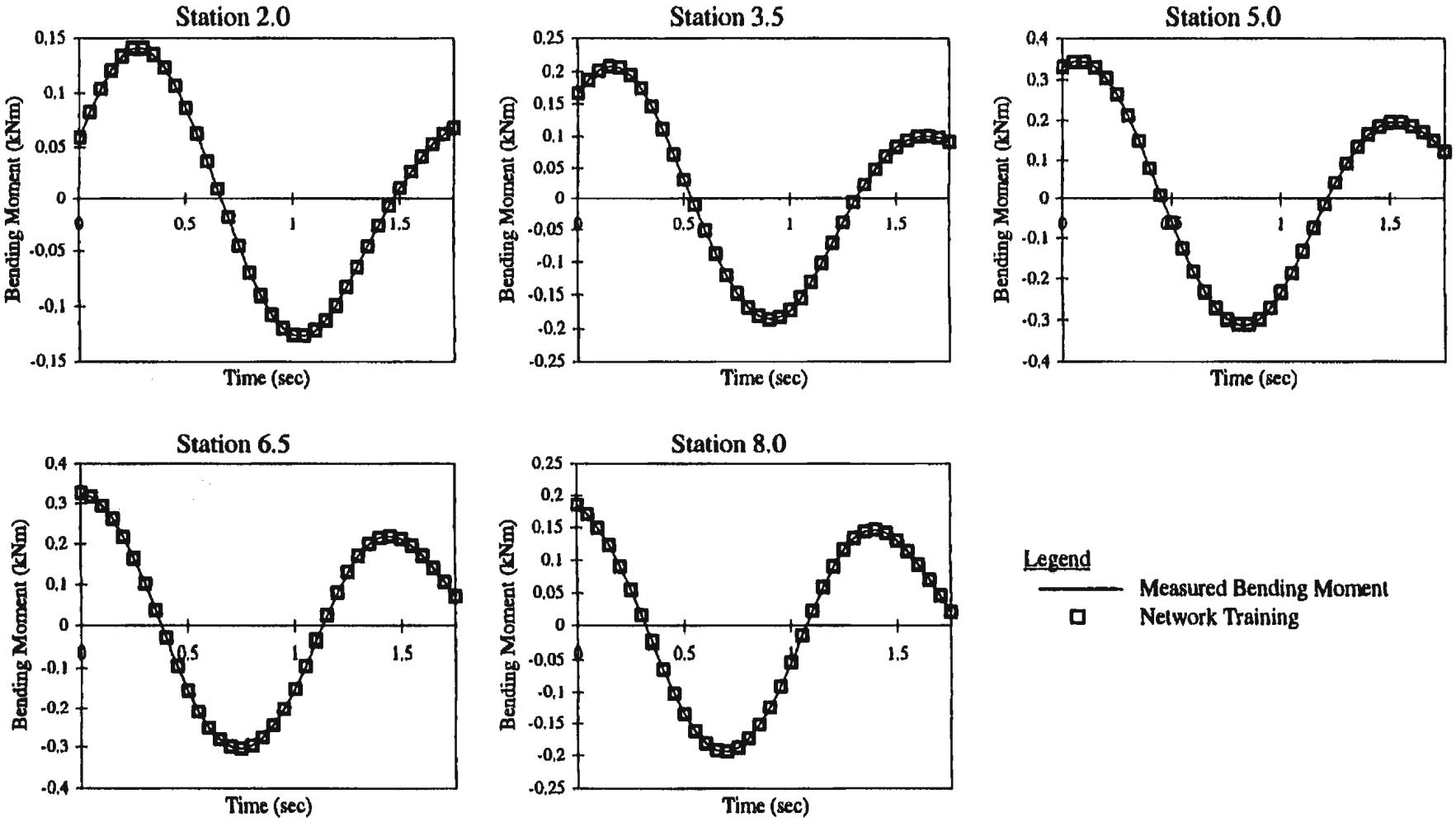

LAKER

Figure B4: Training of Bending Moment^2 Random Decrements

Ship Speed: 14.76 knots Sig. Wave Height: 6.1 m Bretschneider Spectra

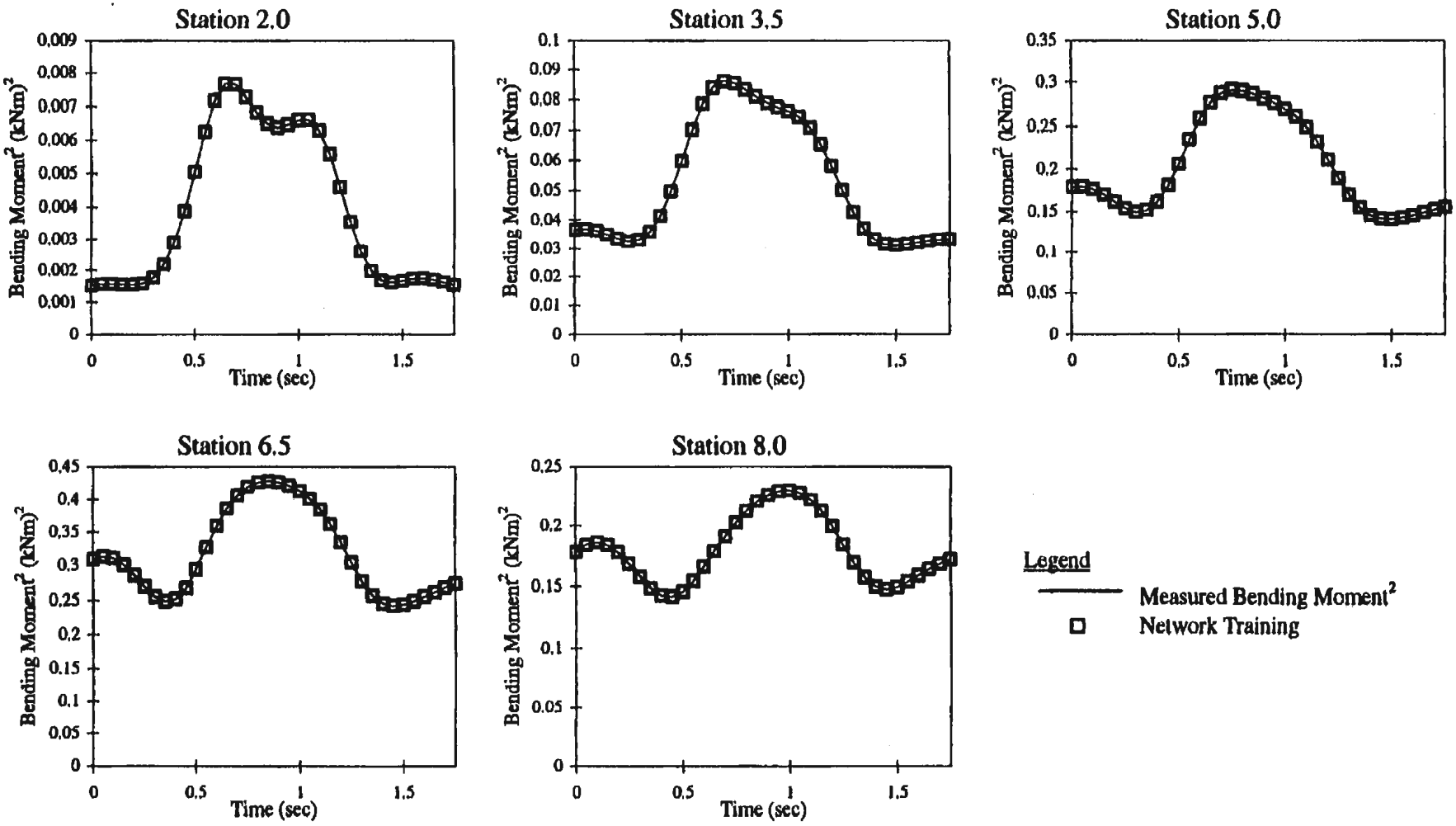

CPF

Figure B5: Training of Bending Moment Random Decrements

Ship Speed: 4.1 knots Sig. Wave Height: 6 m Bretschneider Spectra

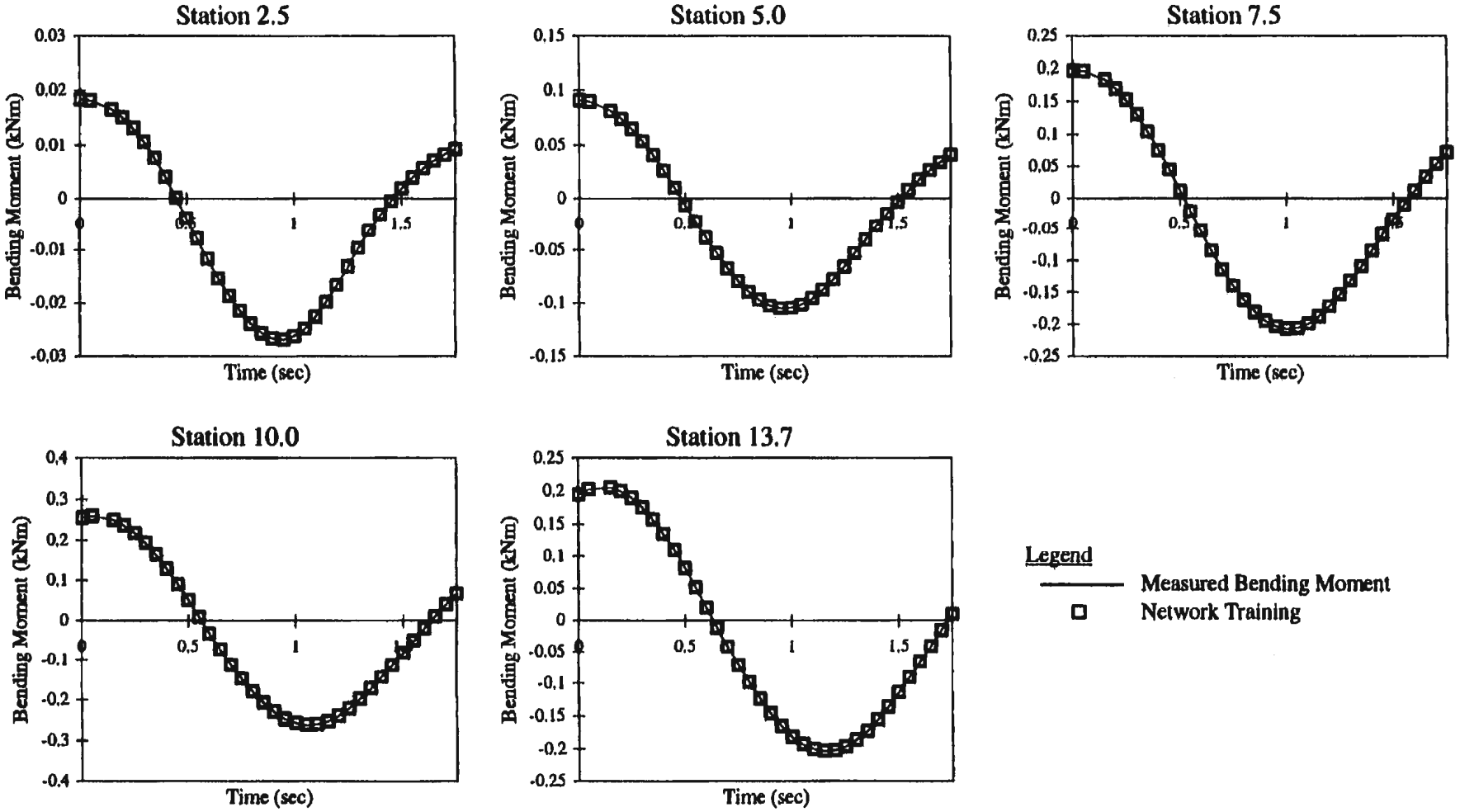

CPF

Figure B6: Training of Bending Moment^2 Random Decrements

Ship Speed: 4.1 knots Sig. Wave Height: 6 m Bretschneider Spectra

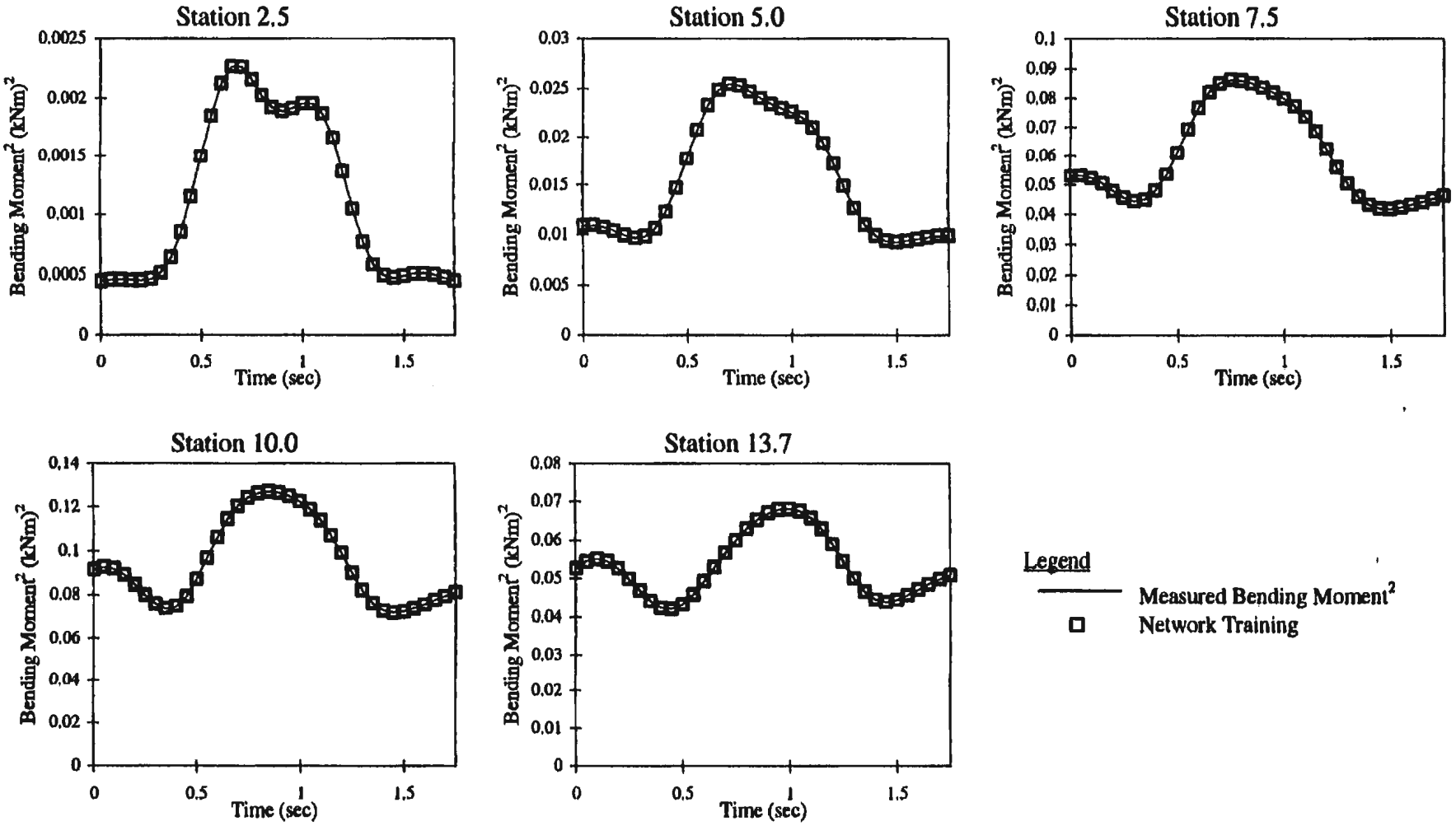

CPF

Figure B7: Training of Bending Moment Random Decrements

Ship Speed: 8.2 knots Sig. Wave Height: 6 m Bretschneider Spectra

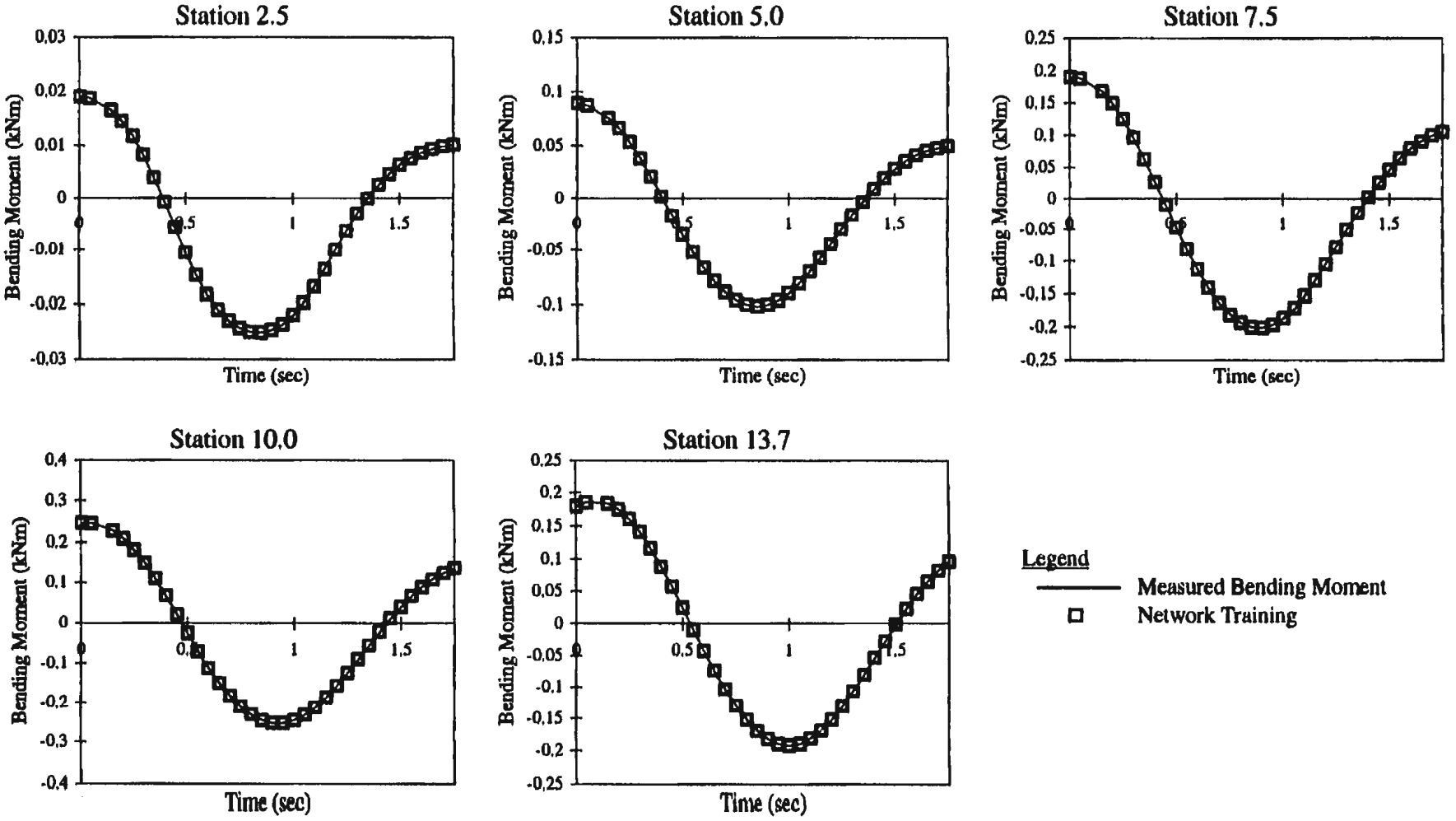

CPF

Figure B8: Training of Bending Moment^2 Random Decrements

Ship Speed: 8.2 knots Sig. Wave Height: 6 m Bretschneider Spectra

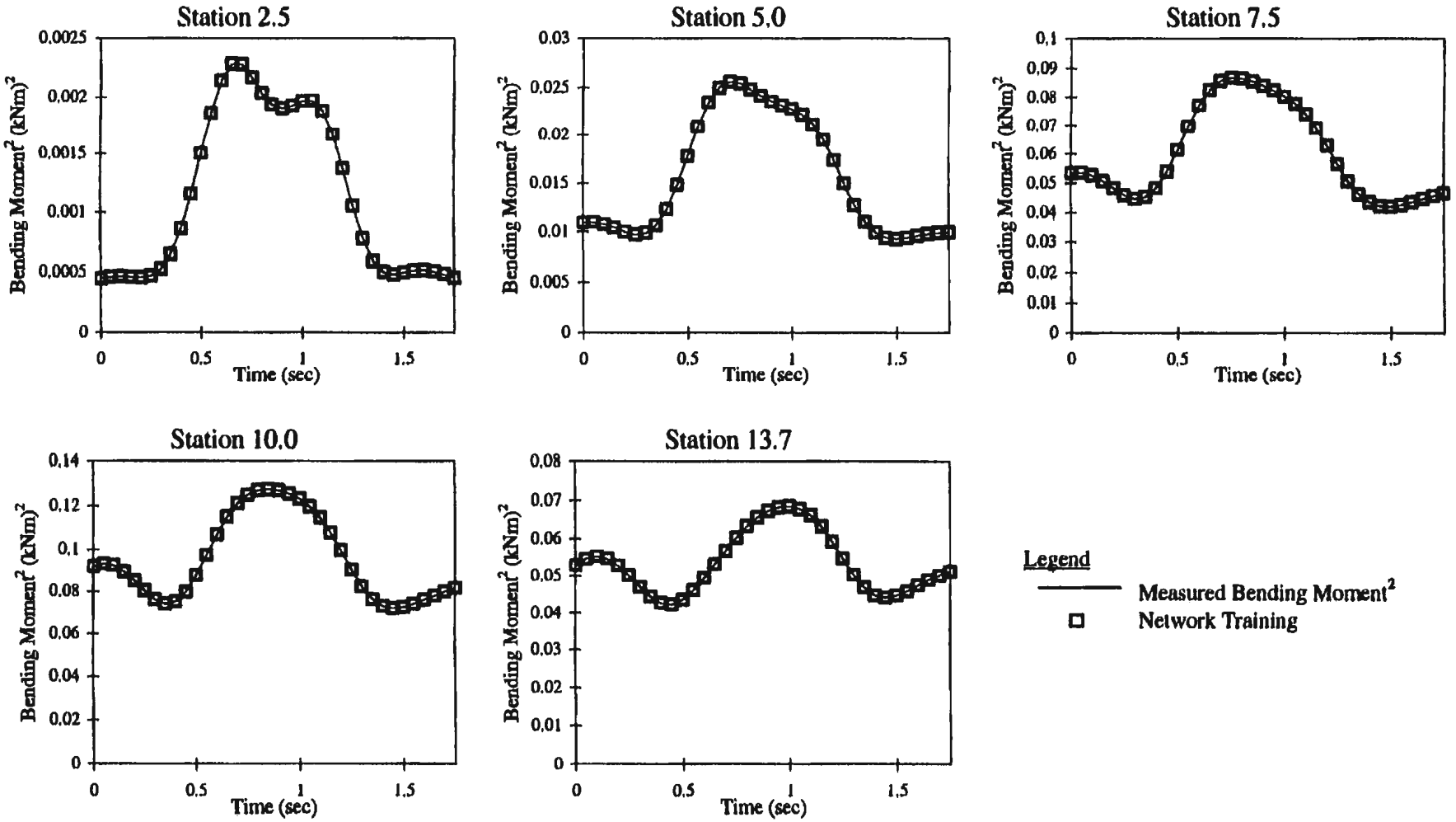

CPF

Figure B9: Training of Bending Moment Random Decrements

Ship Speed: 13.6 knots Sig. Wave Height: 6 m Bretschneider Spectra

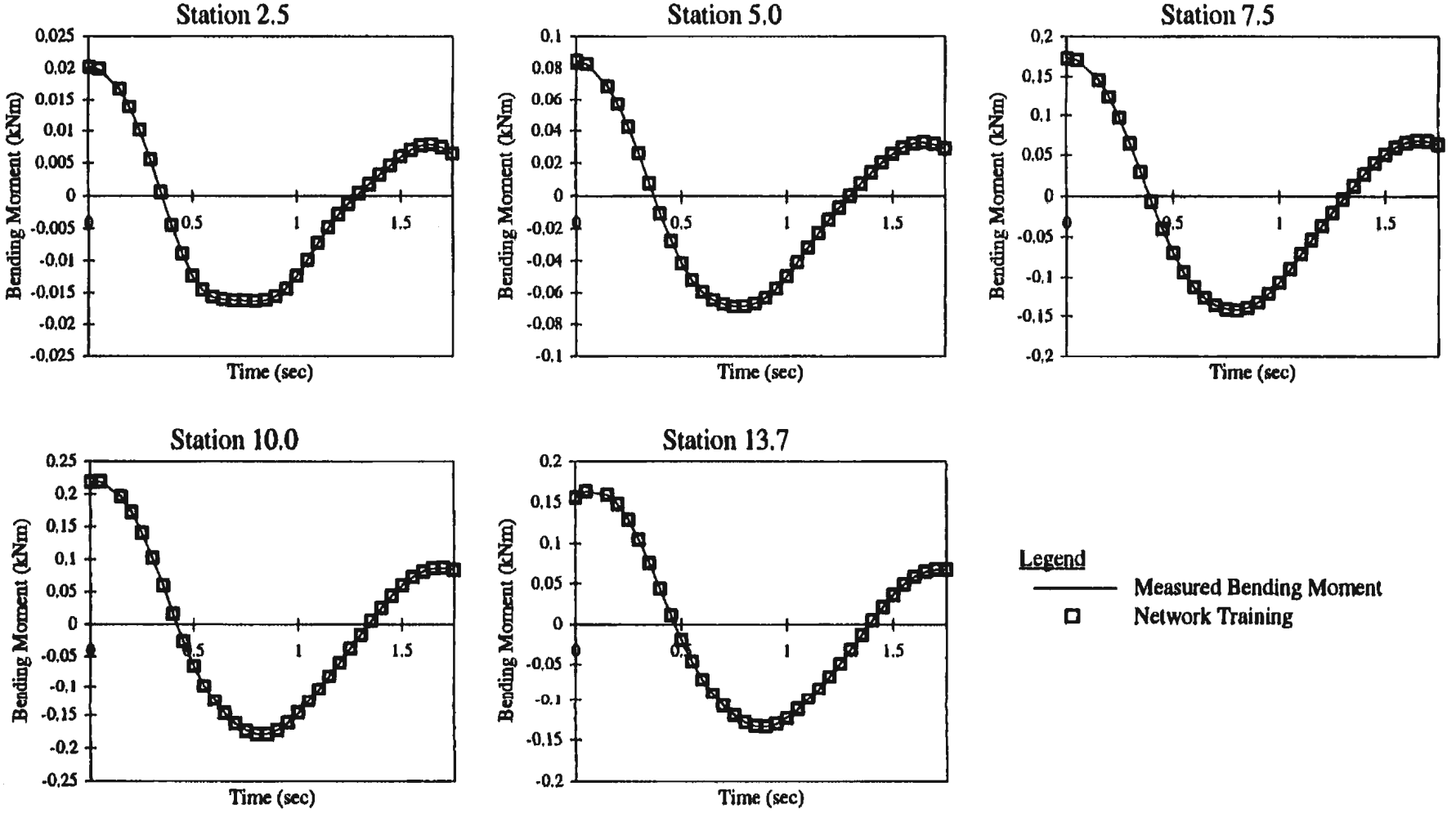

CPF

Figure B10: Training of Bending Moment^2 Random Decrements

Ship Speed: 13.6 knots Sig. Wave Height: 6 m Bretschneider Spectra

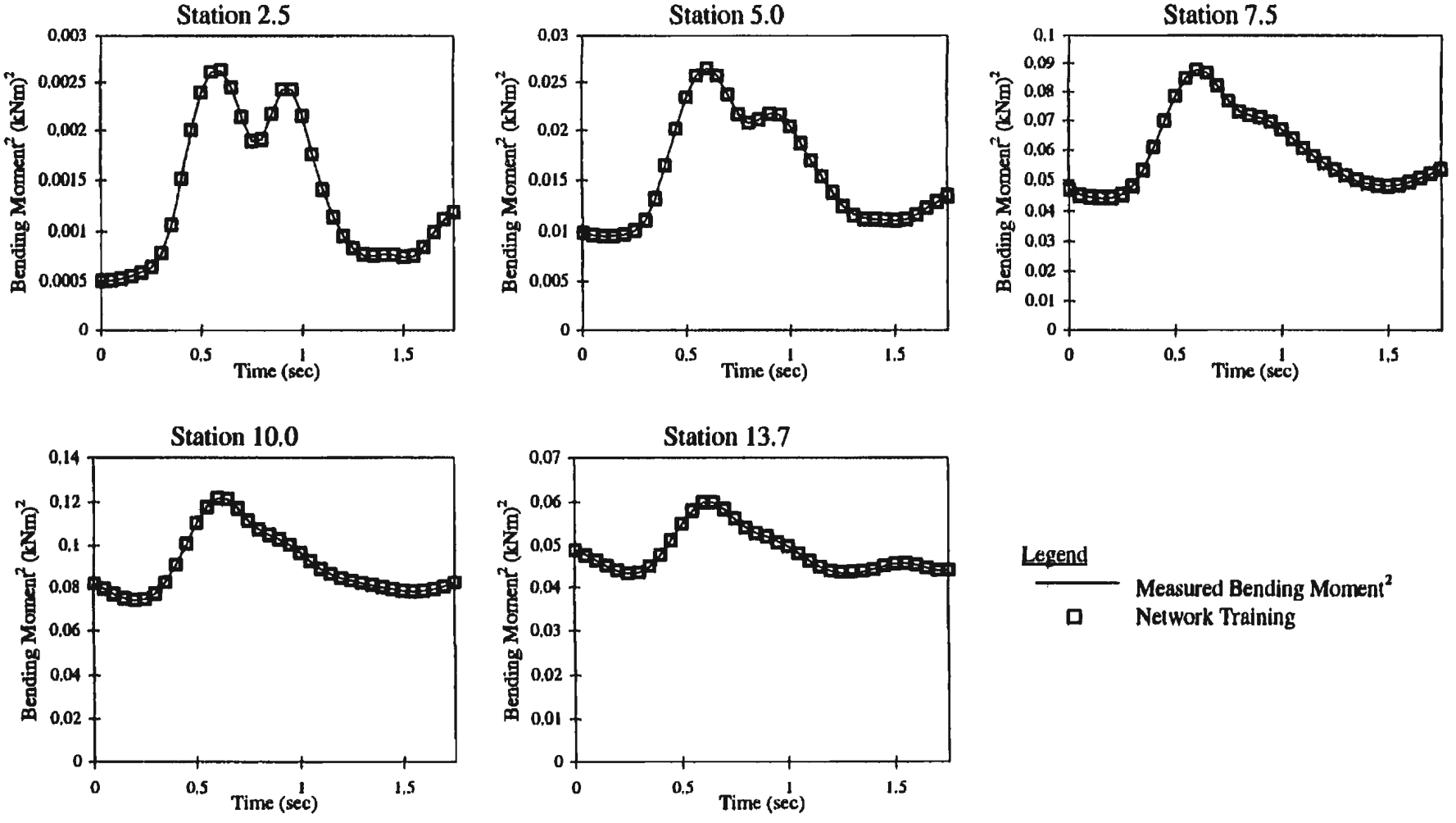

CPF

Figure B11: Training of Bending Moment Random Decrements

Ship Speed: 17 knots Sig. Wave Height: 6 m Bretschneider Spectra

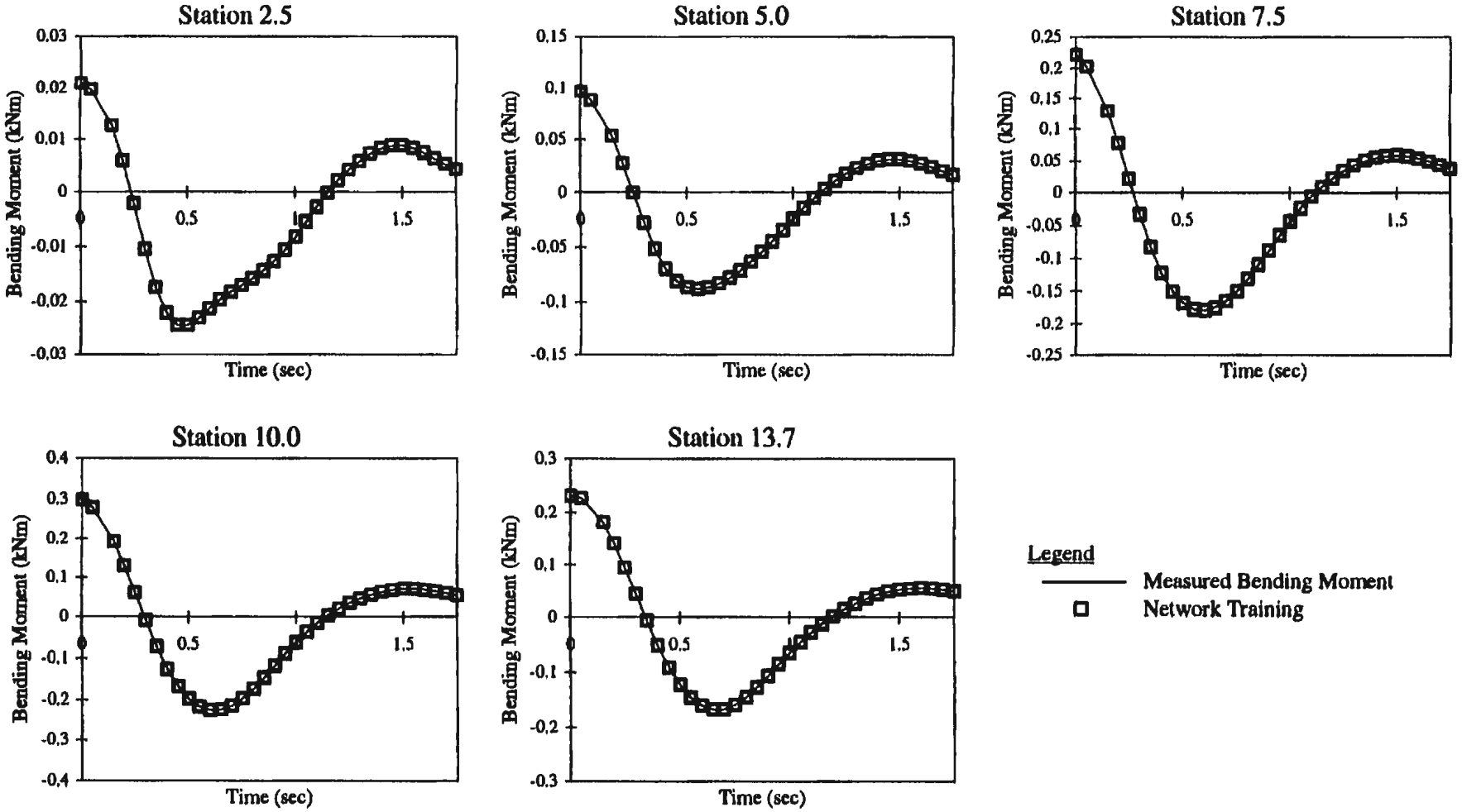

CPF

Figure B12: Training of Bending Moment^2 Random Decrements

Ship Speed: 17 knots Sig. Wave Height: 6 m Bretschneider Spectra

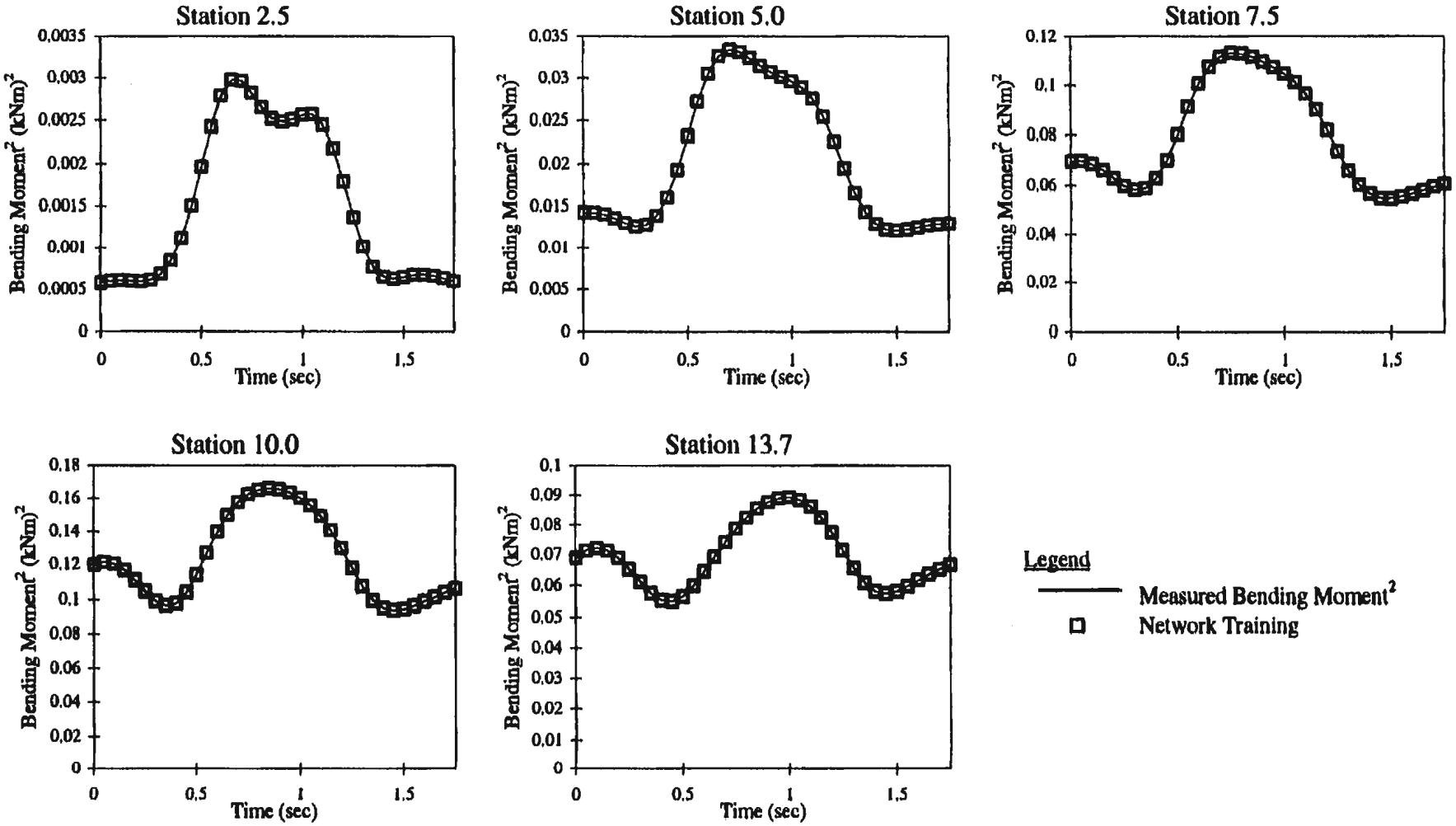

Appendix C: Contribution Factors

LAKER

Figure C1: Contibution Factor Vs. Station for Bending Moment

Ship Speed: 12.15 knots Sig. Wave Height: 6.1 m Bretschneider Spectra

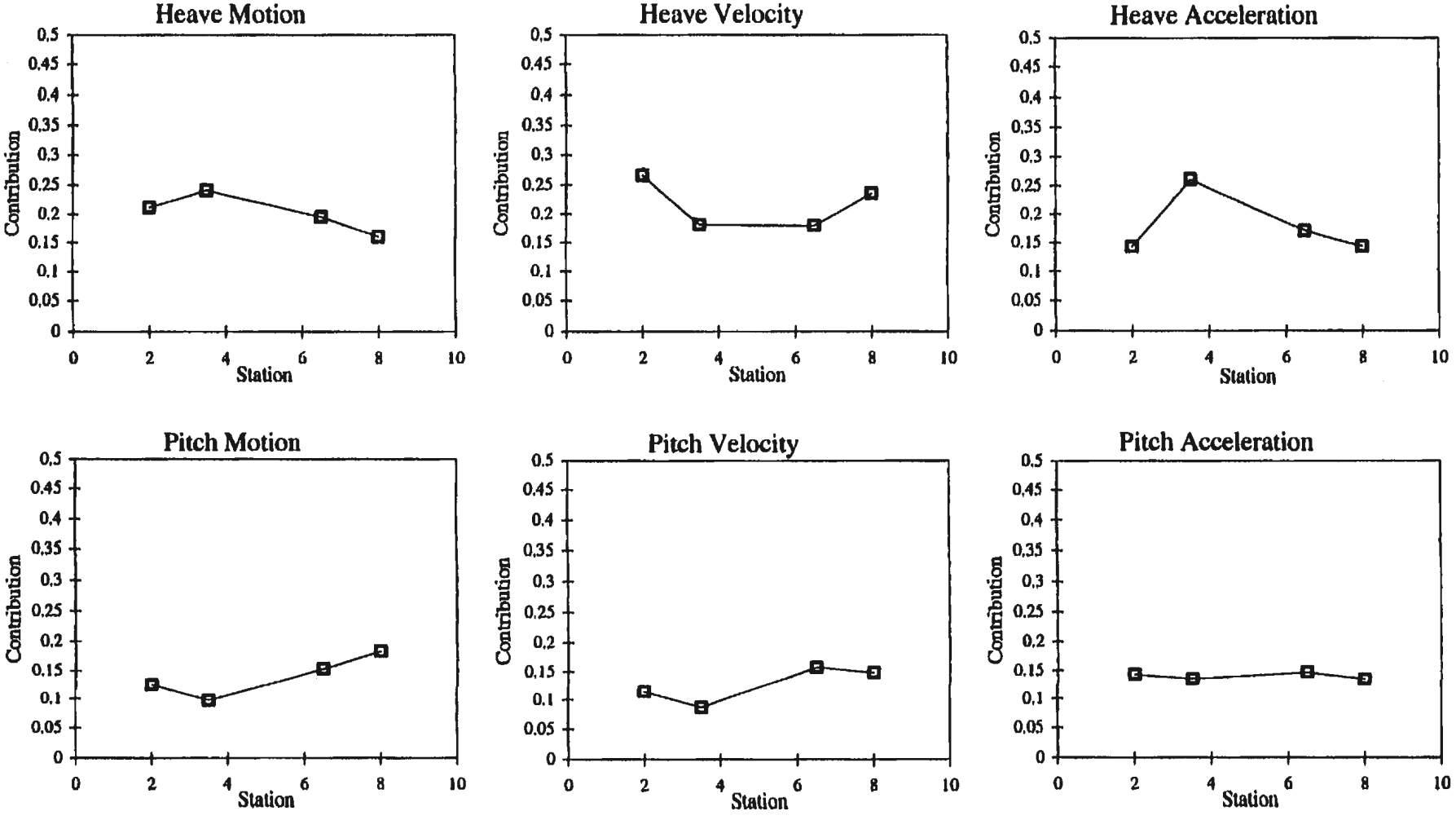

LAKER

Figure C2: Contibution Factor Vs. Station for Bending Moment^2

Ship Speed: 12.15 knots Sig. Wave Height: 6.1 m Bretschneider Spectra

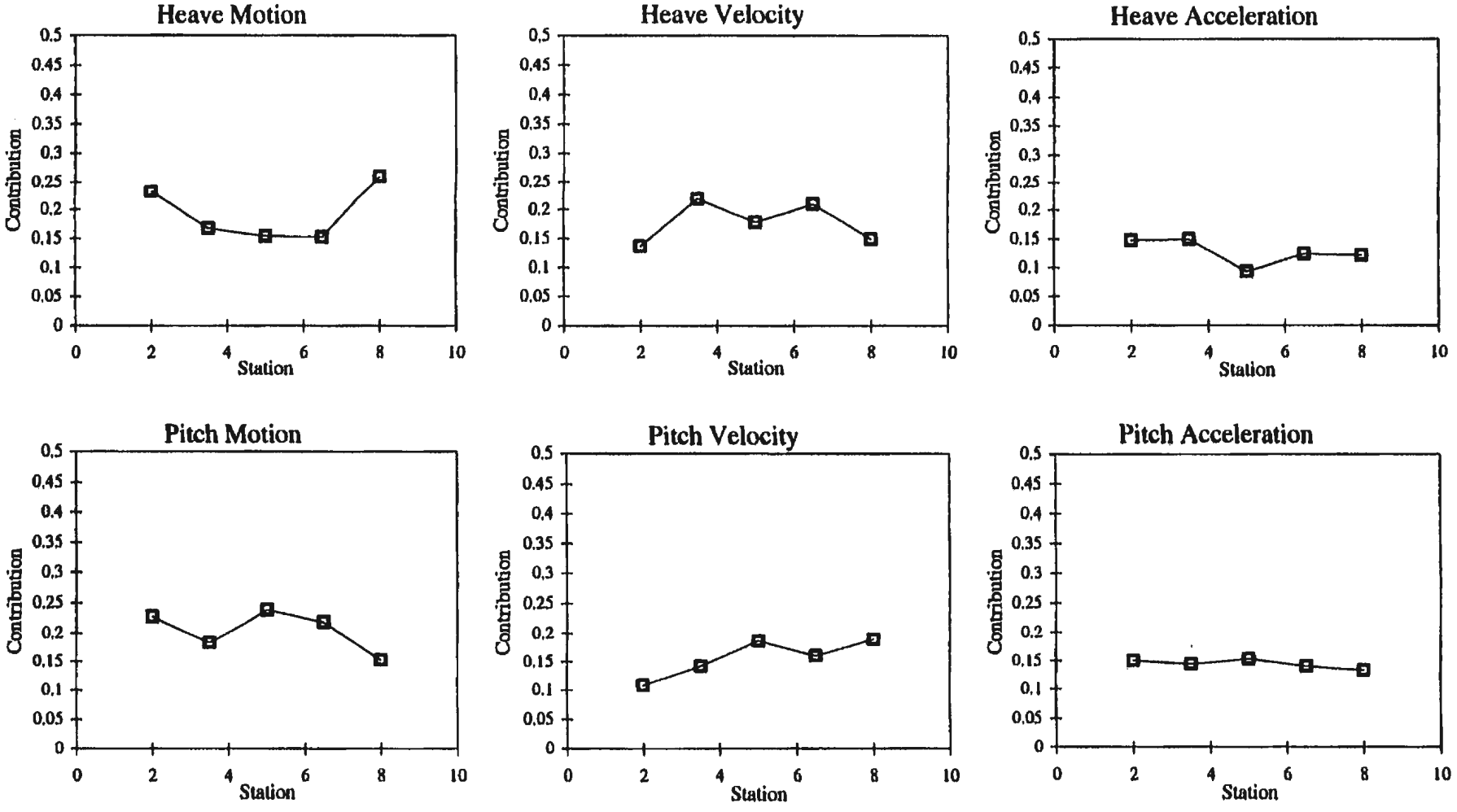

LAKER

Figure C3: Contibution Factor Vs. Station for Bending Moment

Ship Speed: 14.76 knots Sig. Wave Height: 6.1 m Bretschneider Spectra

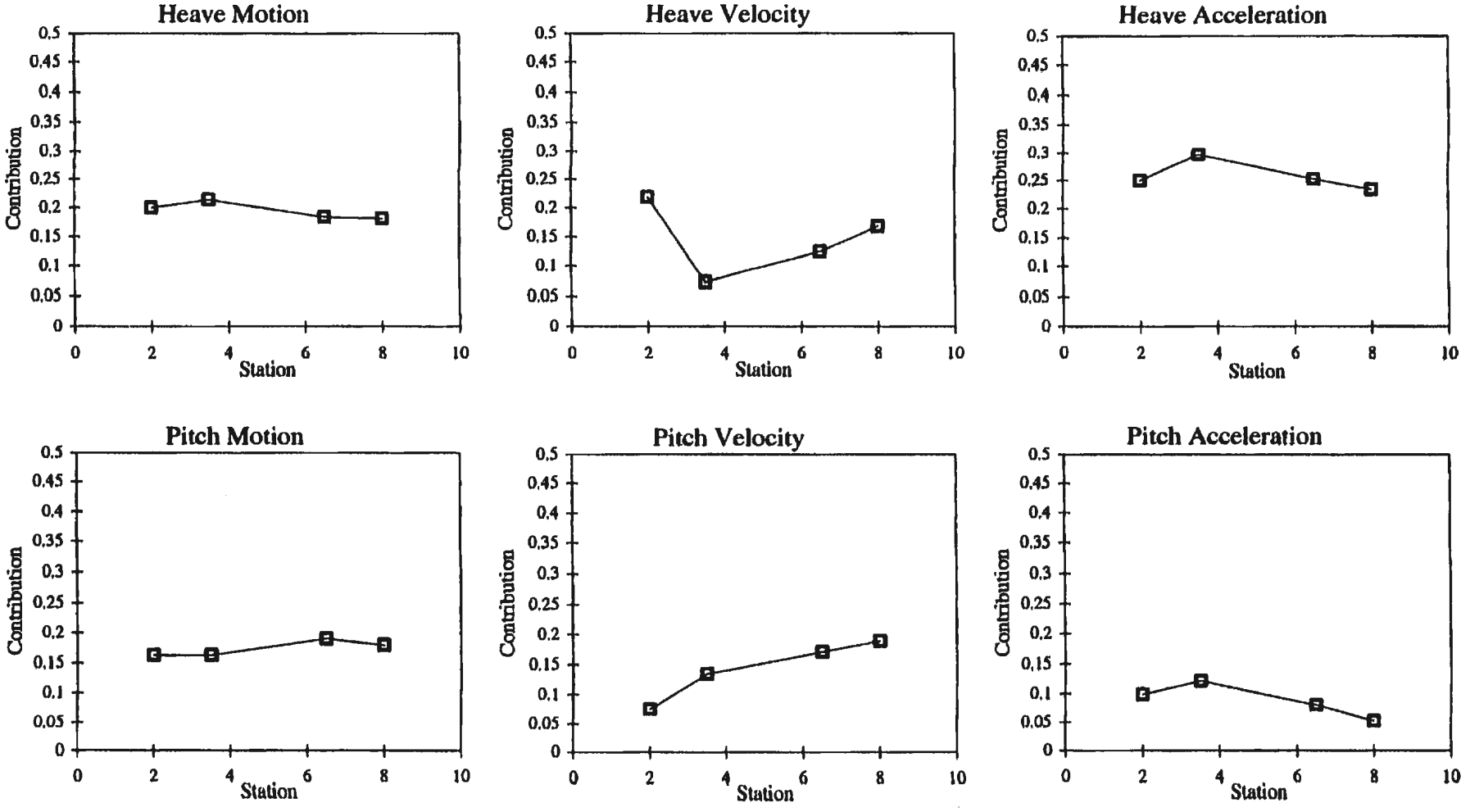

LAKER

Figure C4: Contibution Factor Vs. Station for Bending Moment^2

Ship Speed: 14.76 knots Sig. Wave Height: 6.1 m Bretschneider Spectra

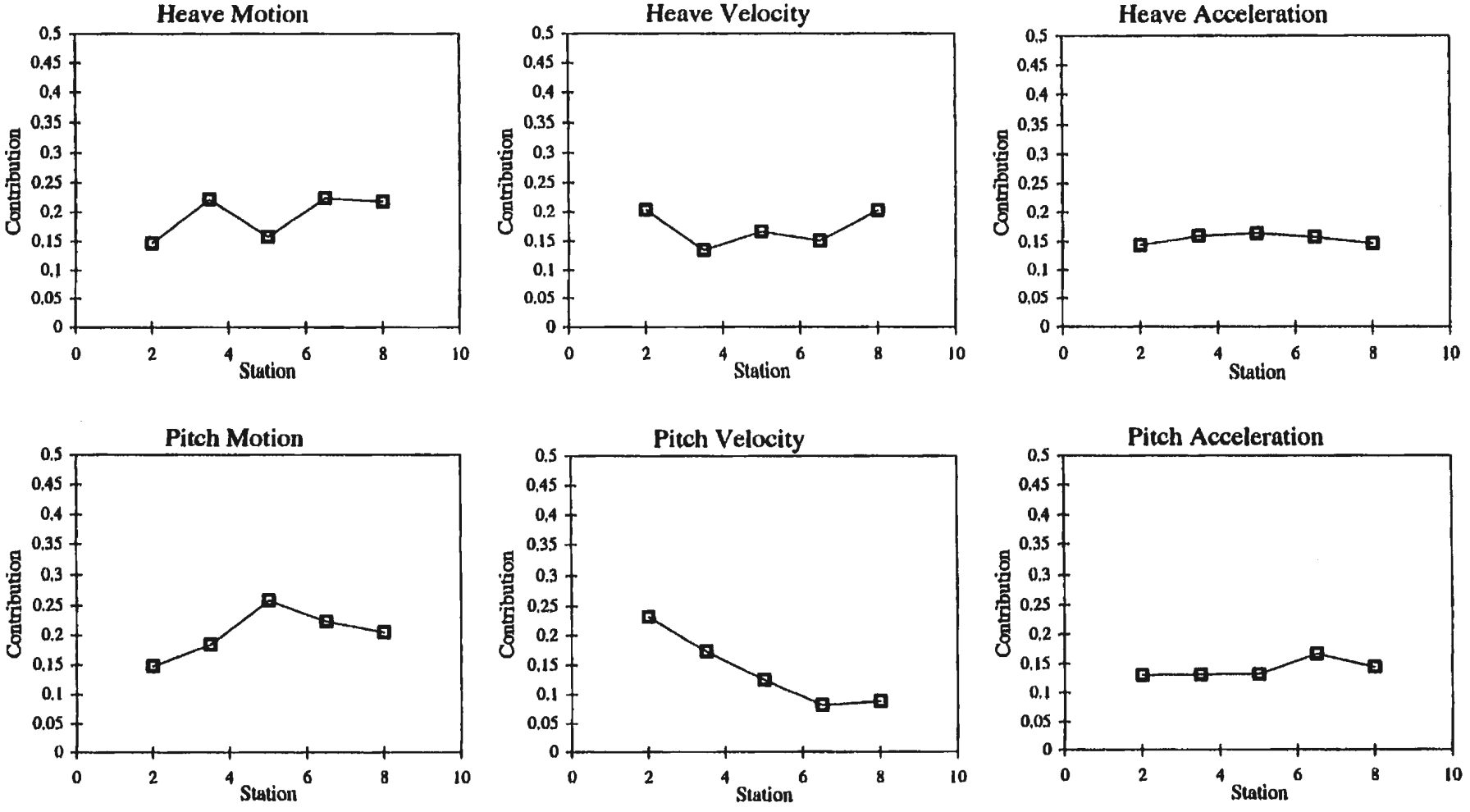

CPF

Figure C5: Contibution Factor Vs. Station for Bending Moment

Ship Speed: 4.1 knots Sig. Wave Height: 6 m Bretschneider Spectra

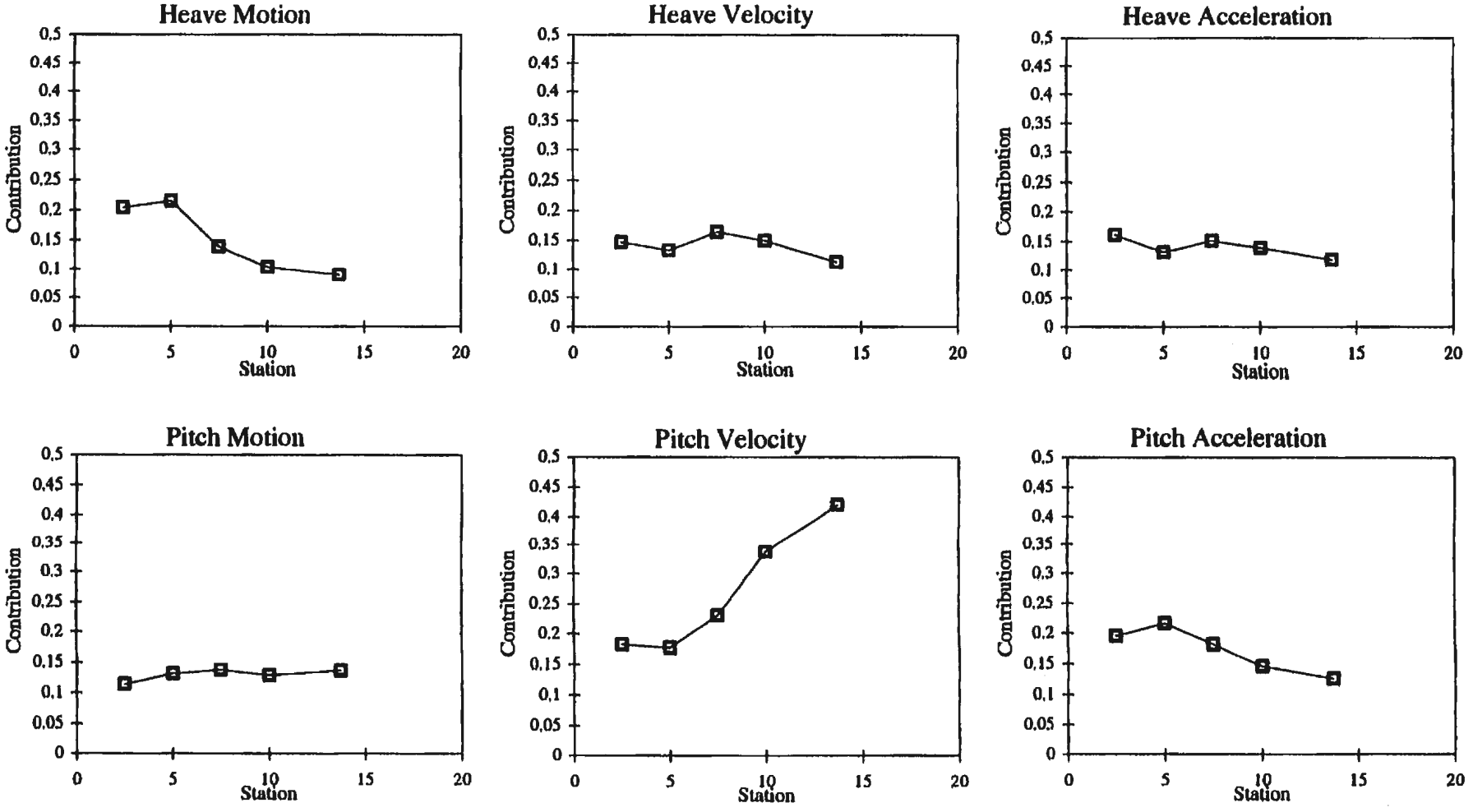

CPF

Figure C6: Contibution Factor Vs. Station for Bending Moment^2

Ship Speed: 4.1 knots Sig. Wave Height: 6 m Bretschneider Spectra

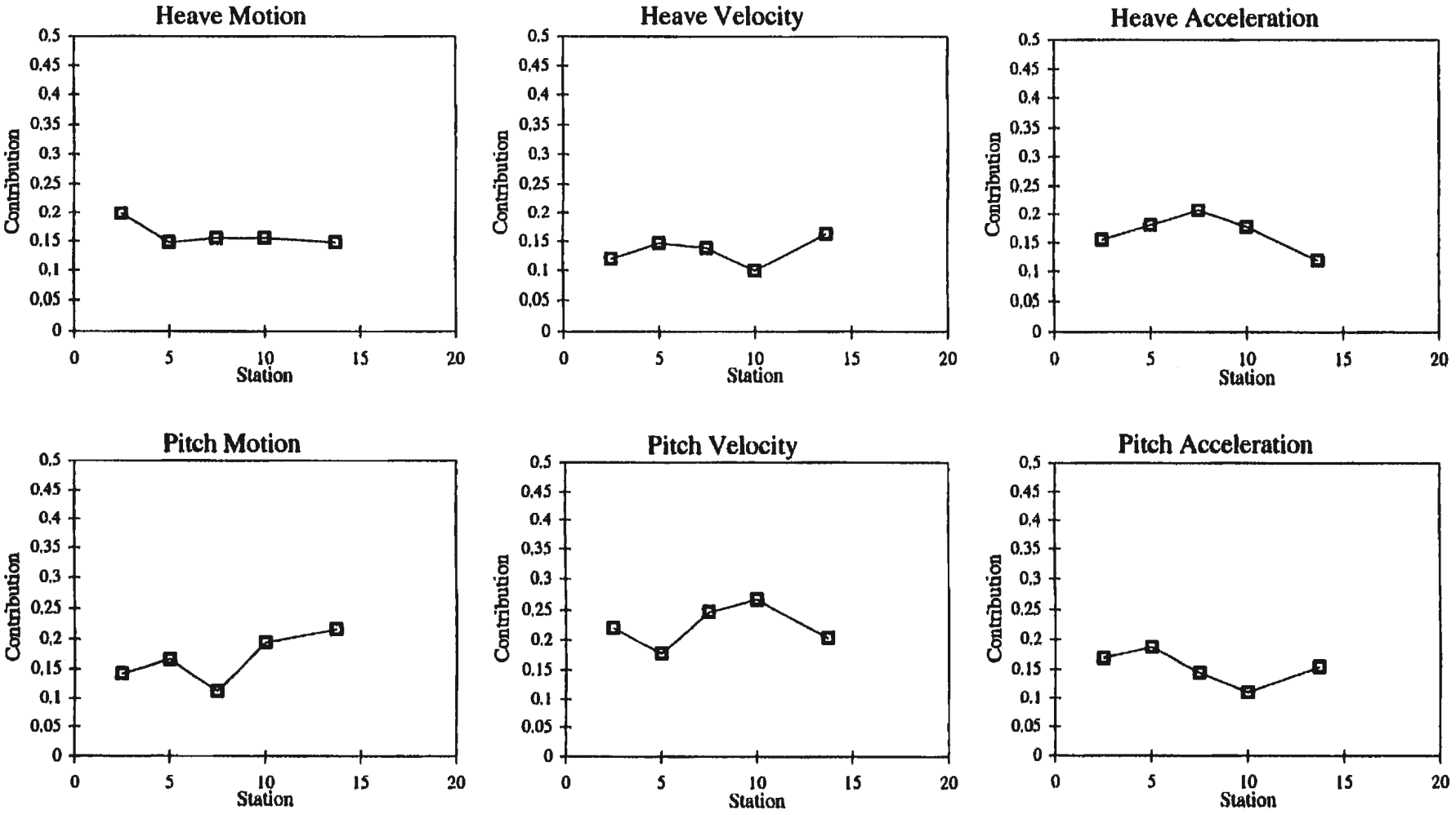

CPF

Figure C7: Contibution Factor Vs. Station for Bending Moment

Ship Speed: 8.2 knots Sig. Wave Height: 6 m Bretschneider Spectra

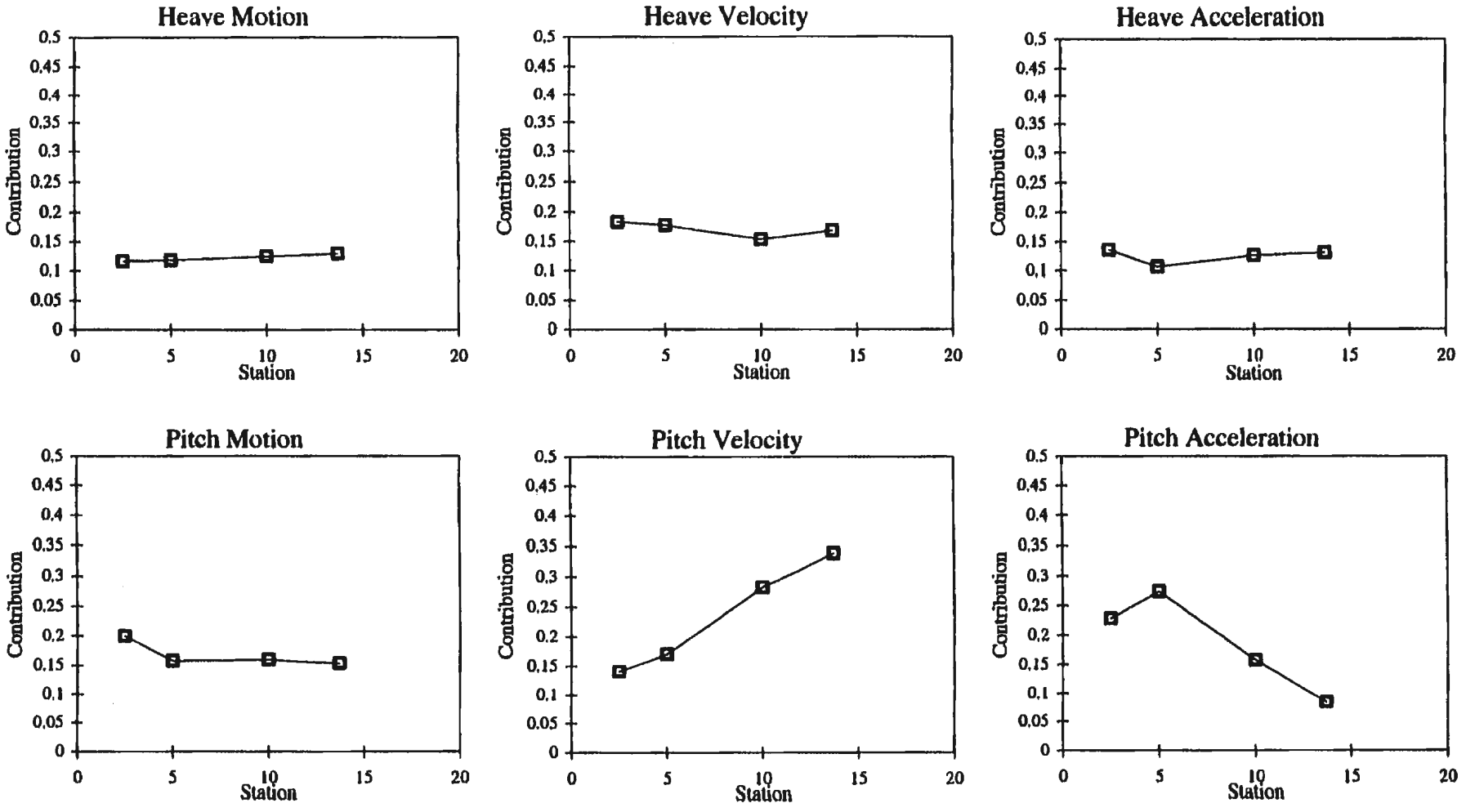

CPF

Figure C8: Contibution Factor Vs. Station for Bending Moment^2

Ship Speed: 8.2 knots Sig. Wave Height: 6 m Bretschneider Spectra

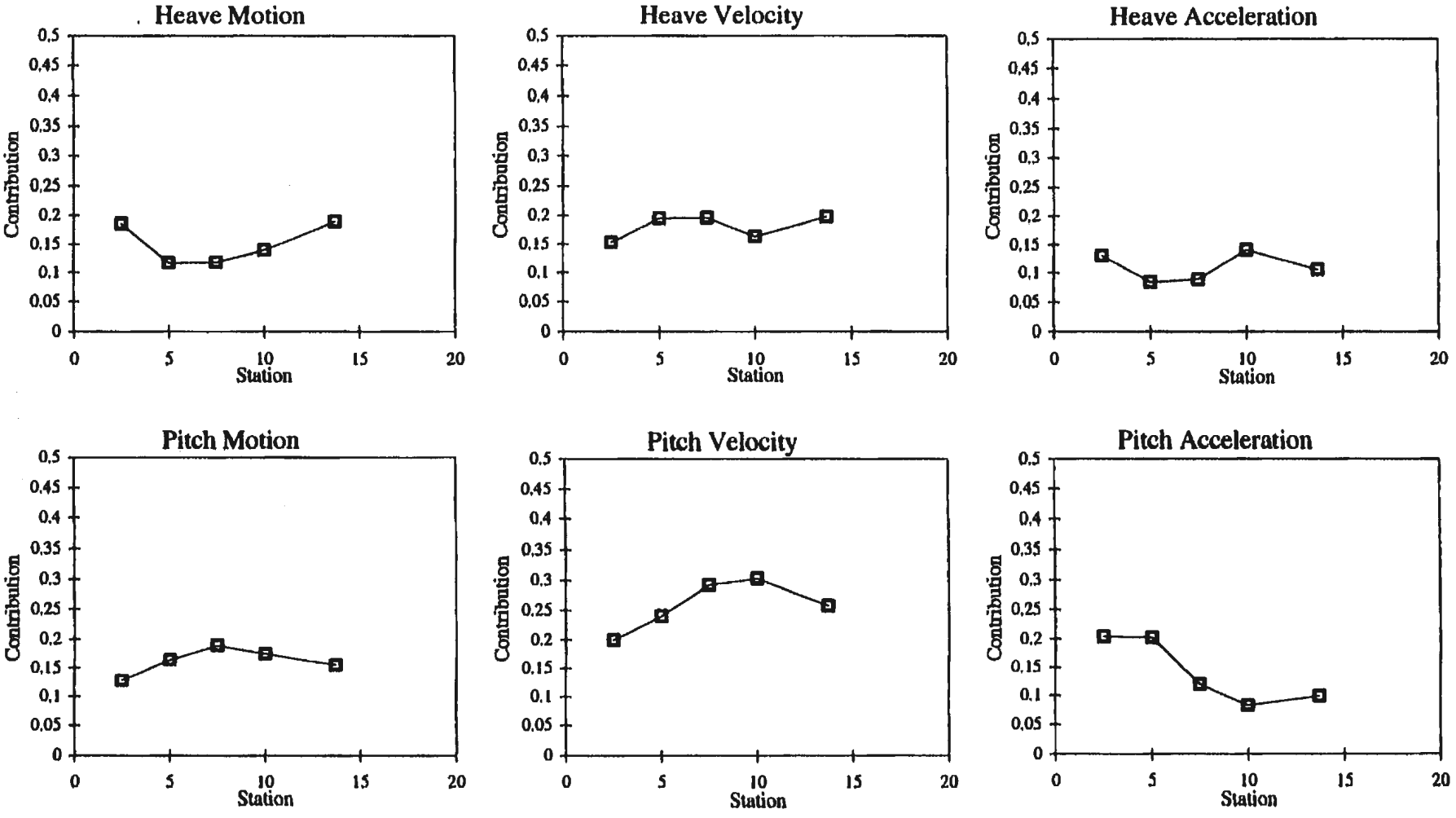

CPF

Figure C9: Contibution Factor Vs. Station for Bending Moment

Ship Speed: 13.6 knots Sig. Wave Height: 6 m Bretschneider Spectra

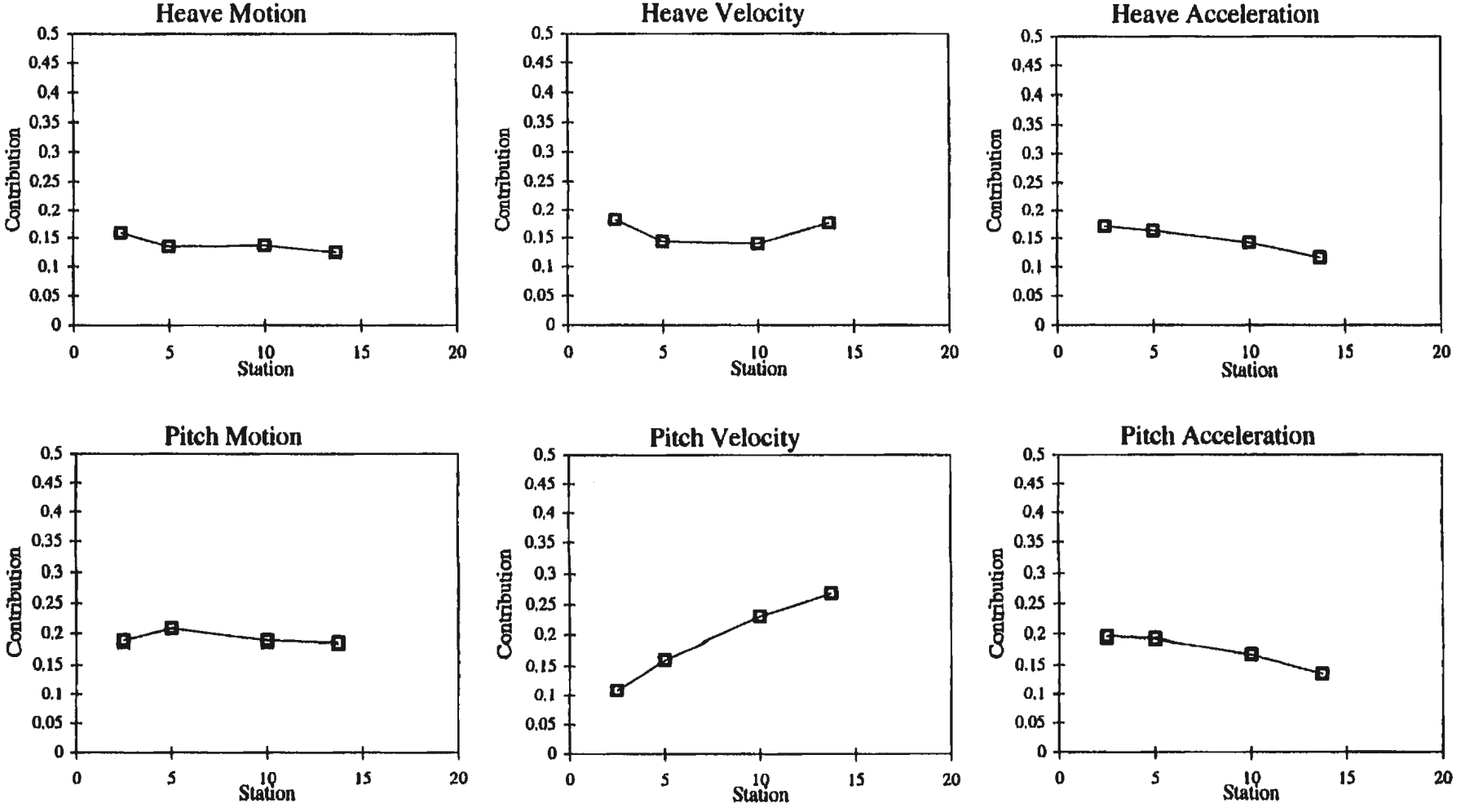

CPF

Figure C10: Contibution Factor Vs. Station for Bending Moment^2

Ship Speed: 13.6 knots Sig. Wave Height: 6 m Bretschneider Spectra

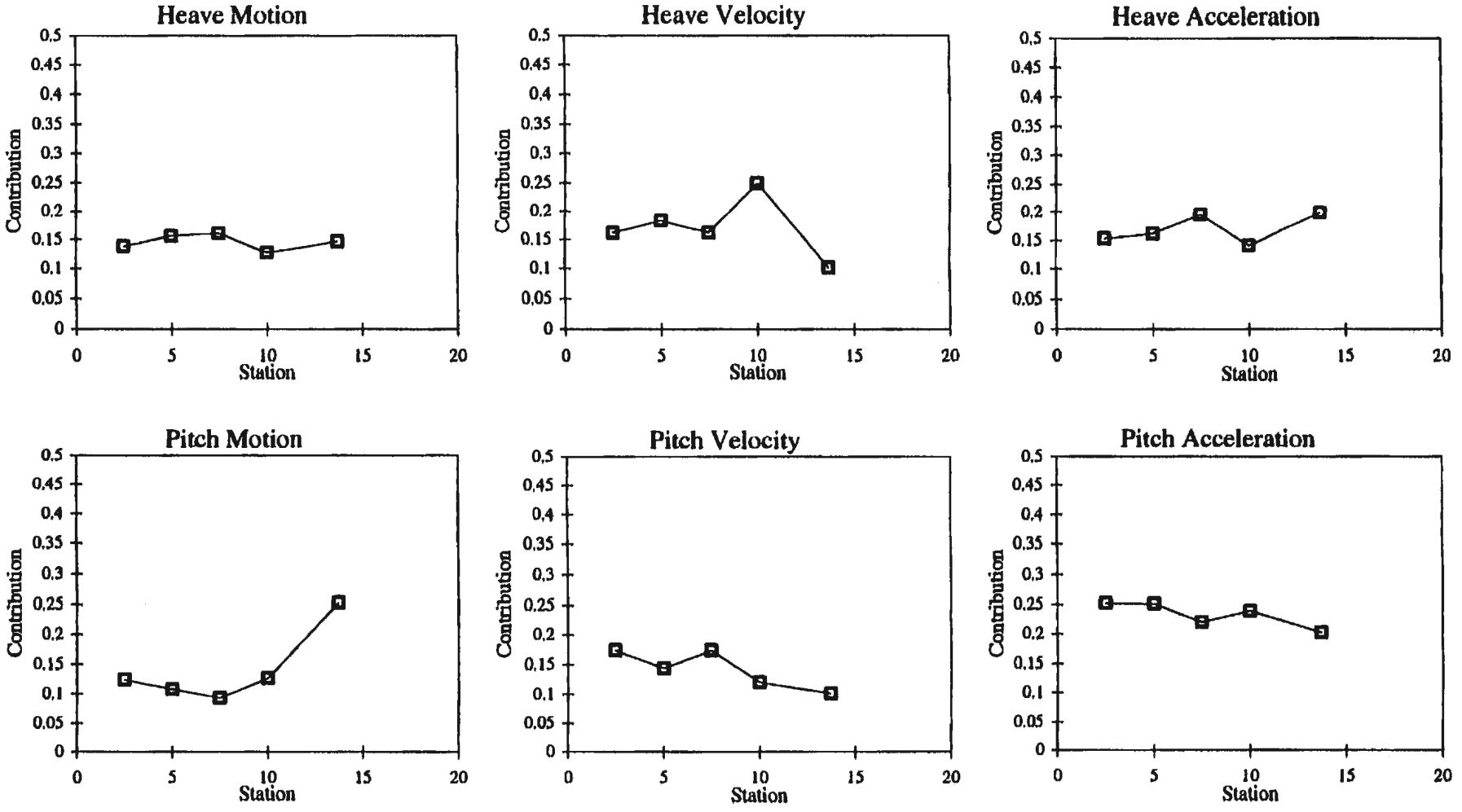

CPF

Figure C11: Contibution Factor Vs. Station for Bending Moment

Ship Speed: 17 knots Sig. Wave Height: 6 m Bretschneider Spectra

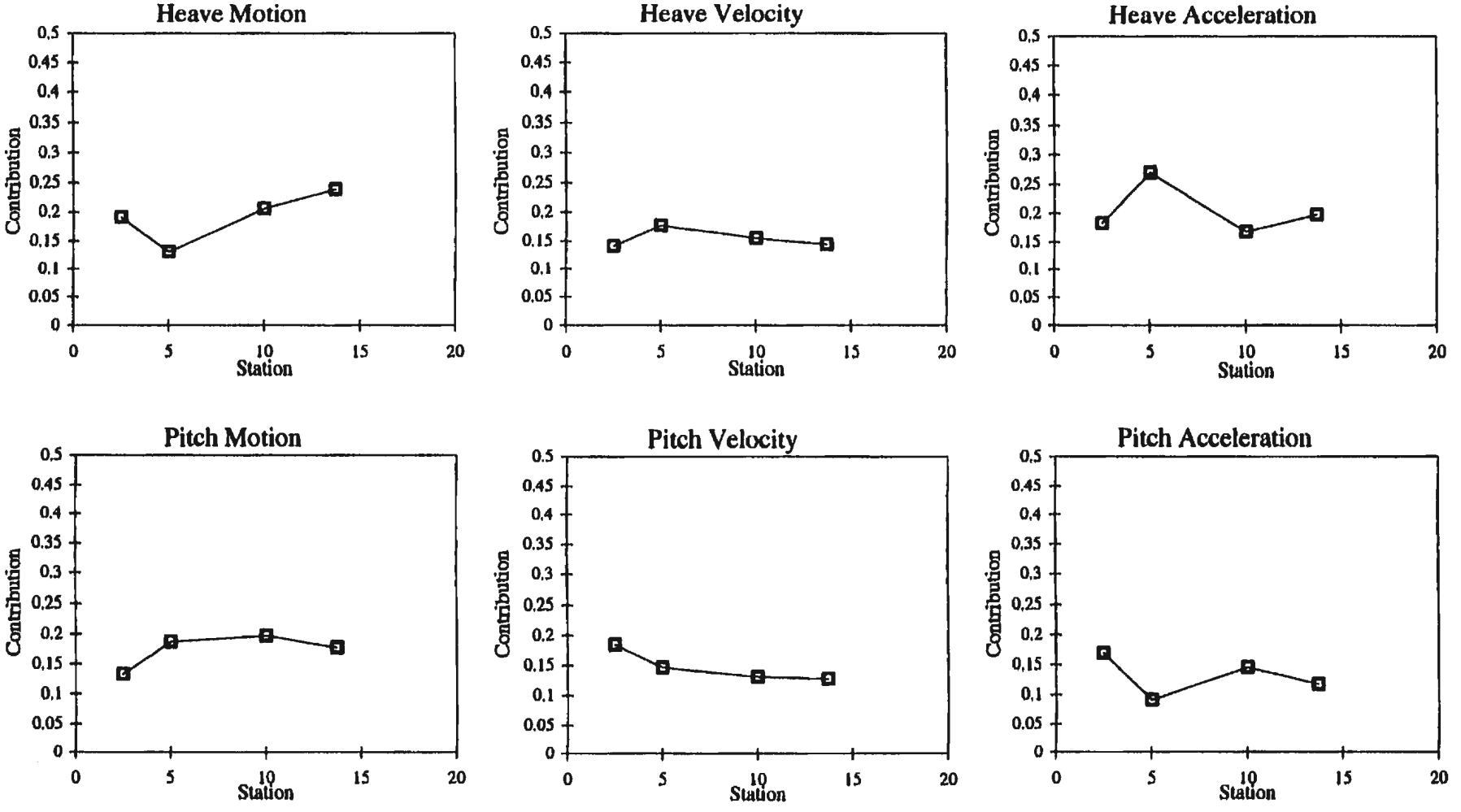

CPF

Figure C12: Contibution Factor Vs. Station for Bending Moment^2

Ship Speed: 17 knots Sig. Wave Height: 6 m Bretschneider Spectra

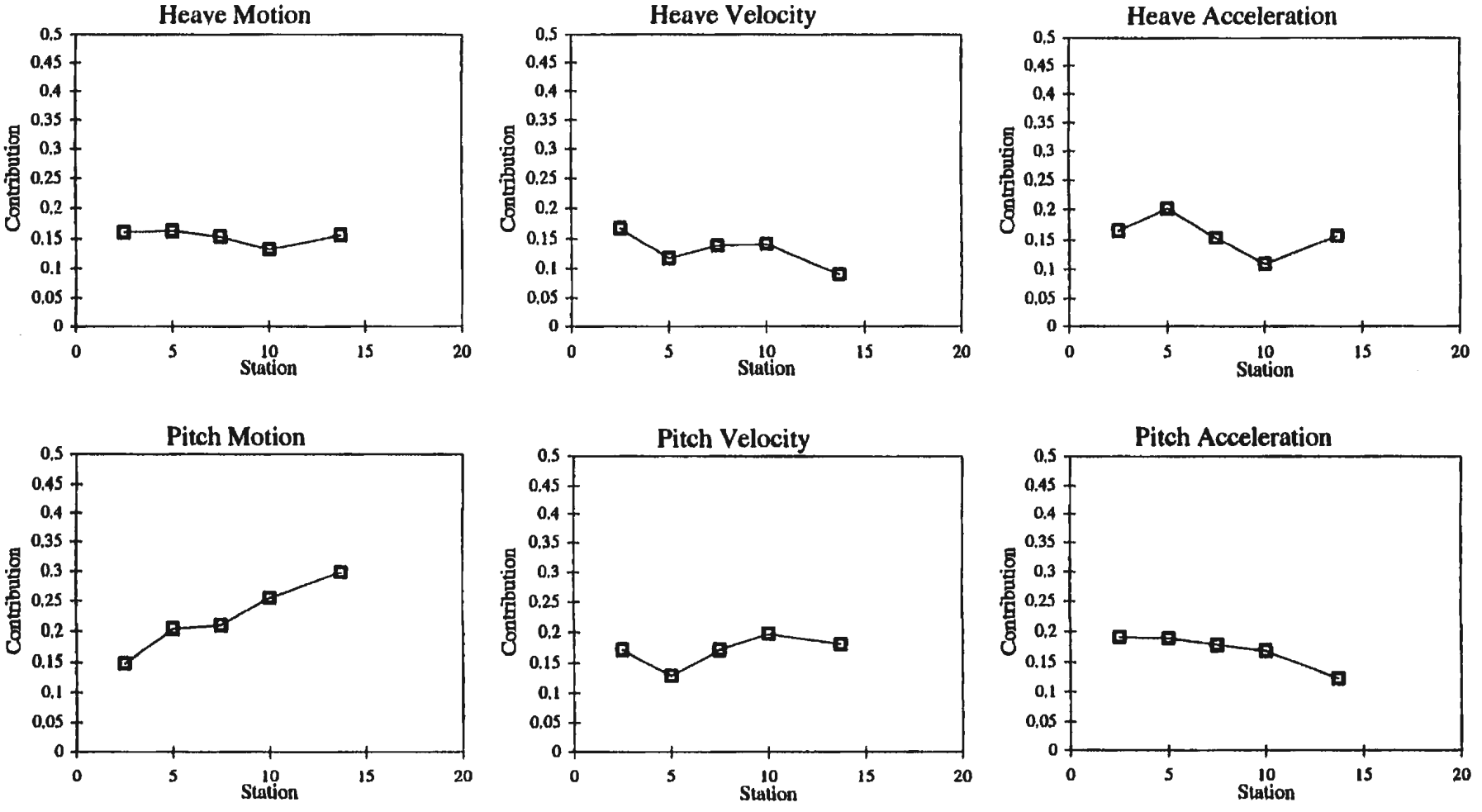

Appendix D: Random Decrement Prediction

LAKER

Figure D1: Prediction of Bending Moment Random Decrements

Ship Speed: 12.15 knots Sig. Wave Height: 3.05 m Bretschneider Spectra

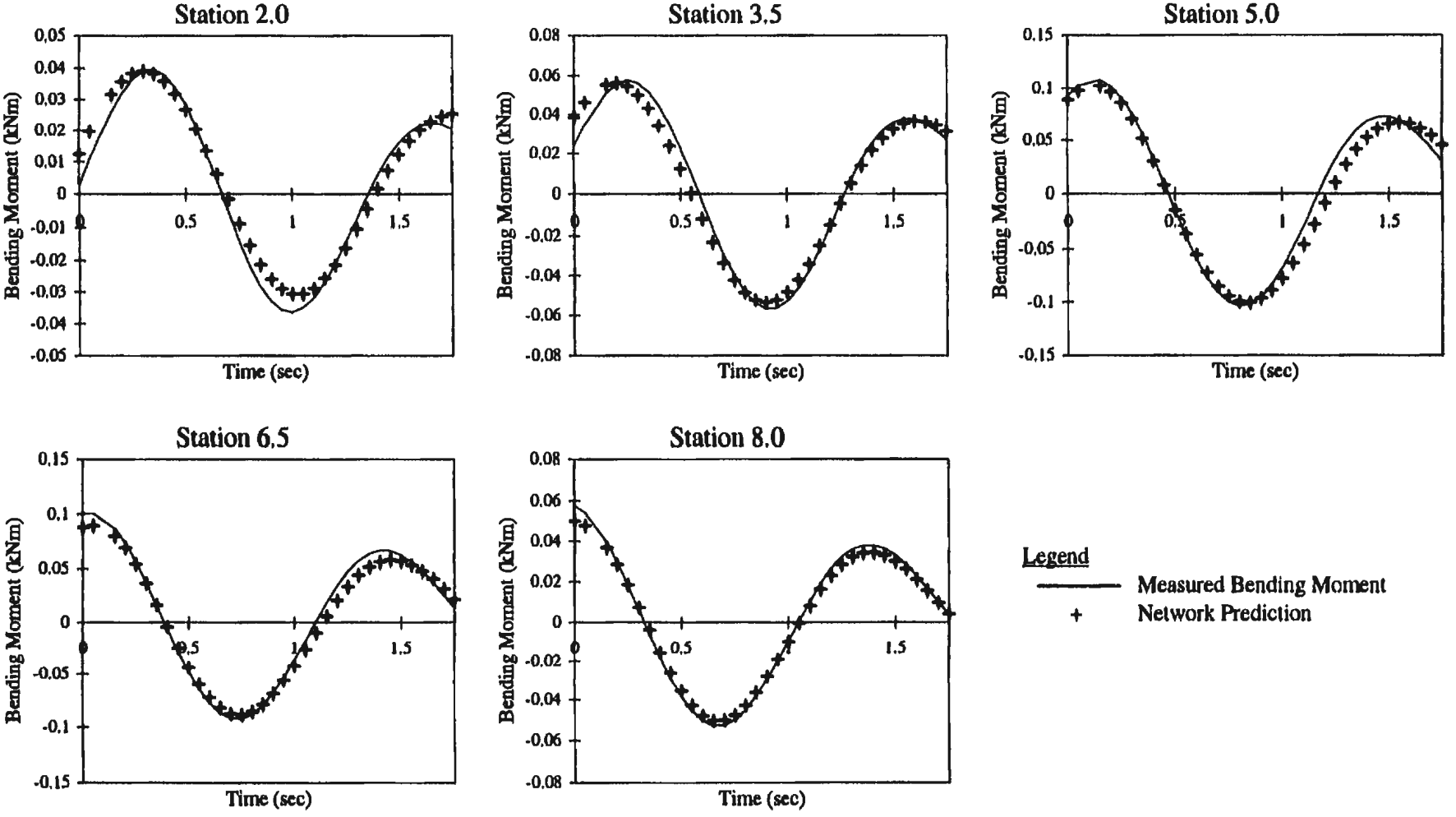

LAKER

Figure D2: Prediction of Bending Moment^2 Random Decrements

Ship Speed: 12.15 knots Sig. Wave Height: 3.05 m Bretschneider Spectra

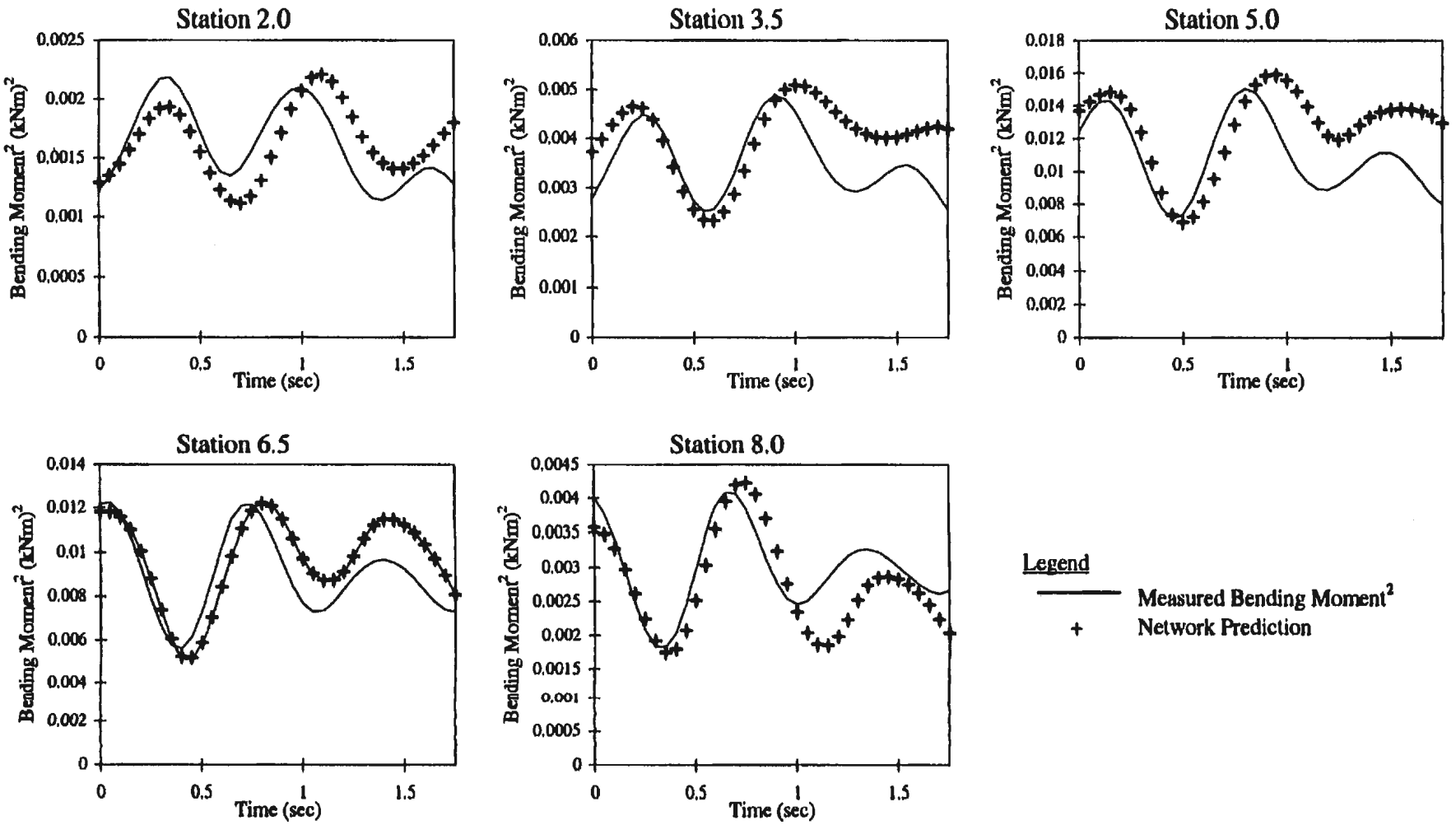

LAKER

Figure D3: Prediction of Bending Moment Random Decrements

Ship Speed: 14.76 knots Sig. Wave Height: 3.05 m Bretschneider Spectra

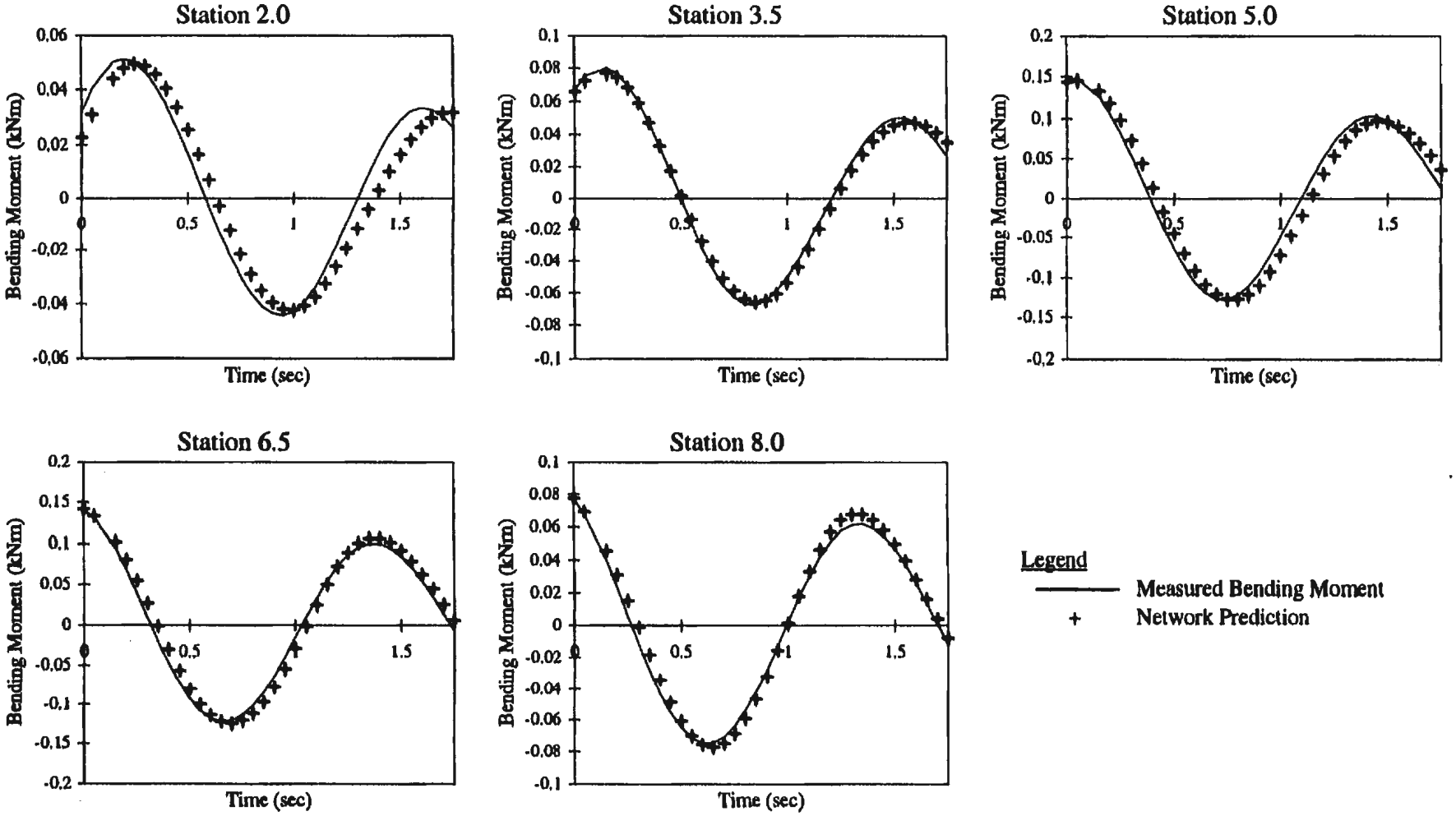

LAKER

Figure D4: Prediction of Bending Moment^2 Random Decrements

Ship Speed: 14.76 knots Sig. Wave Height: 3.05 m Bretschneider Spectra

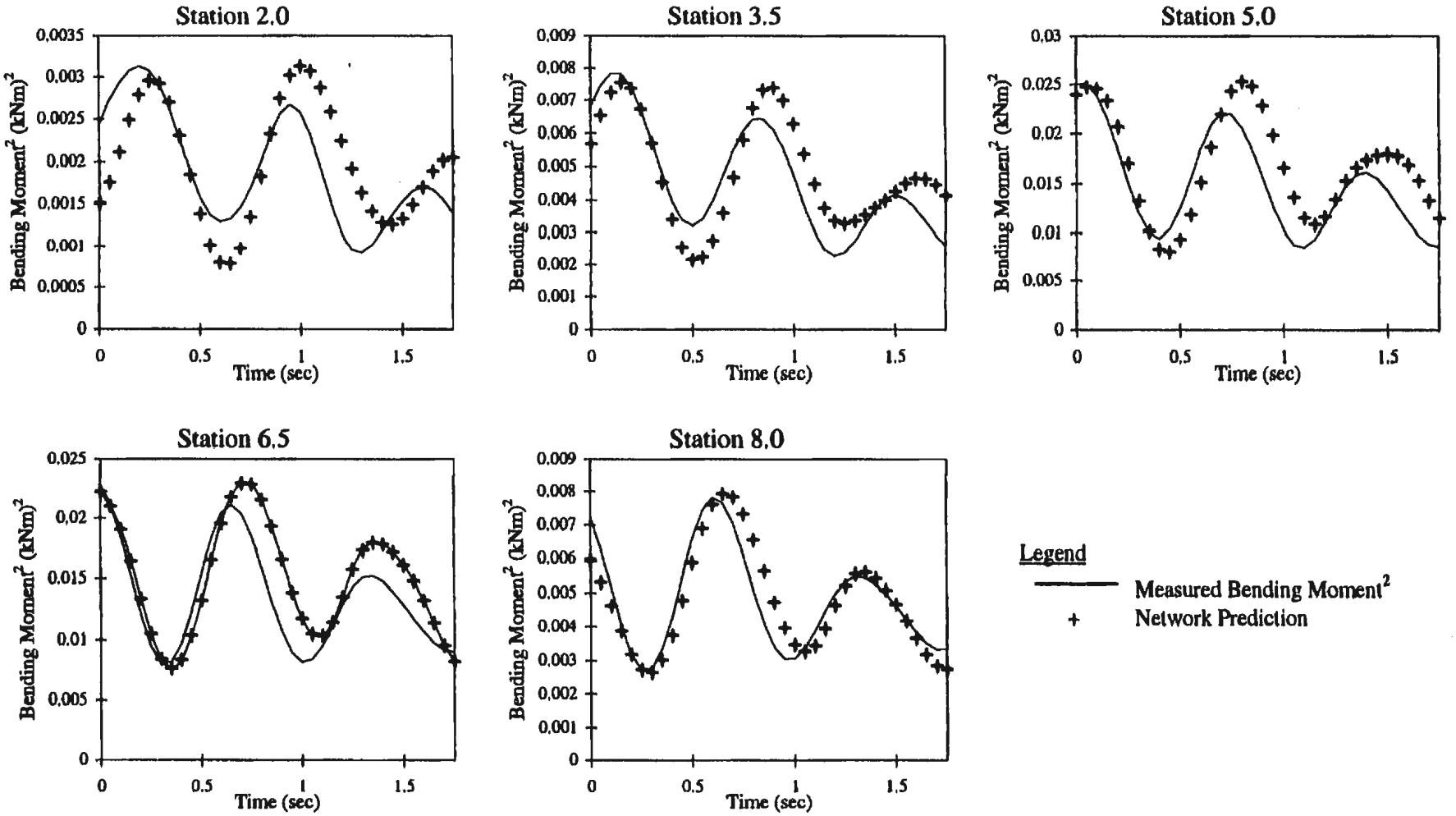

CPF

Figure D5: Prediction of Bending Moment Random Decrements

Ship Speed: 4.1 knots Sig. Wave Height: 4 m Bretschneider Spectra

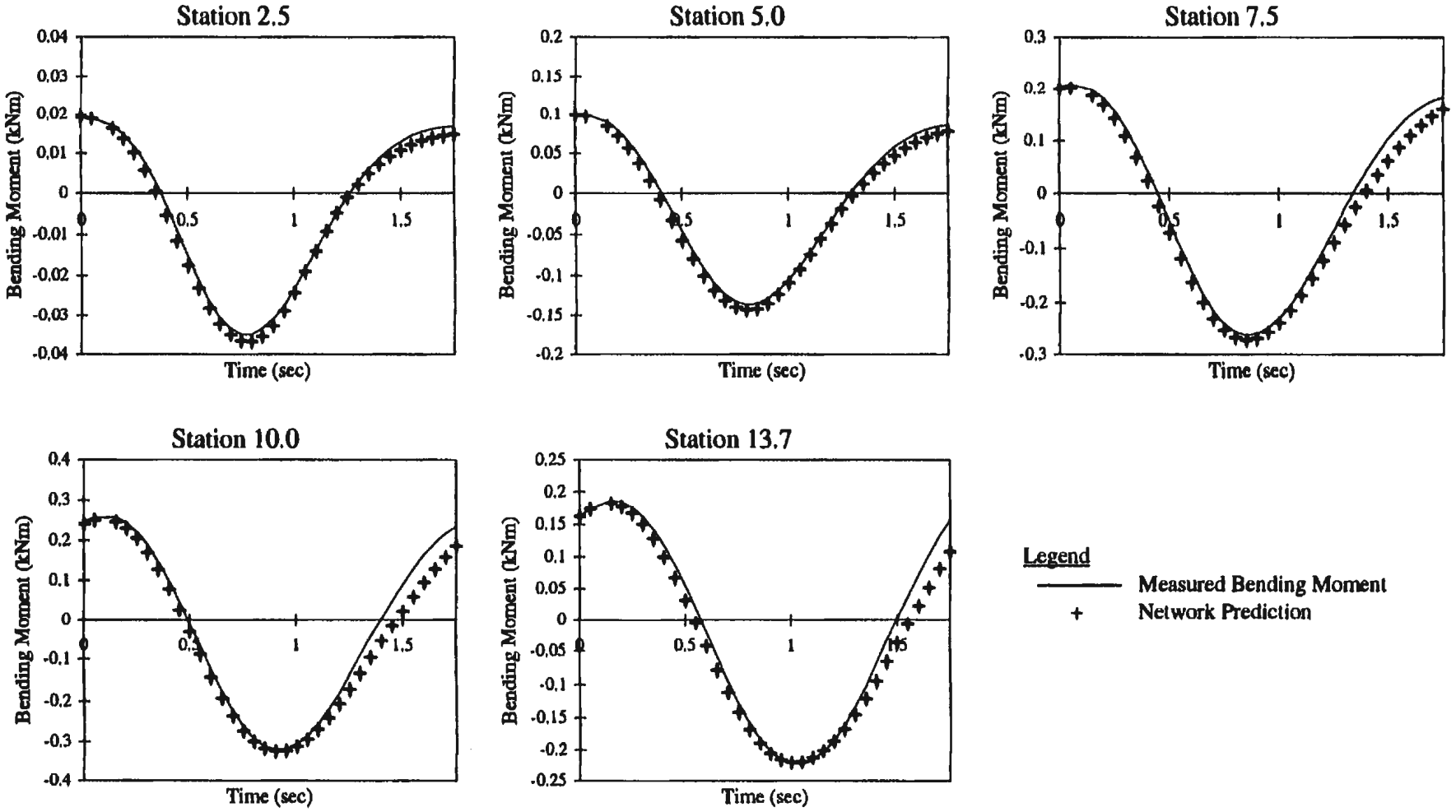

CPF

Figure D6: Prediction of Bending Moment^2 Random Decrements

Ship Speed: 4.1 knots Sig. Wave Height: 4 m Bretschneider Spectra

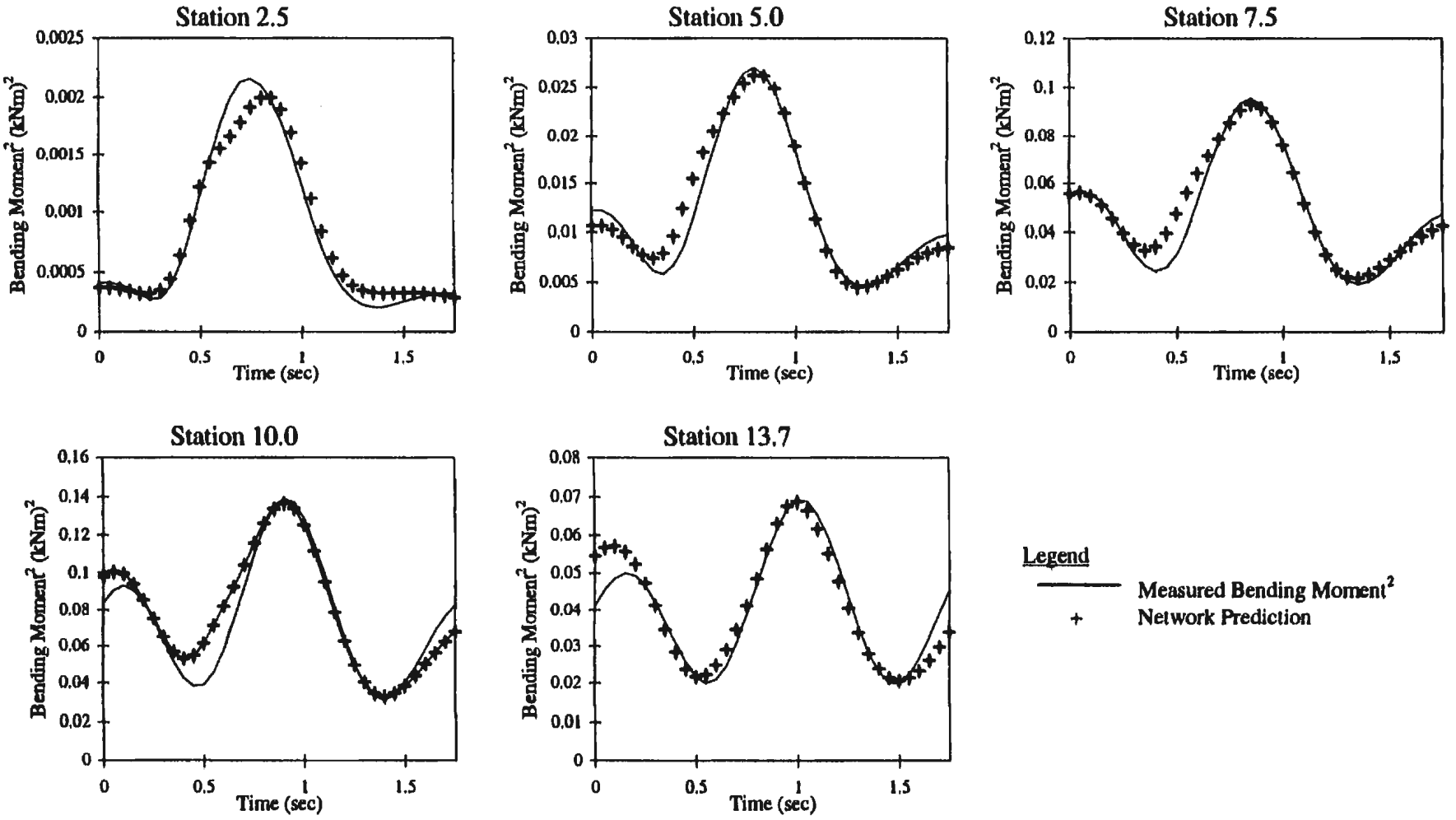

CPF

Figure D7: Prediction of Bending Moment Random Decrements

Ship Speed: 4.1 knots Sig. Wave Height: 5 m Bretschneider Spectra

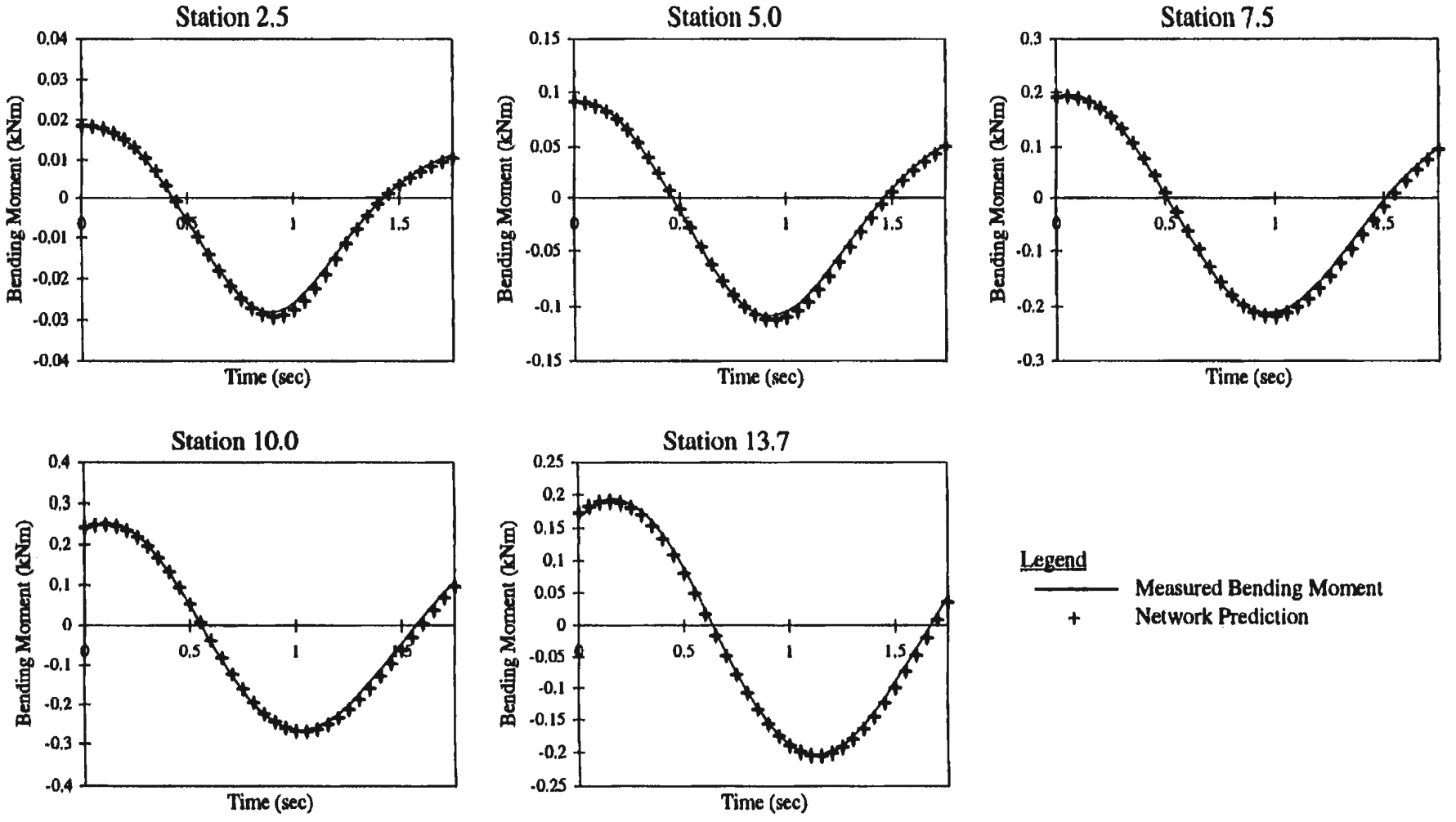

CPF

Figure D8: Prediction of Bending Moment^2 Random Decrements

Ship Speed: 4.1 knots Sig. Wave Height: 5 m Bretschneider Spectra

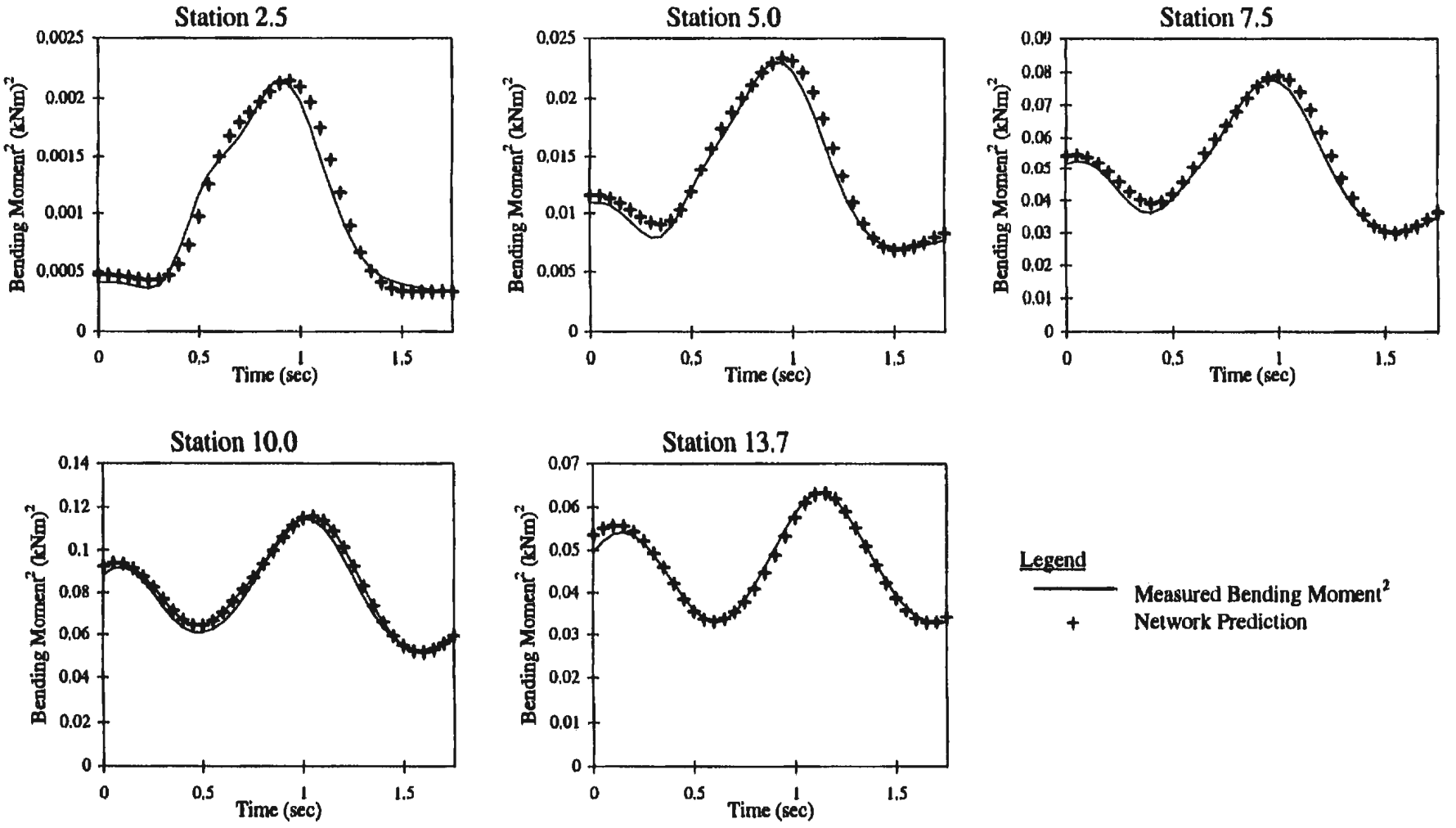

CPF

Figure D9: Prediction of Bending Moment Random Decrements

Ship Speed: 8.2 knots Sig. Wave Height: 4 m Bretschneider Spectra

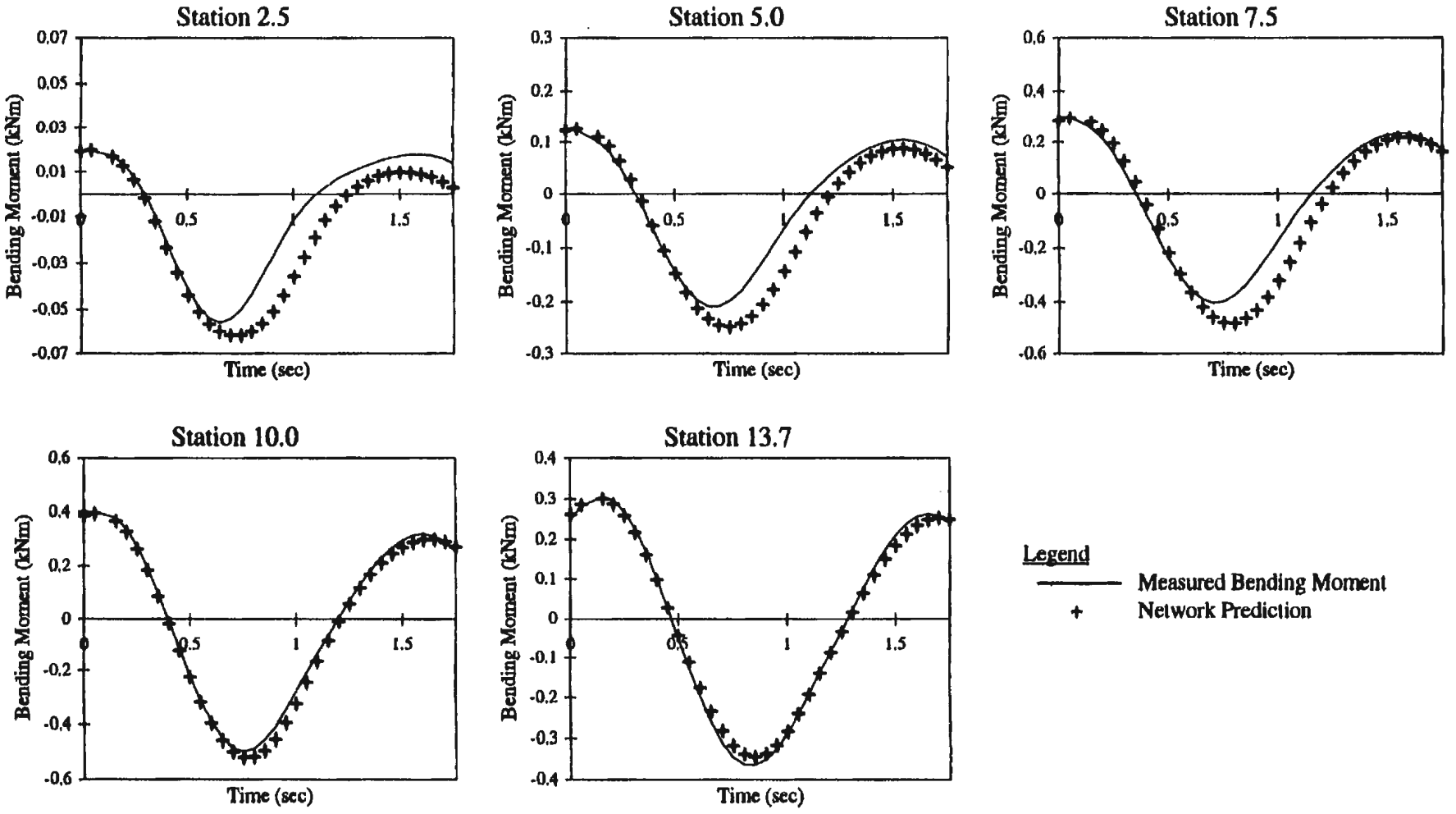

CPF

Figure D10: Prediction of Bending Moment^2 Random Decrements

Ship Speed: 8.2 knots Sig. Wave Height: 4 m Bretschneider Spectra

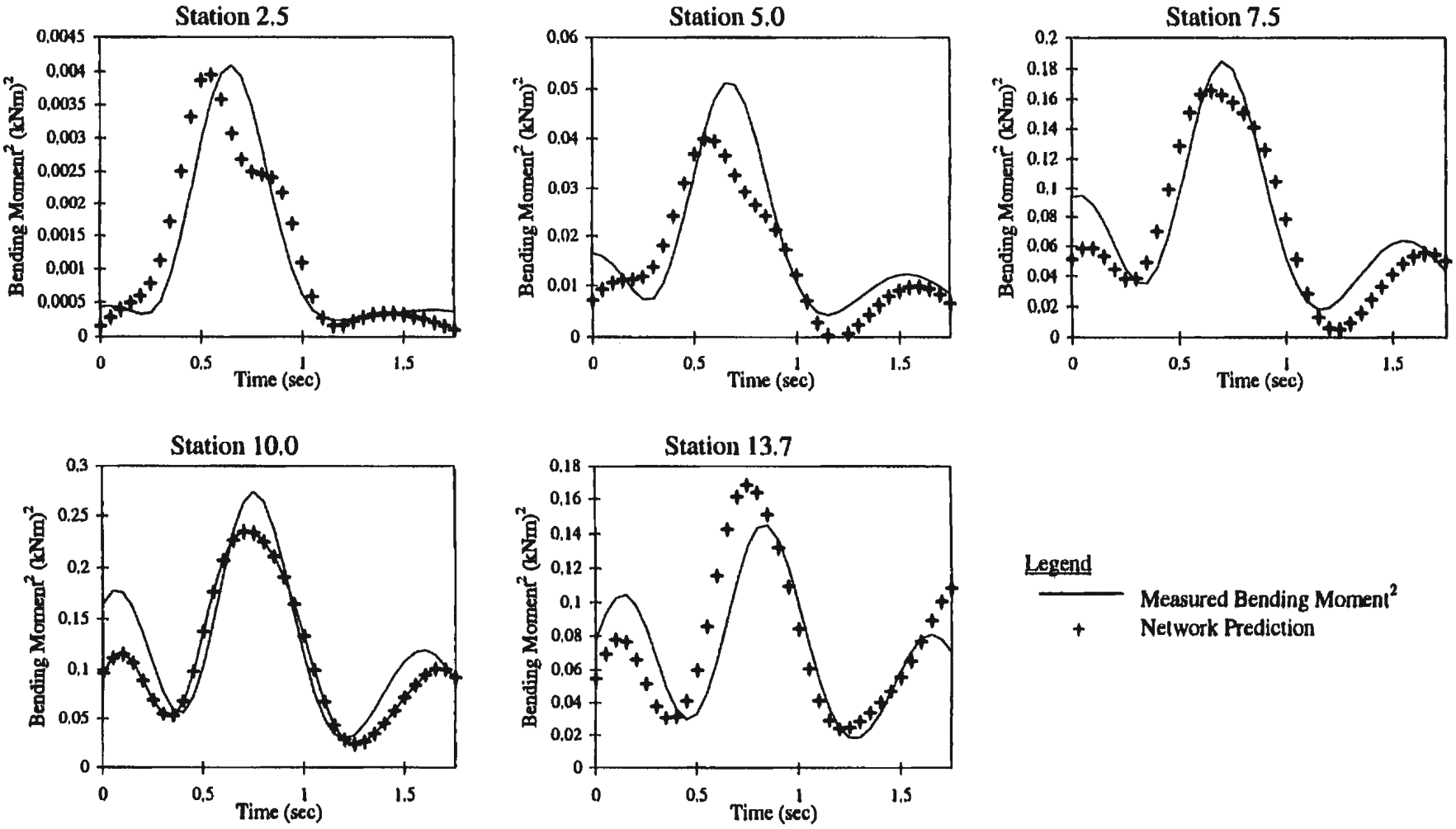

CPF

Figure D11: Prediction of Bending Moment Random Decrements

Ship Speed: 8.2 knots Sig. Wave Height: 5 m Bretschneider Spectra

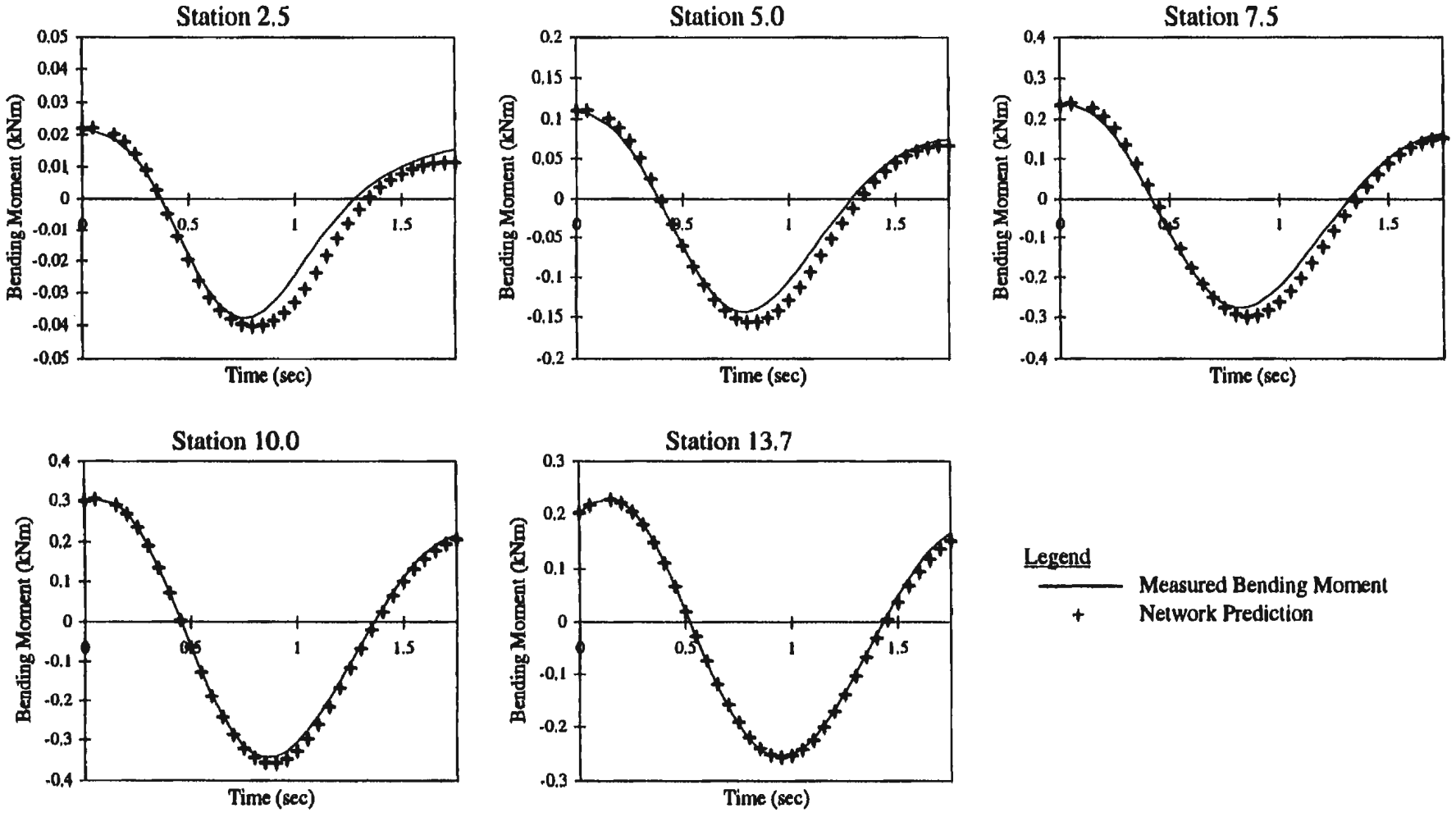

CPF

Figure D12: Prediction of Bending Moment^2 Random Decrements

Ship Speed: 8.2 knots Sig. Wave Height: 5 m Bretschneider Spectra

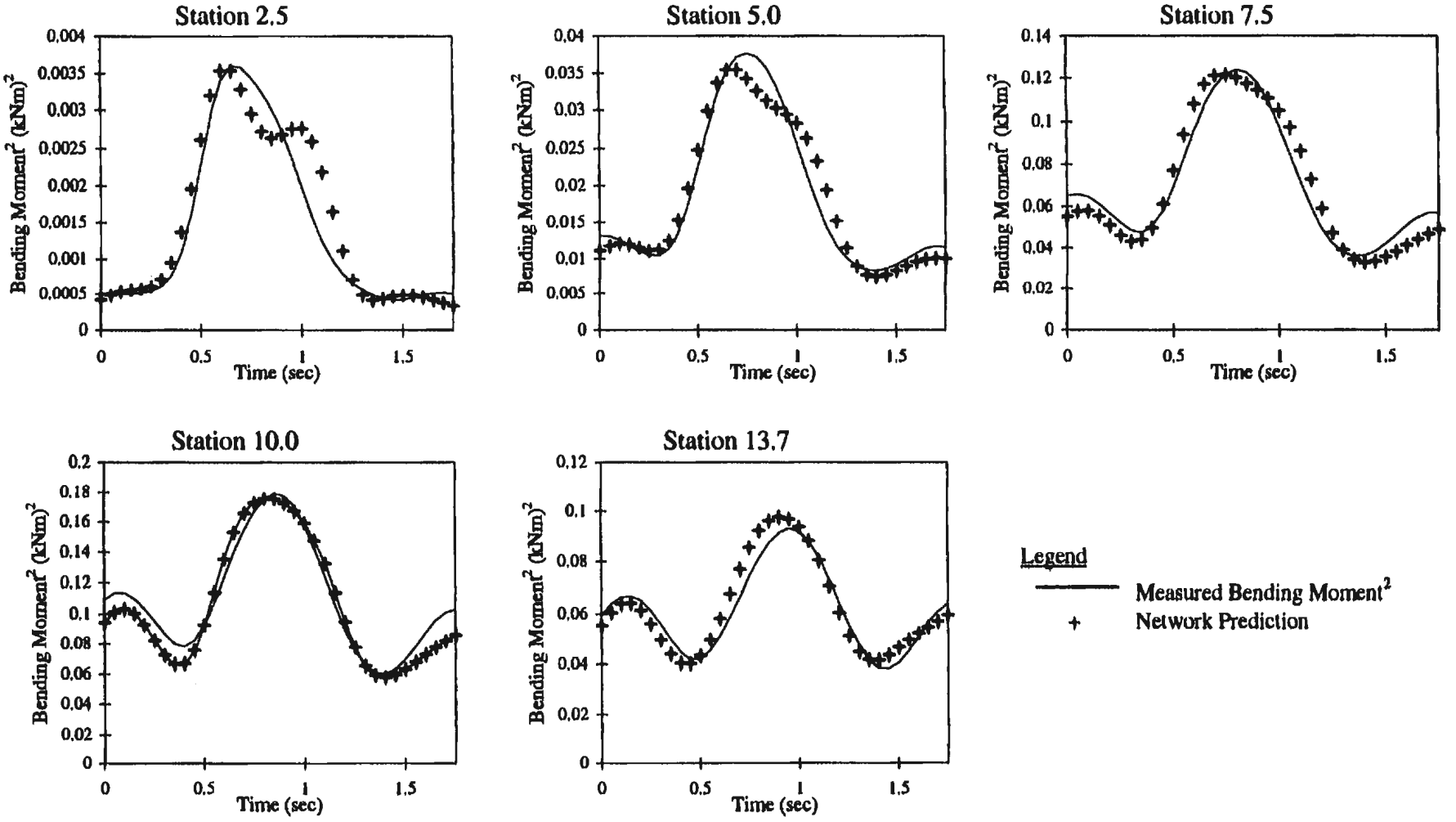

CPF

Figure D13: Prediction of Bending Moment Random Decrements

Ship Speed: 13.6 knots Sig. Wave Height: 4 m Bretschneider Spectra

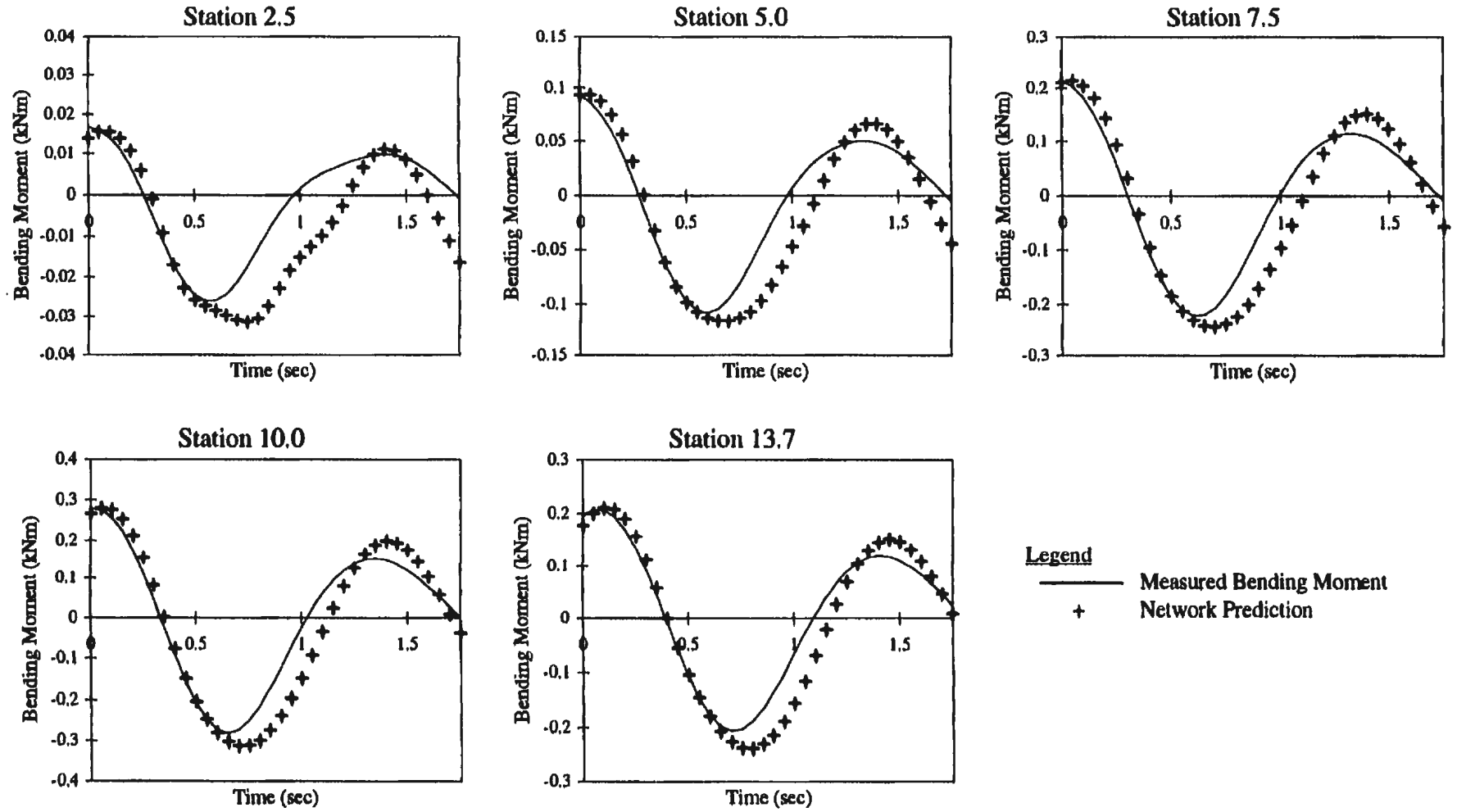

CPF

Figure D14: Prediction of Bending Moment^2 Random Decrements

Ship Speed: 13.6 knots Sig. Wave Height: 4 m Bretschneider Spectra

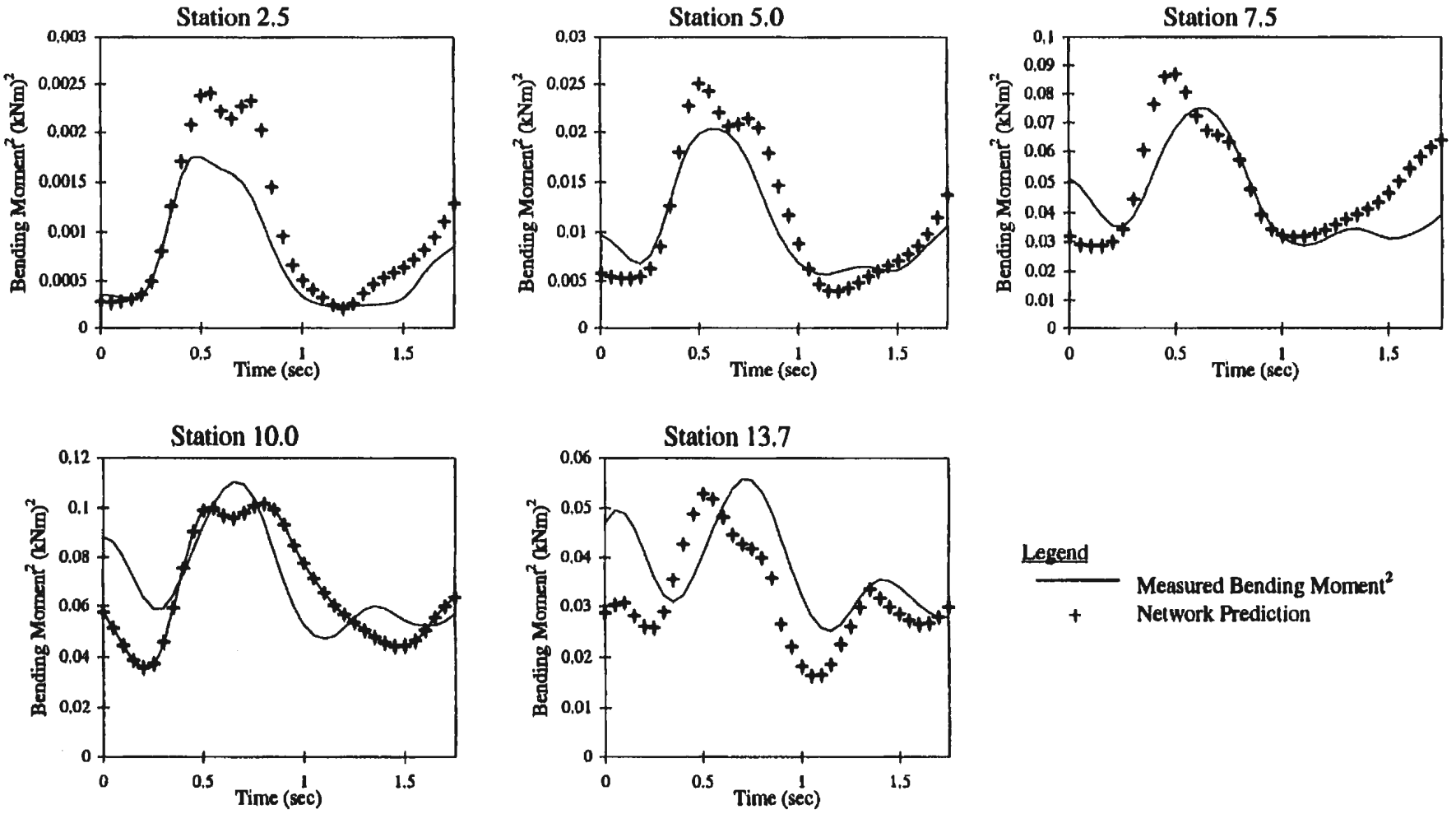

CPF

Figure D15: Prediction of Bending Moment Random Decrements

Ship Speed: 13.6 knots Sig. Wave Height: 5 m Bretschneider Spectra

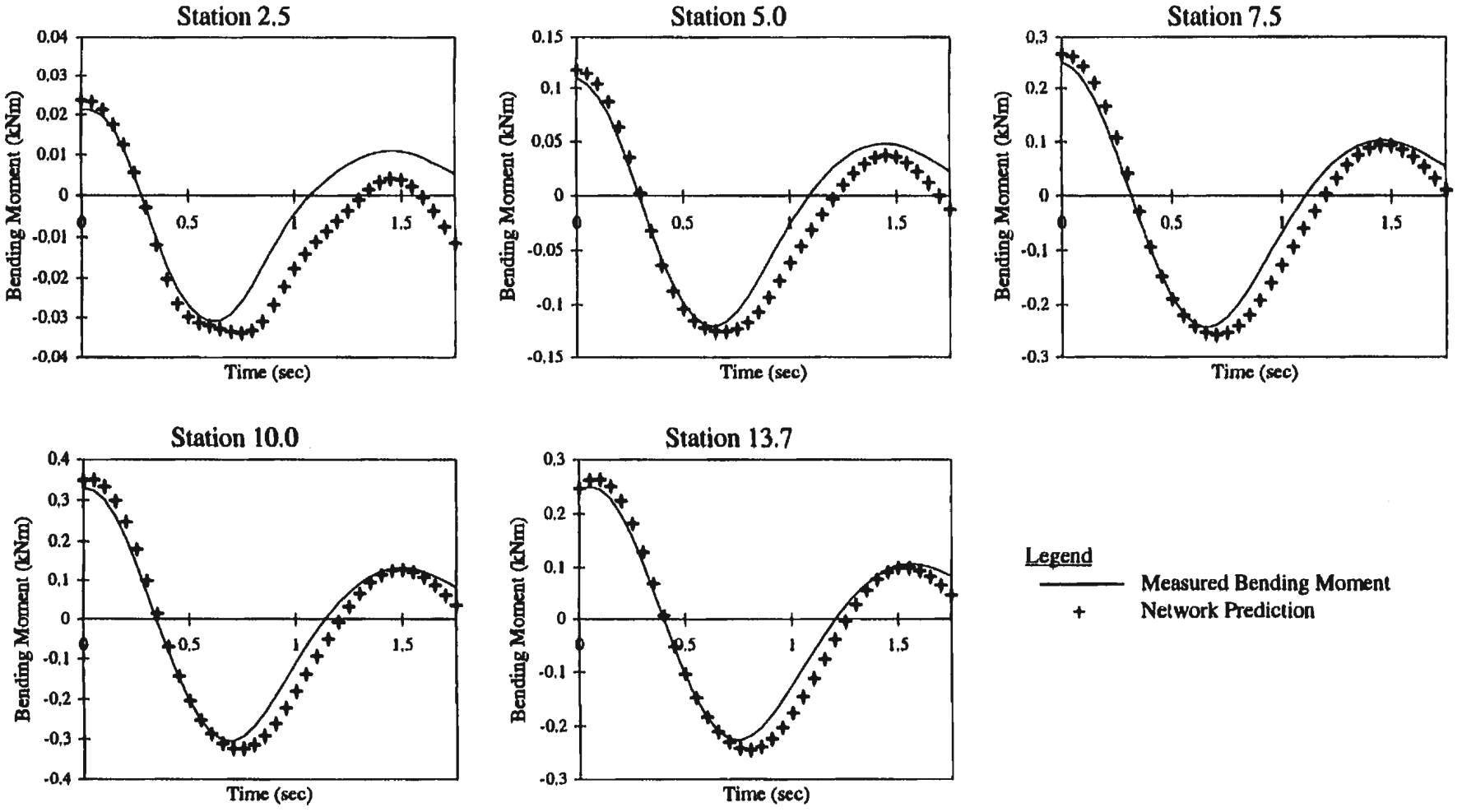

CPF

Figure D16: Prediction of Bending Moment^2 Random Decrements

Ship Speed: 13.6 knots Sig. Wave Height: 5 m Bretschneider Spectra

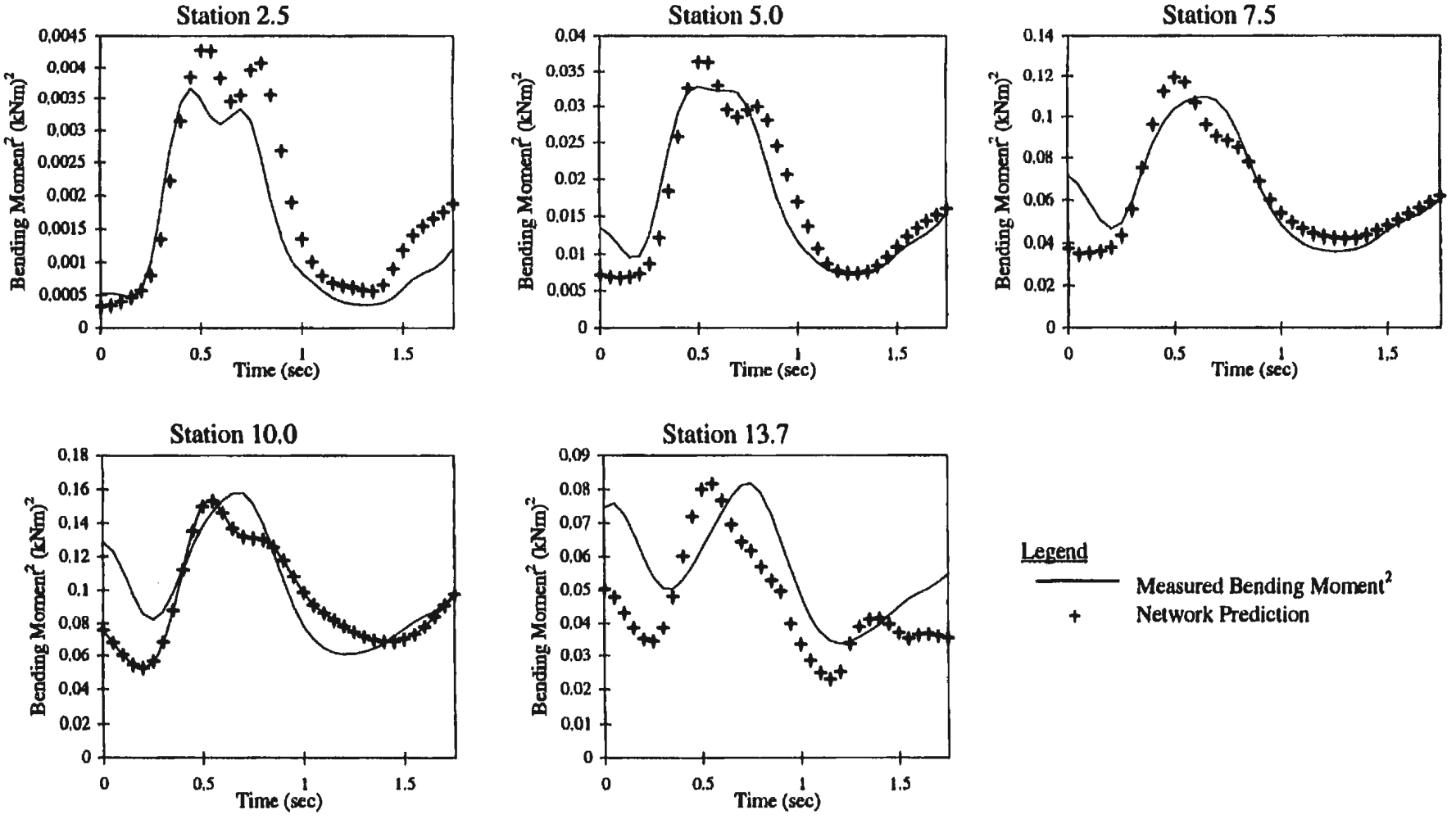

CPF

Figure D17: Prediction of Bending Moment Random Decrements

Ship Speed: 17 knots Sig. Wave Height: 4 m Bretschneider Spectra

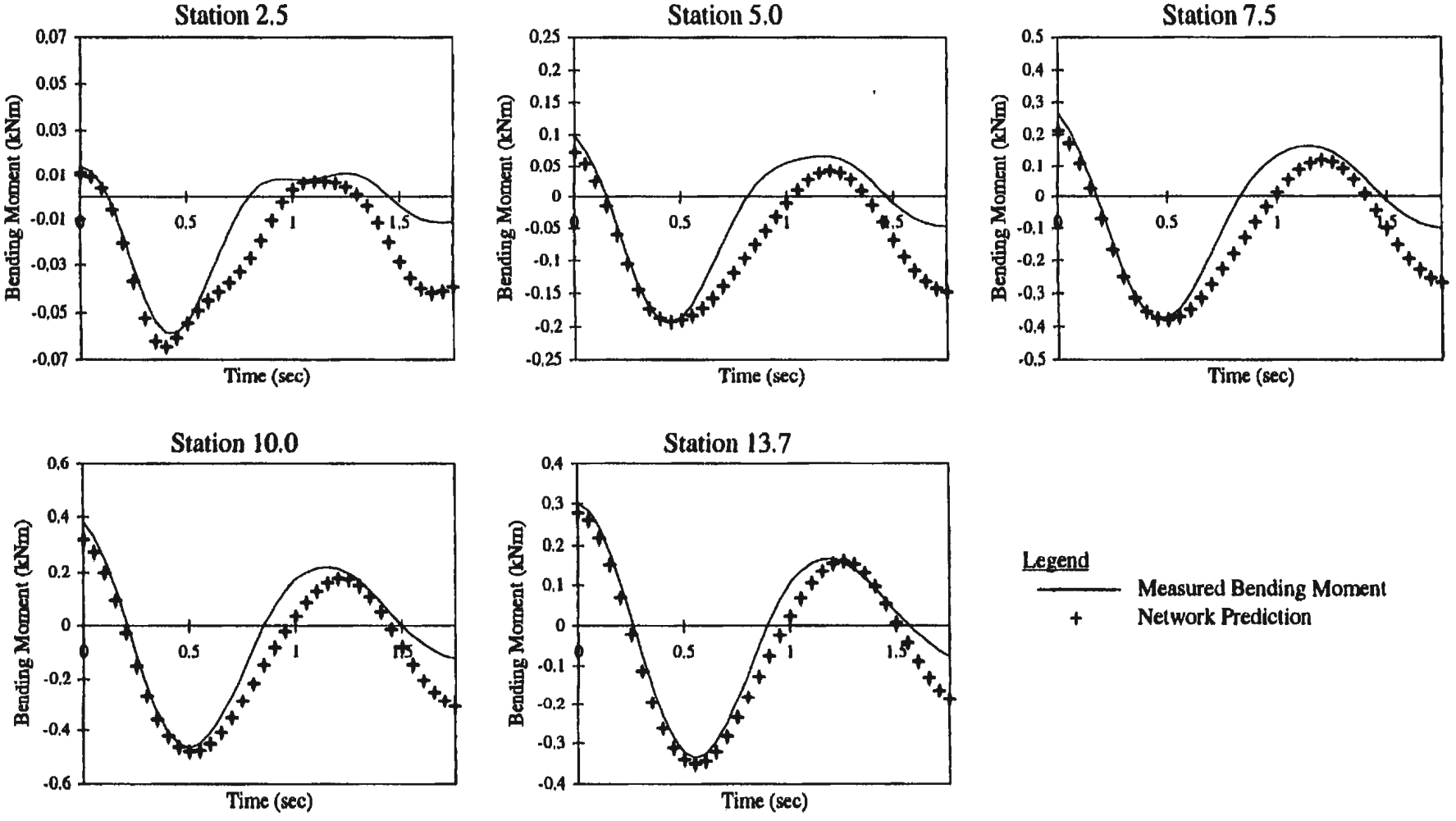

CPF

Figure D18: Prediction of Bending Moment^2 Random Decrements

Ship Speed: 17 knots Sig. Wave Height: 4 m Bretschneider Spectra

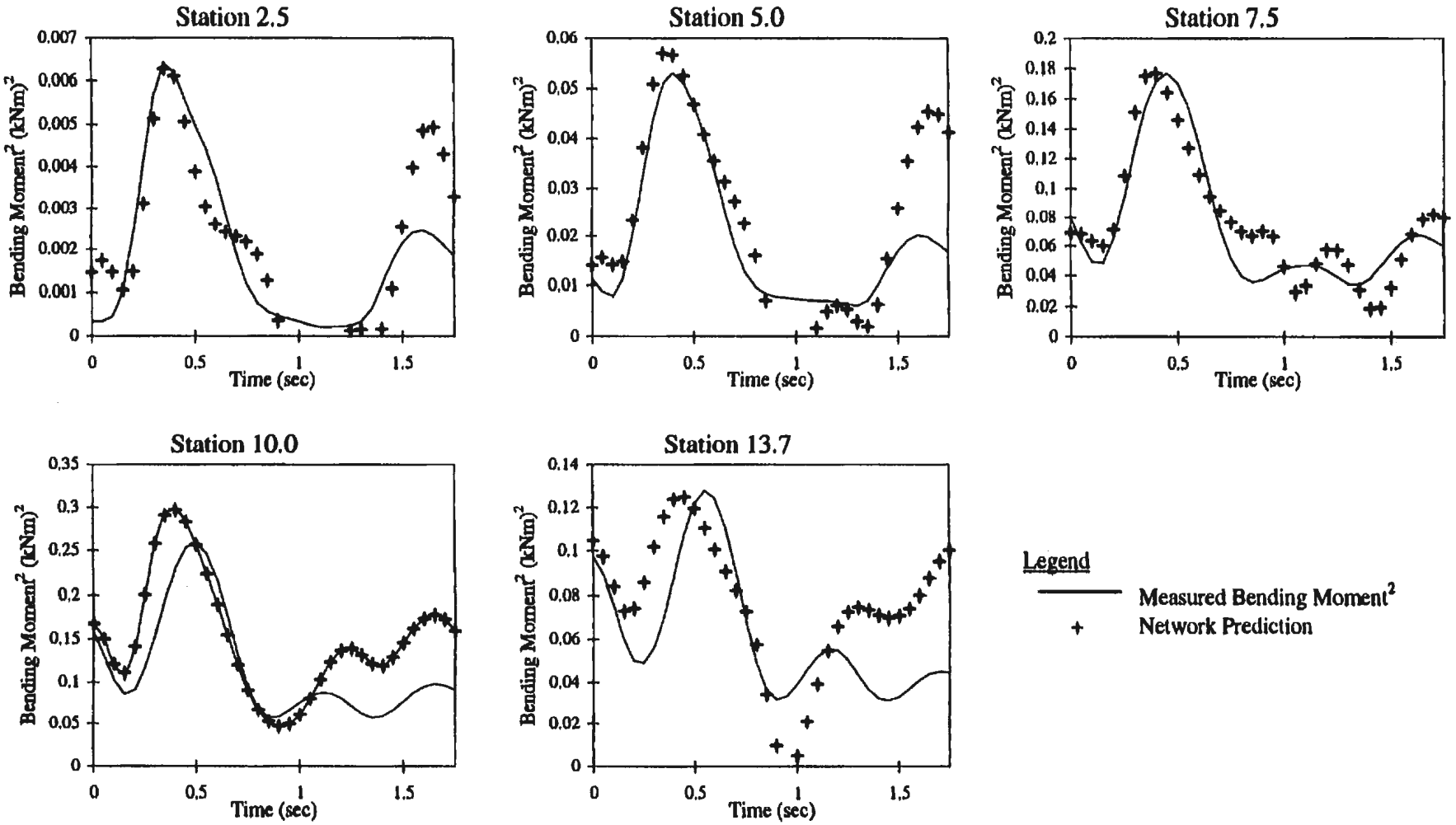

CPF

Figure D19: Prediction of Bending Moment Random Decrements

Ship Speed: 17 knots Sig. Wave Height: 5 m Bretschneider Spectra

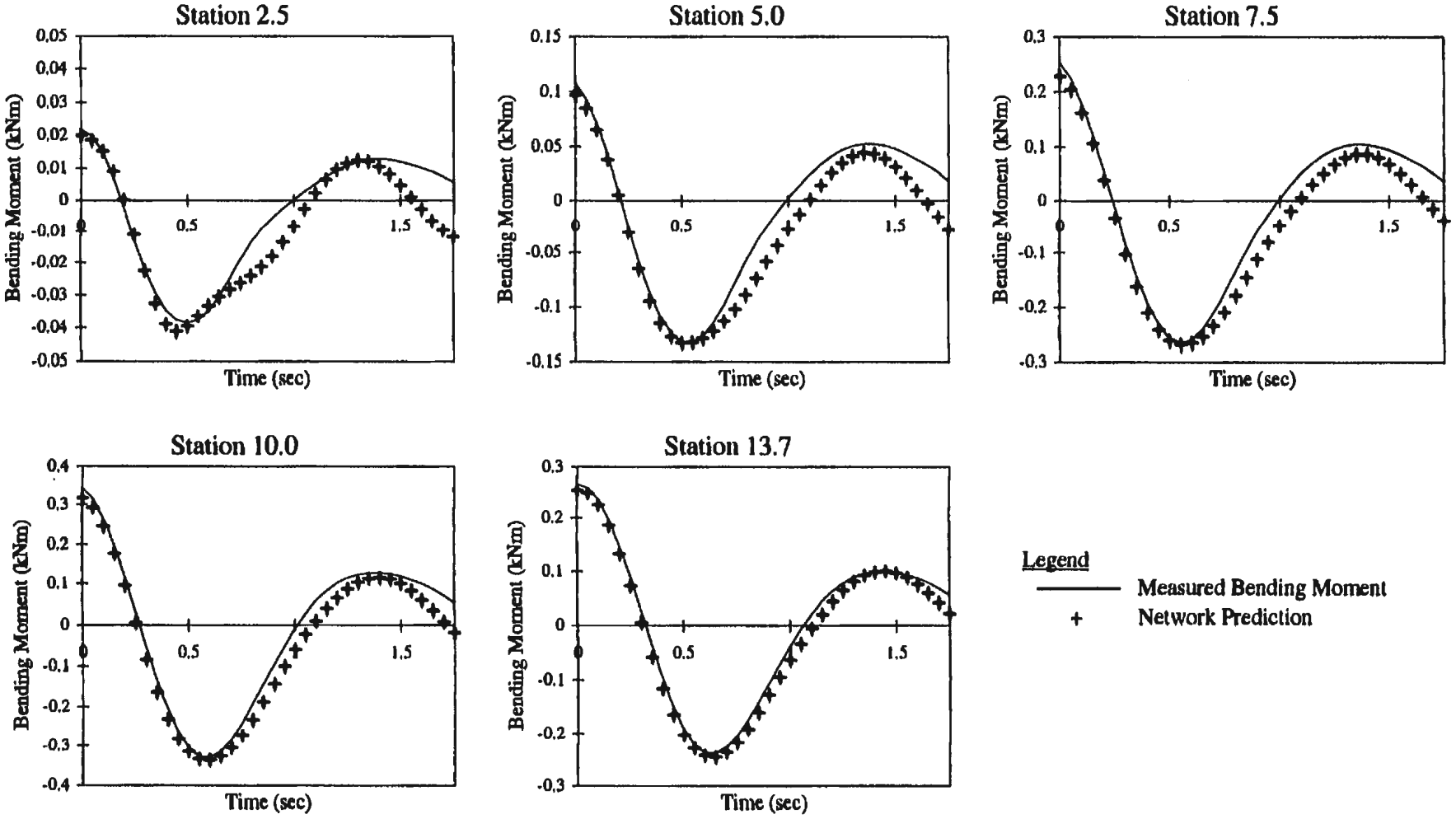

CPF

Figure D20: Prediction of Bending Moment^2 Random Decrements

Ship Speed: 17 knots Sig. Wave Height: 5 m Bretschneider Spectra